

**AIR PRESSURE MEASUREMENT IN THE RAREFIED  
GAS TRANSITION REGION**

*FRED S. BRUNSCHWIG*

*THE BOEING COMPANY*

FOREWORD

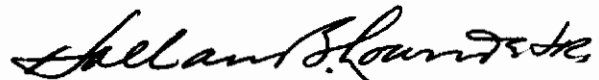
This development project was performed by the Boeing Company, Aerospace Division, Seattle, Washington, under USAF Contract No. AF 33(615)-1793. The work was supervised and this report was prepared by Fred S. Brunschwig, Project Engineer. The contract was initiated under Project No. 1469, "Vehicle Loads Validation", Task No. 146907, "Advanced Technology for Data Sensing". The work described in this document was authorized by and completed under the auspices of the Air Force Flight Dynamics Laboratory, Research and Technology Division, with Mr. William P. Johnson as Project Engineer.

This report covers work conducted from April 1964 to March 1965.

The generous efforts of William Latham and Marilyn Healey, Boeing Electronics Technology, have made this document possible and are gratefully acknowledged.

This Manuscript was released by the author in April 1965 for publication as a RTD Technical Report.

This technical report has been reviewed and is approved.

  
HOLLAND B. LOWNDES, JR.  
Acting Chief  
Structures Division

## ABSTRACT

This report defines parameters and presents pressure corrections for a low air pressure (1-100 p.s.f.a.) measurement system consisting of a pressure transducer and tubing ported to a hot surface at temperatures to 2800°F. Included are results of laboratory measurements with argon and air under conditions of both thermal creep and slip flow occurring together in a pressure transmission tube under temperature gradients. Both temperature functions, thermal creep and slip flow, were found to affect the system pressure. Dynamically, the temperature dependance of slip flow affects time response for tubes since it has the temperature dependancy of gas viscosity. Integration of the tubular time constant, modified for slip flow along the tube's temperature gradient, is carried out and compared to measurements; fair agreement is shown.

For pressure correction, the static (steady state pressure and temperature) differential predicted by Knudsen is found to hold for a closed tubular volume. Additionally, the plotted static results are sufficiently accurate to clearly show the effect of temperature upon viscosity as predicted by integration of Maxwell's viscosity function along the tube.

Other laboratory work reported herein includes calibration of a commercial airborne alpha emission pressure transducer (National Research Corp. Alphation 718). Also, there is considerable data presented on adsorption/oxidation at temperature for pressure tubing material.

TABLE OF CONTENTS

1.0	Introduction	1
2.0	Purpose and Scope	1
3.0	Transducer Survey and Evaluation	1
3.1	Methods of Air Pressure Transduction	1
3.2	Pressure Transducer Packaging	2
3.3	Transducer Evaluation	3
4.0	Tubing Materials Testing	3
4.1	Heating of Tube Materials in Low Pressure Air	3
4.2	Results of Oxidation/Absorption Testing	4
4.2.1	Chemical Reactions	4
4.2.2	Titanium A4O Coating	5
4.3	Tubing Materials Testing - Additional Results	5
5.0	Theory - Steady State	6
5.1	Slip Flow and Transpiration Analysis	7
6.0	Pressure Transmission Investigation	7
6.1	Laboratory Test Program	7
6.2	Discussion of Argon Data	8
6.3	Test with Air-Closed Tube	8
6.4	Discussion of Closed Tube Data	9
7.0	Dynamic Case	10
7.1	Laboratory Technique	10
7.2	Atmospheric Entry Simulation Test	11
8.0	Summary	12
8.1	System Design and Criteria	12
8.1.1	Material	13
8.1.2	Diameter	13
8.1.3	Length	13
8.1.4	Volume	13
8.1.5	Joints	14
8.1.6	Port	14
8.2	Use of Data to Correct Pressure Reading	14

# *Contrails*

9.0	Conclusion	16
	References	17
	Appendix Part I Steady State Creep with Slip a Temperature Function	18
	Appendix Part II Time Response Equation	20

# Contrails

## LIST OF ILLUSTRATIONS

Table 1	Evaluation of Decker Low Gas Pressure Transducer vs. Temperature-145°F	23
Table 2	Evaluation of Decker Low Gas Pressure Transducer Temperature-Room	24
Table 3	Evaluation of Decker Low Gas Pressure Transducer vs. Temperature-45°F	25
Table 4	Alphatron 718 Calibration at 45°F	26
Table 5	Alphatron 718 Calibration at 74°F	29
Table 6	Alphatron 718 Calibration at 160°F	31
Table 7	Alphatron 718 Calibration at 212°F	34
Table 8	Alphatron 718 Calibration at 120°F	36
Table 9	Calibration of Alphatron 718 Pressure Transducer - Full Pressure Range	37
Table 10	Calibration of Alphatron 718 Pressure Transducer - to 5 torr	38
Table 11	Trans-Sonics 120 Calibration Data at 78°F	39
Table 12	Trans-Sonics 120 Calibration Summary	41
Figure 13	Platinum Tubing Facility to Measure Effect of Air Plus Tube Material upon Pressure Measurement	42
Figure 14	Facility to Measure Effect of Air Plus Tube Material upon Pressure Measurement: 1-100psf; 65-2800°F	43
Figure 15	Air Pressure in the Presence of Uncoated Tantalum - 0.3 torr	44
Figure 16	Air Pressure in the Presence of Uncoated Tantalum - 3.0 torr	45
Figure 17	Air Pressure in the Presence of Uncoated Tantalum - 30.0 torr	46

# Contrails

Figure 18	Air Pressure in the Presence of Uncoated Titanium - 0.3 torr	47
Figure 19	Air Pressure in the Presence of Uncoated Titanium - 3.0 torr	48
Figure 20	Air Pressure in the Presence of Uncoated Titanium - 30.0 torr	49
Figure 21	Air Pressure in the Presence of Disilicided Tantalum - 0.3 torr	50
Figure 22	Air Pressure in the Presence of Disilicided Tantalum - 3.0 torr	51
Figure 23	Air Pressure in the Presence of Disilicided Tantalum - 30.0 torr	52
Figure 24	Air Pressure in the Presence of Iridium - 0.3 torr	53
Figure 25	Air Pressure in the Presence of Iridium - 3.0 torr	54
Figure 26	Air Pressure in the Presence of Iridium - 30.0 torr	55
Figure 27	Air Pressure in the Presence of Nickel Plated Titanium - 0.3 torr	56
Figure 28	Air Pressure in the Presence of Nickel Plated Titanium - 3.0 torr	57
Figure 29	Air Pressure in the Presence of Nickel Plated Titanium - 30.0 torr	58
Figure 30	Air Pressure in the Presence of 321 Stainless Steel - 0.3 torr	59
Figure 31	Air Pressure in the Presence of 321 Stainless Steel - 3.0 torr	60
Figure 32	Air Pressure in the Presence of 321 Stainless Steel - 30.0 torr	61
Figure 33	Open Tube Facility for Low Pressure Argon Measurement	62

# Contents

Figure 34	Detail of Open Tube Assembly for Low Pressure Argon Measurement	63
Figure 35	Calibration of Monitor Tube Pressure Against Chamber Pressure	64
Figure 36	Calibration of Monitor Tube Pressure Against Chamber Pressure	65
Figure 37	Argon Static Pressure Difference vs. $K_n$ in an Open Tube	66
Figure 38	Time Response - Argon to 0.4 torr - 0.067" Tube	67
Figure 39	Time Response - Argon to 1.0 torr - 0.067" Tube	68
Figure 40	Time Response - Argon to 5.0 torr - 0.067" Tube	69
Figure 41	Time Response - Argon to 0.40 torr - 0.117" Tube	70
Figure 42	Time Response - Argon to 1.0 torr - 0.117" Tube	71
Figure 43	Time Response - Argon to 0.4 torr - 0.160" Tube	72
Figure 44	Time Response - Argon to 0.8 torr - 0.160" Tube	73
Figure 45	Argon Static Pressure Difference vs. $K_n$ in an Open Tube	74
Figure 46	Tantalum Tube Facility for Low Pressure Air Measurement	75
Figure 47	Tantalum Tube Assembly for Low Pressure Air Measurement	76
Figure 48	Data for Air in Closed Tube	77
Figure 49	Air Static Pressure Difference vs. $K_n$ in a Closed Tube	78
Figure 50	Photograph of Furnace to Heat Tubes	79
Figure 51	Photograph of Tantalum Tube Assembly	80
Figure 52	Photograph of Tantalum Tube Mounted in Furnace	81
Figure 53	Argon Static Pressure Difference vs. $K_n$ in a closed Tube	82



# *Contrails*

<b>Figure 54</b>	<b>Valve Network for Atmospheric Entry Test</b>	<b>83</b>
<b>Figure 55</b>	<b>Atmospheric Entry Test Temperature</b>	<b>84</b>
<b>Figure 56</b>	<b>Atmospheric Entry Test Pressure</b>	<b>85</b>
<b>Figure 57</b>	<b>Atmospheric Entry Test Pressure Differential Data</b>	<b>86</b>
<b>Figure 58</b>	<b>Atmospheric Entry Test Plot of Pressure Differential</b>	<b>87</b>

## LIST OF SYMBOLS

$p$	pressure
$T$	temperature
$T_2$	temperature at hot end of tube
$T_1$	temperature at cold end of tube
$T_0$	transducer temperature
$T_a$	average temperature
$R$	gas constant
$a$	tube radius
$\eta$	coefficient of viscosity
$\gamma$	coefficient of slip
$f$	transfer ratio of momentum
$x$	dimension along tube
$l$	tube length
$P_f$	final pressure
$P_0$	initial pressure
$P_2$	pressure at hot end of tube
$P_1$	pressure at cold end of tube
$V$	transducer volume
$V_T$	tube volume
$K_n$	Knudsen number
$\lambda$	coefficient of the temperature dependence of mean free path
$P_a$	average pressure
$\eta_0$	coefficient of viscosity at room temperature

x

# Contrails

n	power of temperature dependence of viscosity
K	constant which fits the equation, $\eta = K\eta_0 T^n$ at room temperature
C	constant which describes temperature distribution
$C_p$	specific heat at constant pressure
$C_v$	specific heat at constant volume
$\gamma$	ratio of specific heats
k	thermal conductivity
$\tau$	time response

xi

REV LTR

U3 4288-2000 REV. 1/65

**BOEING**

NO.

D2-81314-1

SH.

15

# *Contrails*

## 1.0 Introduction

While physically the correction of pressure measurements for temperature effects has received little attention because the effects are only present for low pressures, measurement of the deviation of gas pressure from that predicted by Boyle's law has been the subject of much physical investigation, for the subject encompasses definition of the equation of state of a gas. Corrections of the gas law to account for molecular volume and intermolecular forces, known as virial coefficients, date back to Amagat in 1870. Soon afterward, Maxwell and Boltzmann showed the statistical significance of thermal velocity of molecules upon the nature of gas dynamics. Knudsen's measurements of temperature-induced pressure effects support the statistical mechanical theory. Lately, Patterson has derived non-isentropic flow theory from Maxwell-Boltzmann statistics. Such non-equilibrium flow defines a part of atmospheric entry physics, and not only the velocity of entry from orbit, but also the concomitantly encountered air temperature requires measurement to interpret the encountered phenomena.

## 2.0 Purpose and Scope

Our purpose here is to report some of the atmospheric entry vehicle research work for the measurement of low gas pressure on a hot surface and to delineate the design of low air pressure measurement systems for the range 1-100 p.s.f.a. where the air pressure can be at temperatures up to 2800°F under airborne conditions. Evaluation of transducers for low air pressure measurement, the effect of temperature upon transmission of air pressure in tubing to 2800°F, and the effect of tubing material on pressure are described. Work measuring the pressure differential of temperature gradient starts where Howard's<sup>2</sup> left off.

Purely from a practical viewpoint, the pressure transducer of the system is assumed to operate in a temperature environment between 45° and 160°F. The transducer is then connected by a tube to the hot surface which is ported to an "outside" environment.

## 3.0 Transducer Survey and Evaluation

### 3.1 Methods of Air Pressure Transduction

Starting with the basic idea of obtaining system accuracy with a pressure sensor least subject to temperature variation, consider the aneroid and diaphragm transducers. The aneroid transducer principle can be represented

by the Computer Instruments Corporation's model 6000A; the diaphragm transducer by the Trans-Sonics' model E2821 DPO.7<sup>3</sup>. The temperature uncertainty and sensitivity of the C.I.C. transducer are respectively  $\pm 0.1$  &  $\pm .003$  p.s.f./ $^{\circ}$ F and of the Trans-Sonics<sup>4</sup> are respectively  $\pm 1.0$  &  $+ 0.03$  p.s.f./ $^{\circ}$ F. Over a range of  $100^{\circ}$ F this implies relative errors at 1 p.s.f. of  $\pm 10\%$ ,  $\pm 30\%$ , and  $\pm 100\% + 300\%$ , respectively. These errors are inherent in the transduction system since they are caused by temperature non-repeatable mechanical hysteresis. Once generated, these errors are fed through the system electronics.

One then looks for a temperature independent transduction principle. Radio-activity satisfies this criteria.

In a changing temperature environment, the emission rate of alpha particles is not a temperature function, while the absolute cross section of gas molecules is an extremely weak temperature function. The resultant ionization current is relatively temperature independent; therefore, temperature compensation for pressure measurement by alpha emission can be accomplished by circuit compensation for temperature changes in the electronics and in the gas (since number density is really measured.)

### 3.2 Pressure Transducer Packaging

Studying the pressure data from the Decker Corporation model 341 and the National Research Corporation's 718 Alphanon, Figures 1-12 (see also the Trans-Sonics 120 Equibar report<sup>5</sup>), one is impressed with the error in pressure which comes about due to instrument electronics temperature change. In fact, the non-linearity of this mechanical transducer is brought out in Figure 11 where the Trans-Sonics 120 has been calibrated against an absolute oil manometer. Since transducer amplifiers have been successfully packaged for airborne use in the temperature and vibration environment of atmosphere re-entry, the packaging of pressure transducer amplifiers merits attention.

The difficulties to be expected in packaging these pressure devices are as follows: It can be seen that the Decker Corporation's transducer is quite sensitive to thermal expansion and compression of the potting compound, causing electrical capacitive variations and hence, changes in pressure measurement response. The Trans-Sonics is also basically a capacitive pressure transducer, and hence, the same difficulties in packaging as with the Decker Corporation's transducer can be expected although it does not have physically exposed capacity. On the other hand, the National Research Corporation 718 Alphanon is basically a counting device, and its electronics is relatively insensitive to amplification variations. This transducer is isolated from the load by a magnetic reluctance effect rather

neatly. It is for this reason that it is recommended that this transducer be packaged for airborne use with temperature compensation.

### 3.3 Transducer Evaluation

An Alphanon 718, packaged for airborne use, was initially calibrated at 45°F, 78°F, 160°F, and 212°F against a Roger Gilmont oil manometer and a Wiancko pressure transducer over the air pressure range of 1-100 p.s.f. (0.359 to 35.9 torr). This data appears in Figures 4-7.

In the Alphanon 718 transducer the 5886 tube, a 2N335 transistor, and a ground lead were replaced in order to make the transducer operable.

Averaging of all Alphanon 718 data for 4 to 6 runs at each temperature resulted in a minimum scatter of  $\pm 47$  percent at 45° F for the 1 p.s.f. point. The scatter decreased with increasing pressure, but increased with increasing temperature. Voltage variation tests and temperature variation tests showed that either can cause data scatter. Because the circuit resistors were not replaced with the component changes, the data did not match that of the vendor's. When both temperature and voltage were carefully held constant, it was possible to hold scatter to  $\pm 4\%$  at 1 p.s.f. at 82°F.

It was also found necessary to isolate the 5886 filament supply from 60 cps pick up. This was done by using a battery.

Further work with the Alphanon 718, involving voltage variation, has determined that the vendor calibration curve can be obtained by reducing the screen of the 5886 tube to 5.1 volts from the previously used 8.1 volts. The calibration data of Figures 8-10 was obtained. This improved result ( $\pm 3$  percent of reading) allowed use of the alphanon 718 as the air pressure reference transducer for the final simulated trajectory heat tests. In this calibration data for the alphanon 718 its output has been also converted from pulse count to analog voltage in Figure 10.

A rebuilt model of the Decker transducer was scheduled for calibration and subsequent evaluation. However, on receiving the model 357 A, the chamber was found to leak excessively so that calibration was impossible.

### 4.0 Tubing Materials Testing

#### 4.1 Heating of Tube Materials in Low Pressure Air

The facility - To determine how a material affects pressure measurement of temperature in air, a sample is inserted into a closed end platinum-10-rhodium tube of 0.170" inside diameter, (See figures 13 and 14). This tube is so positioned inside the furnace that the center of the sample



coincides with the center of the furnace. The thermal gradient from the center of the furnace outward is  $-70^{\circ}\text{F}$  to each end of the 3" sample. The system volume is  $266\text{ cm}^3$ . The sample is retained in position inside the platinum-10-rhodium tube by a platinum wire welded to the platinum tube end.

Initially, the platinum-10-rhodium tube was heated alone to  $2865^{\circ}\text{F}$  to determine if oxidation or diffusion occurred within detectability of the pressure measuring system accuracy. Only slight increases in pressure were observed, which were ascribed to a tendency for the system to always expand a given volume of gas, even when the temperature of each end of the volume is controlled because the furnace slowly gets ahead of the water cooling system. It was possible to hold this thermal drift under  $\pm 1$  percent of pressure reading in 5 minutes at  $2800^{\circ}\text{F}$ . The thermal drift was the same for air and for argon, indicating that the system was leak free.

In order to do the air testing, the Trans-Sonics differential pressure transducer was resealed. While one can measure differential pressure across a leaking diaphragm instantaneously, eventually the system pressure will be affected by the leak, and in these tests the pressure must be constant over a five-minute time interval. The transducer was recalibrated against the Roger Gilmont oil manometer and the Wiancko pressure standard; the reading was found accurate to  $\pm 3$  percent as indicated by the meter.

## 4.2 Results of Oxidation/Adsorption Testing

Data for tantalum, titanium, and tantalum disilicide on tantalum are shown in Figures 15 through 23. These data were obtained by observing air pressure inside the platinum-10-rhodium tube after pressure and temperature had stabilized. The gettering of air for tantalum to  $2800^{\circ}\text{F}$  and for titanium to  $2000^{\circ}\text{F}$  are recorded. The getter action was so severe for titanium that no tests were run above  $2000^{\circ}\text{F}$  because the volume of low pressure air disappeared in a few minutes at 1 p. s. f. (0.359 torr reduced to 0.011 torr).

### 4.2.1 Chemical Reactions

There was no observed chemical reaction between tantalum and the platinum-10-rhodium tube to  $2800^{\circ}\text{F}$ . The titanium showed a small dot of chemical reaction at  $2000^{\circ}\text{F}$  at the point it touched the platinum tube. When the silicide coated tantalum was being tested at  $2500^{\circ}\text{F}$ , the platinum-10-rhodium tube blew in at just this point. At  $2800^{\circ}\text{F}$ , on later retest of the disilicided tantalum, the tube again blew in. A

4



tantalum wire separated the disilicide from the platinum during this test to prevent direct grain boundary attack by silicon. This time there was a tantalum-platinum eutectic reaction at 2800°F. While there may have been silicon grain boundary attack of the platinum-10-rhodium tube, the position of the holes indicates that the titanium and platinum formation of a low temperature eutectic at 2000°F, and tantalum and platinum at 2800°F caused the tube blow-ins. Since the tube's external environment is argon to protect the tantalum furnace heater, there is no serious effect upon the system during a blow in. In no case was there any noticeable effect on the samples after test.

#### 4.2.2 Titanium A40 Coating

An attempt to disilicide the titanium A40 tubing was not successful. The process destroyed the tubing with simultaneous flaking of any coating which formed. The titanium tubing does take a nickel plate; the nickel plated material was tested. Also, 321 stainless steel and Iridium were tested in air for their effect upon pressure measurement.

#### 4.3 Tubing Materials Testing - Additional Results

Additional tubing material tests in air to 2800°F are presented in Figures 24-32. These materials include iridium, nickel plated titanium, and 321 stainless steel. None of these three appear superior to disilicided tantalum at 2800°F for 0.360 torr of air pressure. While iridium has less pressure error at 3 and 30 torr, there is really not that much difference. To 2000°F, uncoated tantalum is stable enough to measure low pressure air in tube systems.

On the basis of the material pressure measurement data, it was decided to use disilicided tantalum to 2800°F and uncoated tantalum to 2000°F as a pressure monitor tube in forthcoming simulated heat trajectory tests of system pressure measurement accuracy.

None of these statements is to be confused to suggest that platinum-10-rhodium is not the most oxidation resistant tubing material to 2800°F. As was stated at the beginning of these material tests, the accuracy standard for the tests is platinum-10-rhodium, which displays no observable oxidation pressure change for five minutes of radiant heating at 2800°F temperature.

The inside of the tantalum monitor tube and 0.160" I.D. tantalum tube for the low air pressure trajectory heat tests were disilicided.

The brazing of tantalum presents a problem; it can be welded; and indeed this is how square sheets of tantalum, bent on a bar, were constructed into a one-inch diameter monitor tube. The disilicided material is brazable at 1100°F with silver brazing alloy. Above this temperature, abrading off the disilicide coating, followed by welding, suffices for a gas tight joint. A braze of 75% platinum - 25% "paliney 7" (m.p. 2800°F) failed to wet the disilicide, and hence tantalum joints which must operate above 1100°F were welded. The possibility of using FS-80 (columbium alloy) in place of tantalum can be recommended. The columbium is only half the weight of the tantalum, while its oxidation resistance is less than half that of tantalum.

## 5.0 Theory - Steady State

The theory of thermal creep, slip, and transpiration can be found in Loeb and Kennard, who both report Knudsen's work. Here we start with an expression derived by Kennard (p 331) which describes the tube flow under local temperature conditions. Slipping at the walls with the main flow is an additional return flow induced by the resultant pressure of thermal creep at the walls. The thermal creep is set up at the walls by a temperature gradient which causes molecular rebound at hot surfaces to occur more often than at the cold surface; hence, a rarefaction occurs at the cold end of the tube. The integration is carried out in Part I of the appendix. The key to the integration along a tube of this equation is in noting that the coefficient of slip is a temperature function by virtue of its viscosity dependance.

Inspection of the resulting eq. (16) shows that the static equation for tube pressure involves only the tube end point temperatures; that is, the value of pressure difference is independent of the temperature distribution along the tube. The difference of end pressures squared is not a strong function of  $\lambda$  (about as the inverse first power). This leaves only the question of Maxwell's transfer ratio of  $f$ . A value near unity is usually assigned on the basis of R.A. Millikan's measurements. Presumably, the data here could be used to determine the value of  $f$  and if another parameter is required.

It is to be noted that for a temperature there is a continuation of pressure corrections versus pressure, and that for a different temperature there is a different continuum. So that when the pressure correction is plotted

versus Knudsen number there occurs a curve for each tube end temperature.

5.1 Slip Flow and Transpiration Analysis

Because molecules in the hot end of the tube, at about the same pressure as those in the cold end, are heated to mean free paths five times those of the cold end, free molecular flow can occur in the hot end while slip flow takes place at the cold end. For the case of free molecular flow (transpiration) in the tube

$$P_2^2 - P_1^2 = P_1^2 (T_2 - T_1) / T_1$$

while for slip flow

$$P_2^2 - P_1^2 = \frac{4R}{a^2} 3K^2 \eta_o^2 \int_{T_o}^T \frac{T^{2n}}{1 + \lambda T^n + 1/2} dT$$

In the free molecular flow equation the difference of the square of pressures depends upon pressure squared. But in the slip flow equation the difference of the squares of pressures increases less than as pressure (through the mean free path). Furthermore, inspection of the data shows that the corrections are pressure dependent at pressures where the mean free path is of the order of the tube diameter. Hence, a method of combining slip flow with free molecular flow along the tube is required. Logically, one integrates the slip expression until  $Kn = 1/2$  and then calculates the remaining error under the transpiration, or free molecular flow, condition.

6.0 Pressure Transmission Investigation

6.1 Laboratory Test Program

Returning to the original thought of the introduction, the laboratory philosophy for determining those creep and slip effects on pressure induced by temperature consisted in measuring pressure differences directly. For the work a monitor, or standard tube, was made with diameter large enough to ensure neglect of wall effects and therefore to give true measurement of ambient pressure. In this way, both static and dynamic pressure difference measurement were effected for various tube radii. For those cases where system time response was too fast, excess volume was added to slow the system time response.

Where flow theory alone was being checked, Argon was substituted for air to eliminate oxidation effects (an accepted simulation technique).

## 6.2 Discussion of Argon Data

For this series of tests, an 0.902" inside diameter 321 stainless steel tube served as a pressure monitor tube. The tube under test was parallel to the monitor tube as shown in Figures 33 and 34. Calibration of the monitor tube pressure against chamber pressure is shown in Figures 35 and 36. The static pressure differences and time response curves are graphed in Figures 37-44. The time response data were taken by recording alpha-tron pressure reading every fifteen seconds. The result was so smooth that no single points are shown on the graphs. But as a result of the scatter in the static data, the tests were repeated to gain accuracy with a tantalum monitor tube extending completely into the furnace. The Trans-Sonics was rebuilt and used differentially with the Alphasatron 718 as the absolute pressure measuring device. The results were extremely accurate ( $\pm 1 \times 10^{-3}$  torr) and are plotted in Figure 45.

Inspection of the plot of argon steady state pressure difference due to temperature gradient effect yields the following conclusions:

The temperature dependent slip calculations for argon fall on those of Knudsen for hydrogen and Howard for air. The argon measurements are scattered about this line. If at the point of demarkation of the slip theory from the Knudsen empirical line, ( $Kn = 1/2$ ), the integration is modified to extend from the cold end to the point where  $Kn = 1/2$  and to continue with free molecular flow to the hot end of the tube, the dashed line results.<sup>8</sup> This analysis of the phenomena is in agreement with Skreekanth, who also says that slip flow holds until  $Kn = 1/2$ ; a conclusion he reaches measuring mass flow across an orifice.

## 6.3 Tests with Air - Closed Tube

A one-inch diameter tantalum tube was constructed and disilicided in order to make a monitor tube for low air pressure measurement. There is welded on the side of this tube, as shown in Figures 46 and 47, an 0.160" inside diameter tantalum pressure measurement tube. Those portions of both tubes which are above 2000°F have been disilicided to minimize oxide formation. A set of tests, similar to those run with argon, were run to determine the system time response as a temperature function, and to determine the steady state thermal creep pressure differences as pressure and temperature functions; the tests are summarized in Figure 48 and plotted in Figure 49. The time responses are in the right hand column; the pressure differences at each pressure are indicated in microns. The steady state data agrees with the integrated equation for tube pressure



difference reported earlier up to a Knudsen number of 0.5; above this value the pressure differences fall off rather more steeply than predicted by Knudsen. Photographs of the furnace built around the tantalum tubing are shown in Figures 50-52.

The data plot of Figure 53, measured in the disilicided tantalum tube, brings out very nicely the effect of temperature upon the steady state pressure differential occurring along the tube. At each temperature a discrete viscosity has given rise to a temperature identifiable flow. On each temperature curve, the point at the higher Knudsen number is measured at 0.079 torr.

6.4 Discussion of Closed Tube Data

The fit of the data for argon and air to a temperature dependent slip flow integration along the tube (see Figures 49 and 53) suggests that at all temperatures slip flow holds below a Knudsen number of one-half. Above Knudsen number of one-half the values of  $\Delta P/P_a / \Delta T/T_a$  branch off at each temperature toward an appropriate free molecular flow limit. For free molecular flow ( $\Delta P/P_a$ ) is fixed by the quantity  $\Delta T/(T_a + \sqrt{T_1 T_2})$ , a number of the order of one-half. As the temperature increases, the transition from slip flow to free molecular flow disappears, and the flow tends to go directly from slip flow to free molecular flow. The limits of the pressure difference expression are then:

$$\text{At } 2780^\circ\text{F} \quad \frac{\Delta P/P_a}{T/T_a} = 0.60$$

$$\text{At } 1090^\circ\text{F} \quad \frac{\Delta P/P_a}{T/T_a} = 0.526$$

Data taken at 2800°F shows this limit line to level at the 0.78 value of  $\Delta P/P_a / \Delta T/T_a$  before Knudsen number of four, some distance above the 0.60 value predicted by free molecular flow.

This tendency of the temperature curves for air to follow the slip flow calculation rather than an argon type transition as found by Knudsen and Howard can be attributed to oxidation of the tantalum and tantalum disilicide. We make the following argument: The rate of air reaction in a tube is proportional to its radius. The amount of air is proportional to the tube's radius squared. Therefore, a small tube is a more effective getter than a large tube on a pressure (molecular number density) basis. This being so, some part of the pressure differential can be due to reaction of the surface with the air in the small tube. Since data for reaction rates were not taken below 0.360 torr, it is not surprising to find noticeable gettering action taking place at 0.050 torr, the largest Knudsen number point on the curves for air.

Essentially, the data defines the pressure corrections in a closed system for air to below 1 p.s.f. (0.359 torr) at 2800°F (1805°K). The data also shows a separate transition flow for each temperature.

**7.0 Dynamic Case**

Calculation results with the integrated time response equation of Part II of the appendix tend to yield times one-quarter too short at the lower temperatures and times too long at the higher temperatures. Examining the results of air measurement, Figure 48, the product  $(\tau) \cdot (P_f)$  is nearly constant at each temperature in agreement with Sinclair and Robins<sup>9</sup> for the room temperature case. Hence, a good value of time response can be obtained by considering the temperature effect on viscosity. The values of argon and air viscosity versus temperature used in calculation can be found in references 10 and 11, respectively.

As with the isothermal time response equations of reference 9, inertial and velocity gradient terms are negligible. We must examine the analysis more carefully. Following R. D. Fay<sup>12</sup> it is possible that the difficulty with our dynamic analysis lies in the heat conduction of the gas to the walls of the tube. This heat conduction can be included by modifying the viscosity to an effective viscosity as given by

$$\eta_e = \eta \left[ 1 + \left( \sqrt{\gamma} - \frac{1}{\sqrt{\gamma}} \right) \sqrt{k/c_p \eta} \right]^2$$

This expression, at least to the first order is independent of temperature since the thermal conductivity can be written  $k = (5/2)\eta C_v$  and then  $\sqrt{k/c_p \eta} = \sqrt{5/2} \cdot 1/\sqrt{\gamma}$  where  $\gamma = C_p/C_v = 1.4$ , the ratio of specific heats is practically constant over a large temperature range. This gives a constant value of 2 to multiply the viscosity. Hence, all hot time constant calculations can be increased by a factor of two. Since the time response calculations are low at lower temperature and high at the higher temperature, this course of correction would seem to be eliminated.

More logically, in eq. (7) of Part II of the Appendix, a temperature gradient parameter appears. Unlike the static pressure equations, the dynamic equation depends upon the functional character of the temperature distribution. Any unknown quality of the temperature distribution can cause discrepancy between theory and measurement in the time response equation.

**7.1 Laboratory Technique**

A few words are devoted here to the method of obtaining the argon system pressure time response. The chamber pressure in the facility is manually stepped by a valve. This operation takes from 5-10 seconds for a final

pressure to be set in the chamber and to be recorded through the monitor tube by the Trans-Sonics differential pressure transducer whose reference side is evacuated. Since the pressure time response of the tube and Alphanon 520 is of the order of minutes, this operation allows presentation of data of pressure time response to a step in pressure at the hot end of the tube. The fact that the system time responses are of the order of minutes comes about through the large (28 cu. in.) volume of the Alphanon 520. The tube lengths are 36 in.

In order to obtain reasonably slow time responses in the closed tube for air with the 718 Alphanon supplementary volume of 498 cc (or 30.4 cu. in.) was added to the tube volume here. Also, to prevent pressure drift after a pressure jump, a large tank of 302 cu. in. was attached to the system so that system pressure would be maintained while air crept in to fill the small bore tube. The data for air were actually plotted on a recorder and later reduced to find the time response at the 63% response value.

## 7.2 Atmospheric Entry Simulation Test

Looking at the two flow terms (in equation (1) of Appendix Part I) for one-quarter inch diameter tubing, the flow term due to temperature is approximately twice the flow term due to time varying atmospheric entry pressure head. This result is independent of the tube length. Under these conditions, if there is no net flow, the pressure head necessary to maintain the temperature flow can be found. Presumably,  $dp$  thus found is the pressure correction to be applied to measurements made through the hot tubing. There is, however, the question of establishing that the gas in the tube is in thermal equilibrium, for Kennard's derivation of the flow equation relies upon an equilibrium condition. That is; eq. 65a, page 49, Kennard, is used to calculate average thermal equilibrium molecular velocity. The agreement of these equations with measurement indicates that the gas in the tube is in thermal equilibrium.

By letting air in and out of the disilicided tantalum tubes with a pump around flow network of valves (see Figure 54), it was possible to linearly simulate atmospheric entry air pressure conditions. At the same time, an appropriate temperature history was run to simulate the entry temperature

at the pressure port. The aim of this rather complicated data production was to verify that steady state values of pressure differentials can be used to correct dynamic pressure histories. The simultaneous temperature and pressure histories are shown in Figures 55 and 56. The corresponding pressure differential in time between the air pressure in the monitor tube and its tube's time response of one second at room temperature and the lagging 0.160" tantalum tube is shown in Figure 57, plotted in Figure 58 (two seconds at 2800°F) or  $\pm 6$  to 12 microns. The sign depends on whether the pressure is ramping up or down. The check of this pressure difference data against the previously measured steady state values for air showed that indeed for pressure rates of the order of  $\pm 6$  microns/sec. the steady state corrections are accurate.

By way of illustration, the largest pressure differential occurs at the lowest pressure, highest temperature condition at thirteen minutes. The steady state value at 1800°F, 0.350 torr is 0.037 torr of pressure differential. If the values 0.056 torr and 0.0217 torr are averaged to remove the system time lag on the change from increasing to decreasing pressure, there results 0.039 torr. The data are within two microns of steady state prediction, substantiating the equilibrium statement in the first paragraph.

The valve network shown in Figure 54 allows air-in-rate and air-out-rate to be set independently too, without the pump-around feature there would be an in-leak during pump down cycles. With only on-off valves, a linearly (fixed needle valve sitting) simulated atmospheric entry curve of pressure can be followed. The needle valves face the tubular volume to isolate it from air shocks caused by the on-off valves' reversal for pressure rate reversals.

8.0 Summary

8.1 System Design and Criteria

Without attempting to discuss here the mounting of tubing to survive vibration environment in a vehicle, but confining ourselves to the measurement of pressure, there are enough materials data to describe how to build a low pressure air measurement system for minimum pressure error. Additionally, the temperature induced pressure differentials have been determined so that correction can be made where needed.



**8.1.1 Material**

Reviewing the tube material data, one cannot recommend titanium for any hot pressure application. Even at 1000°F there is obvious evidence of gettering. But to 1000°F 321 stainless steel is quite resistant to air absorption. Tantalum is adequate to 2000°F. Above this temperature, platinum-10-rhodium or disilicided tantalum are least prone to oxidize. Above the melting point of platinum-10-rhodium, 3350°F, Iridium can be considered as tubing material; however, there is here no data for its oxidation resistance above 2800°F. There is some weight advantage in using tantalum over platinum; if weight is a factor, columbium (FS-80) is lighter though 2-1/2 times less oxidation resistant than tantalum. Columbium was not tested. While there seems little advantage in going to the refractory metals if platinum will suffice, there are many pitfalls in the use of platinum, some of which have been related.

**8.1.2 Diameter**

Diameter of tubing is the only available parameter with which one can adjust a system to collect uncorrected pressure, or with which to compensate for a heavy tube material. If pressure corrections must be made, then weight can be saved by reducing diameter of tubing and accepting a larger pressure correction. Tube wall thicknesses for this work have been 10-15 mils.

**8.1.3 Length**

Tubing length is, of course, pretty well fixed by vehicular design. In general, because time response depends upon tube length both directly and through the tube volume, the length of tube run should be minimized. Obviously, minimum length gives minimum weight.

**8.1.4 Volume**

The transducer volume is the remaining parameter free to adjust. For fast time response, it should be minimized. Hot pressure systems have as much or more volume in the tubing as in the transducer so that time response gains to be realized this way are limited. The effect of temperature upon time response has been seen to be severe. Temperature affects time response through air viscosity dependency directly and to the extent slip flow is present since the slip coefficient is temperature dependent.

8.1.5 Joints

At and near room temperature, with reasonable precautions, nylon taped standard threaded joints can be leak free relative to 50 microns. All high temperature joints have been brazed or welded in this work as indicated. The making of a leak free screw joint to operate at high temperatures is a question of picking the inside tubing material to have the greater coefficient of thermal expansion. Preventing chemical reaction and/or oxidation at the thread interface would seem to vitiate any advantage in threaded joints.

8.1.6 Port

There is the consideration that where large tube openings bear against hot boundary layers, a stagnation region can form causing extreme local heating and flow distortion. A holed cap can be welded to the tube end. A hole in a cap should be of reasonable dimension - a tenth of an inch diameter. As long as the system time response is viscosity limited, a cap is not considered to cause any degradation of time response.

8.2 Use of Data to Correct Pressure Reading

With eq. (16) of part I of the appendix, it is possible to accurately correct quasi-steady state air pressure reading in a tube subject to temperature gradient. In the quasi-steady state condition, only the transducer temperature  $T_0$  and the tube hot end temperature  $T$  must be known in addition to the transducer pressure  $p(0)$  to calculate from air data the pressure at the hot end of the tube  $p(l)$ . Pressure correction under these conditions is independent of the form of the temperature distribution along the tube.

For the sake of convenience, these corrections can be obtained for air pressure from Figure 49, as follows:

1. The value of  $\Delta p$  is estimated from the transducer pressure,  $p$ .
2. Compute average pressure,  $p_a$ , from transducer pressure,  $p$ , and estimated  $\Delta p$ .
3. "Average" mean free path,  $\lambda$ , is found from  $p_a$  at room temperature (300°K). (This is tabulated in "US Standard Atmosphere, 1962" 13).
4. "Average" Knudsen number,  $K_n$ , is found by multiplying "average" mean free path by the ratio of hot end temp,  $T$ , to room temperature,  $T_0$ , and dividing by the tube radius,  $a$ .
5. From Fig. 49 the factor  $\frac{\Delta p/p_a}{\Delta T/T_0}$  is found from the graph by going from the Knudsen number  $K_n$ , to the appropriate temperature curve.
6. Since  $\Delta T$  and  $T_0$  are determined by the tube end temperatures and  $p_a$  has been picked, the pressure differences can now be determined.

USE FOR TYPEWRITTEN MATERIAL ONLY

A check of the end pressure then determines how good a value of  $p_a$  was used with Figure 49. If the new value of  $\Delta p$  is quite different from the old, the process is iterated until repeated values of  $\Delta p$  are constant.

Now the pressure correction for two cases is worked out as explained above. The first case is at 2800°F, 2 torr. The second case occurs at 2000°F, 0.4 torr. The transducer is taken at 300°K (room temperature) for the calculations. The value of tube radius is 0.080 inch. The value of pressure correction  $\Delta p$  is assumed. The value of  $\Delta p$  is positive since the pressure at the transducer is reduced from the pressure of the hot end of the tube due to viscous flow.

Case	$p$ (torr)	Assumed $p$ (torr)	Estimated $p_a$ (torr)	$T_o - ^\circ K$ ( $T_o - ^\circ F$ )	$\frac{T}{T_a}$	$\lambda$ (in)(Room Temp) 300°K)
1	2.00	0.80	2.04	1805 (2800)	1.52	$0.94 \times 10^{-3}$
2	0.40	0.04	0.42	1360 (2000)	1.28	$4.5 \times 10^{-3}$

$\frac{T}{T_o}$	$K_n$	$\frac{\Delta p/p_a}{\Delta T/T_a}$	Resulting $p$	Oxidation/ Adsorption Error (torr)	Corrected $p$
6.0	.07	0.008	.025	0.2	2.225
4.5	.25	0.080	.043	0	0.443

First, the average tube pressure in case 1 was fair enough because the factor of 3 error in the choice of  $\Delta p$  produces less than two percent error in average pressure,  $p_a$ , and in turn in "average" Knudsen number. In case 2, the assumed value of  $\Delta p$  turned out to be close to the calculated value of  $\Delta p$ . Now look at the resulting pressure corrections. The higher temperature 2800°F, higher pressure 2.0 torr, case gives a pressure correction of only 1.2 percent while the lower temperature 2000°F, lower pressure 0.40 torr, case has a correction of 11 percent.

Now separately, the error due to oxidation/adsorption of air must be estimated from the appropriate material-pressure curve. Presumably, this pressure value is not great, but some care is required in noticing that the curves represent the pressure change in air for a given area of material at temperature. Twice the area will have twice the pressure error under the same conditions. Too, if the pressure error is significant under these conditions, it is time dependent, and time at temperature must be known for pressure correction. It is obviously an advantage to design around the oxidation/adsorption problem.

By way of example, consider the 0.160" inside diameter tantalum tubing used in this work. For heating to 2800°F, the end of the tube is disilicided. The disilicide extended to the elbow joint some eight inches from the furnace center (see Figure 53 ). The temperature at the joint was found to be less than 2000°F. Inspection of the oxidation/adsorption data for disilicided tantalum (Figures 21-23) to 2800°F and for tantalum (Figures 12-13 ) to 2000°F shows that only disilicided tantalum at 3 torr and 2800°F contributed any oxidation/adsorption pressure error. Now from Figures 55 and 56 where the temperature-pressure history is shown, it can be seen that the total time above 2500°F is two minutes at a pressure where the tubular pressure correction is not serious. From Figure 21 the oxidation/adsorption error is 0.2 torr for 3.6 torr; about a five percent negative error, a value assumed to hold at 2.0 torr also.

The net result is that the higher temperature case which has the 5 percent oxidation/adsorption error has additionally only a 1 percent pressure correction. The uncorrected lower temperature case requires an 11 percent pressure correction.

Assigning to the alphasatron 718 data between 78°F and 81°F ± 3 percent of absolute pressure error, the system error for the corrected data here is maximum at the 2800°F point, due to oxidation/adsorption. It is then for the system the root sum square of -5% and -1% and ± 3%, giving ± 6% of reading for the 0.160 inch disilicided tantalum tube. Uncorrected for the lower pressure case, the system error is the root sum square of ± 0% and ± 3%, giving ± 12% of reading.

9.0 Conclusion

It is feasible to measure low pressure air in the range 1-100 p.s.f.a. with an accuracy better than ± 6% of reading throughout the range if pressure corrections based on temperature are used. If temperature is unknown, the accuracy at 1 p.s.f.a. can be no better than + 4, - 12% of reading in a 0.160" inside diameter tube.

This accuracy value increases as pressure increases to + 4, - 6 % of reading at 3 p.s.f.a. where temperature induced pressure effects become almost negligible.

Since this pressure discrepancy is inversely proportional to square of the tube diameter, a factor of two increase in tube diameter to 0.320" improves accuracy to + 4, - 5% of reading at 1 p.s.f.a.

The system time response of 3 feet of 0.160" inside diameter tubing is of the order of a second with the Alphasatron 718. Hence, at pressure rate changes of 5 u/second the system time lag is of little significance above 1 p.s.f.a.

## REFERENCES

1. Patterson, G. N., "Molecular Flow of Gases", 1956, John Wiley & Sons, New York.
2. Howard, W. M., "The Effect of Temperature on Pressure Measured In a Hypersonic Wind Tunnel", *Journal Aero/Space Science*, November 1959, p. 764.
3. Computer Instruments Corporation, Form No. 262.
4. Trans-sonics, Inc., Specification No. 11743 F.
5. "Evaluation of Trans-Sonics Type 120 Equibar Pressure Meter", The Boeing Company, 2-5435-7725, Seattle, Washington.
6. Loeb, L. B., "The Kinetic Theory of Gases", 1961, Dover Pub. Inc., New York.
7. Kennard, E. H., "Kinetic Theory of Gases", 1938, McGraw Hill Book Co., Inc., New York.
8. Skreekanth, A. K., "Review of Progress in B.S.R.L. for last Six Months of 1963", p. 14, February 15, 1964.
9. Sinclair, A. R. and Robins, A. W., N.A.C.A. TN2793, "A Method for the Determination of the Time Lag in Pressure Measuring Systems Incorporating Capillaries".
10. Guggenheim, E. A., "Elements of the Kinetic Theory of Gases", p. 45, Pergamon Press, 1960.
11. "Thermophysical and Transport Properties of Air in Dissociation and Ionization Equilibrium", D2-5129, The Boeing Company, Seattle, Washington.
12. Fay, R. D., "Attenuation of Sound in Tubes", Vol. 12, 1940, pp. 62-67. J.A.S.A.
13. Champion, K. S. W., O'Sullivan, W. J. Jr. and Tewles, Sidney, U. S. Standard Atmosphere 1962, U. S. Govt. Printing Office, Wash., 25, D.C. December 1962.



APPENDIX PART I

STEADY STATE CREEP WITH SLIP A TEMPERATURE FUNCTION; by Kennard  
p. 331, Kinetic Theory of Gases equation (1) is found to be for no net flow:

$$0 = -\frac{\pi}{8} \frac{a^4 p}{R\eta} (1 + 4 \frac{\delta}{a}) \frac{dp}{dx} + \frac{3\pi}{4} \frac{\eta}{T} \frac{dT}{dx} a^2 \quad (1)$$

or

$$pdp = \frac{2R}{a^2} (3\eta^2 dT) / (1 + 4 \delta/a) \quad (2)$$

Now assume  $\eta = K\eta_0 T^n$  for viscosity where K and n are determined by curve fit. (3)

$$\delta = \sqrt{\pi r/2} \left( \frac{2-f}{f} \right) \frac{\eta}{p} \sqrt{RT} \text{ for slip coef.} \quad (4)$$

and f is defined later.

then

$$pdp = \frac{2R}{a^2} (3K^2 \eta_0^2 T^{2n}) dT / (1 + \lambda T^{n+1/2}) \quad (5)$$

where  $\lambda = \frac{4}{a} \sqrt{\pi r/2} \left( \frac{2-f}{f} \right) K \eta_0 \frac{\sqrt{R}}{p}$  (6)

to integrate eq. (5)

lets  $y = 1 + \lambda T^{n+1/2}$  (7)

then:  $y - 1 = \lambda T^{n+1/2}$  and  $T = \left( \frac{y-1}{\lambda} \right)^{\frac{1}{n+1/2}}$  (8)

therefore:  $T^{2n} = \left( \frac{y-1}{\lambda} \right)^{2n/(n+1/2)}$  (9)

also:  $dT = \frac{1}{n+1/2} \left( \frac{1}{\lambda} \right)^{\frac{1}{n+1/2}} \cdot (y-1)^{\frac{1}{n+1/2}-1} dy$  (10)

$$= \frac{1}{n+1/2} \left( \frac{1}{\lambda} \right)^{\frac{1}{n+1/2}} \cdot (y-1)^{\frac{(1/2-n)(n+1/2)}{n+1/2}} dy \quad (11)$$

finally:  $\int_{T_0}^T \frac{T^{2n} dT}{1 + \lambda T^{n+1/2}} = \frac{1}{n+1/2} \cdot \left( \frac{1}{\lambda} \right)^{\frac{1}{n+1/2}} \cdot \left( \frac{1}{\lambda} \right)^{\frac{2n}{n+1/2}} \cdot \int \frac{1}{y} \cdot (y-1)^{\frac{(1/2-n)(n+1/2)}{n+1/2}} \cdot (y-1)^{\frac{2n}{n+1/2}} \cdot dy$  (12)

$$\int_{T_0}^T \frac{T^{2n} dT}{1 + \lambda T^{n+1/2}} = \frac{1}{n+1/2} \left(\frac{1}{\lambda}\right)^{\frac{2n+1}{n+1/2}} \int \frac{y-1}{y} dy \quad (13)$$

$$= \frac{1}{n+1/2} \left(\frac{1}{\lambda}\right)^2 [y - \ln y] \quad (14)$$

and substituting for y:

$$\int_{T_0}^T \frac{T^{2n} dT}{1 + \lambda T^{n+1/2}} = \frac{1}{n+1/2} \left(\frac{1}{\lambda}\right)^2 \left[ (1 + \lambda T^{n+1/2}) - \ln(1 + \lambda T^{n+1/2}) \right]_{T_0}^T \quad (15)$$

so that the integral of eq. (5) is:

$$p^2 (l) = p^2 (e) + \frac{4R}{a^2} (3 K^2 \eta_0^2) \frac{1}{n+1/2} \left(\frac{1}{\lambda}\right)^2 \left[ (1 + \lambda T^{n+1/2}) - \ln(1 + \lambda T^{n+1/2}) \right]_{T_0}^T \quad (16)$$

where  $\lambda = \frac{2-f}{f} \frac{4}{a} \sqrt{\frac{\pi}{2}} K \eta_0 \frac{\sqrt{R}}{p}$

by Maxwell  $f$  = transfer ratio of momentum

$f = 1$  molecules are reflected diffusely

$f \geq 1$  molecules are reflected backward

$f \leq 1$  molecules are reflected forward

or  $f$ , fraction, are reflected diffusely and  $1-f$  specularly.

**APPENDIX PART II  
TIME RESPONSE EQUATION**

Modifying the NACA TN 2793<sup>8</sup> time response equation for slip flow results in:

$$\tau = \frac{8 \eta l}{\pi r^4 p_f} \cdot \frac{1}{(1 + 4 \delta/a)} \cdot (V + \frac{V_T}{2}) \ln \frac{(p_0 - p_1)(p + p_1)}{(p_0 + p_1)(p - p_1)} \quad (1)$$

where  $\delta = \sqrt{\pi/2} \left(\frac{2-f}{f}\right) \frac{\eta}{p} \sqrt{RT}$  (2)

and we define  $\lambda = \frac{4}{a} \sqrt{\pi/2} \left(\frac{2-f}{f}\right) K \eta p \sqrt{\frac{R}{p}}$  (3)

let also  $B = \frac{8}{\pi r^4 p_f} (V + \frac{V_T}{2}) \ln \frac{(P_0 - P_1)(P + P_1)}{(P_0 + P_1)(P - P_1)}$  (4)

then  $\tau = B \int \frac{\eta dl}{1 + 4 \delta/a}$  where viscosity (5)

and slip are temperature functions and temperature varies with length.

Let there be a linear temperature distribution:

$$T = c l + T_0 \quad \text{so} \quad dT = c dl \quad (6)$$

and assume  $\eta = K \eta_0 T^n$  (6a)

then  $\tau = \frac{B K \eta_0}{c} \int_{T_0}^T \frac{T^n \cdot dT}{1 + \lambda T^{n+1/2}}$  (7)

In order to integrate set (8)

$$y = 1 + \lambda T^{n+1/2}$$

so  $y-1 = \lambda T^{n+1/2}$  and  $T = \left(\frac{y-1}{\lambda}\right)^{\frac{1}{n+1/2}}$  (9)

therefore  $T^n = \left(\frac{y-1}{\lambda}\right)^{n(n+1/2)}$  (10)



# Contrails

also 
$$d T = \frac{1}{n+1/2} \left(\frac{1}{\lambda}\right) \frac{1}{n+1/2} \cdot (Y-1) \frac{1}{n+1/2} = 1 \quad (11)$$

$$= \frac{1}{n+1/2} \left(\frac{1}{\lambda}\right) \frac{1}{n+1/2} (Y-1)^{1/2-n/n+1/2} dy \quad (12)$$

finally substituting Eqs. (8), (10) and (12) into Eq. (17)

$$\frac{\tau_a}{B K \tau_o} = \int_{T_o}^T \frac{T^n d T}{1 + \lambda T^{n+1/2}} = \frac{1}{n+1/2} \int \left(\frac{1}{\lambda}\right) \frac{1}{n+1/2} (1/2-n/n+1/2) (y-1)^{n/n+1/2} \cdot \left(\frac{1}{\lambda}\right) \frac{n/n+1/2}{y} dy \quad (13)$$

$$= \frac{1}{n+1/2} \left(\frac{1}{\lambda}\right) \frac{(n+1)/(n+1/2)}{y} \int (y-1)^{1/2/n+1/2} dy \quad (14)$$

expanding the numerator inside the integral results in

$$(y-1)^{1/2/(n+1/2)} = (y-1)^{\frac{1}{2n+1}} = y - \left(\frac{1}{2n+1}\right) y^{\frac{1}{2n+1}-2} + \left(\frac{1}{2n+1}\right) \left(\frac{1}{2n+1}-1\right) \frac{1}{2!} y^{\frac{1}{2n+1}-2} \quad (15)$$

then

$$\frac{(y-1)^{1/2n+1}}{y} = y - \frac{1}{(2n+1)} y^{\frac{1}{2n+1}-2} + \left(\frac{1}{2n+1}\right) \left(\frac{1}{2n+1}-1\right) \frac{1}{2!} y^{\frac{1}{2n+1}-3} \quad (16)$$

and

$$\int \frac{(y-1)^{1/2n+1}}{y} dy = (2n+1) y^{\frac{1}{2n+1}-1} - \frac{1}{2n+1} y^{\left(\frac{1}{2n+1}-1\right)} + \frac{1}{2} \frac{1}{2n+1} \left(\frac{1}{2n+1}-1\right) \left(\frac{1}{2n+1}-2\right) y^{\left(\frac{1}{2n+1}-2\right)} \dots \quad (17)$$

# Contrails

now 
$$\frac{1}{\frac{1}{2n+1} - 1} \cdot \frac{1}{2n+1} = \frac{1}{-2n} \quad (18)$$

and 
$$\left( \frac{1}{\frac{1}{2n+1} - 2} \right) = \frac{2n+1}{-4n-1} \quad (18a)$$

so 
$$\int \frac{(y-1)^{1/2n+1}}{y} dy = (2n+1) y^{\frac{1}{2n+1}} + 2ny^{-\frac{2n}{2n+1}} + \frac{1}{4n} \frac{2n+1}{4n+1} y^{-\frac{4n+1}{2n+1}} + \dots \quad (19)$$

and finishing the derivation:

$$\int_{T_0}^T \frac{T^n dT}{1 + \lambda T^{n+1/2}} \cong \frac{1}{n+1/2} \left( \frac{1}{\lambda} \right)^{1/(n+1/2)} \left[ (2n+1) y^{\frac{1}{2n+1}} + 2ny^{-\frac{2n}{2n+1}} + \frac{1}{4n} \frac{2n+1}{4n+1} y^{-\frac{4n+1}{2n+1}} \right]_{T_0}^T \quad (20)$$

In which  $y = 1 + \lambda T^{n+1/2}$

Substitution of eqs. (20) and (4) into eq. (7) yields the time response integrated over a linear temperature (steady state) distribution.

**EVALUATION OF DECKER LOW GAS PRESSURE TRANSDUCER VS. TEMPERATURE**

**AMBIENT TEMPERATURE: 140°F**

**TRANSDUCER TEMPERATURE: 145°F**

Not readable at 160°F -- erratic output

Calibration Number 1			Calibration Number 2		Calibration Number 3	
Trans-Sonics Type 120 Pressure MM Hg	Wiancko (1) Frequency 522B HP Counter CPS	Decker (2) Transducer Output Volts	Wiancko CPS	Decker Volts	Wiancko CPS	Decker Volts
.035	40004	-1.371	40006	-1.449	40006	-1.449
.359	40017	-1.344	40019	-1.428	40019	-1.432
1.000	40042	-1.297	40043	-1.385	40043	-1.393
5.0	40195	-1.048	40196	-1.120	40198	-1.119
10.0	40387	-.743	40389	-.787	40390	-.778
15.0	40580	-.432	40582	-.444	40582	-.429
20.0	40772	-.108	40775	-.085	40775	-.068
25.0	40965	+.208	40967	+.266	40968	+.282
30.0	41158	.514	41159	+.608	41160	+.618
35.0	41351	.821	41350	.949	41350	.942
40.0	41545	1.140	41544	1.303	41545	1.295
45.0	41732	1.464	41731	1.663	41732	1.647
40.0			41544	1.302		
35.0	41346	.807	41350	.942	41350	.927
30.0			41159	.604		
25.0	40965	.202	40967	.264	40968	.258
20.0			40775	-.086		
15.0	40578	-.432	40583	-.444	40582	-.444
10.0			40390	-.786		
5.0	40195	-1.028	40197	-1.117	40198	-1.113
1.000			40044	-1.383	40043	-1.379
.359			40019	-1.426	40019	-1.420
.035	40004	-1.319	40006	-1.449	40005	-1.440

**ZERO SHIFT OF DECKER OUTPUT-VOLTS**

Trans-Sonics Pressure MM Hg	45°F	100°F	145°F
.011	-.739	-.910	-1.432

Stabilized temperature and output volts

Thermocouple attached to Decker Housing inside case, all temperatures.

NOTES: (1) See 45°F data for Wiancko Reading  
(2) Thermal creep is ±0.95% to 70°F as Decker Transducer tube correction.

TABLE 1

**EVALUATION OF DECKER LOW GAS PRESSURE TRANSDUCER VS. TEMPERATURE**

AMBIENT TEMPERATURE: 80°F

TRANSDUCER TEMPERATURE: 100°F

START 10:30 A.M.

STOP 4:15 P.M.

TRANSONICS ZERO DRIFT + .009 MM

	Calibration Number 1		Calibration Number 2		Calibration Number 3	
	Trans-Sonics Type 120 Pressure MM Hg	Wiancko (1) Frequency 522B HP Counter CPS	Decker (2) Transducer Output Volts	Wiancko CPS	Decker Volts	Wiancko CPS
.035	40005	-.530	40005	-.624	40005	-.682
.359	40017	-.495	40017	-.585	40017	-.640
1.000	40043	-.418	40042	-.506	40041	-.562
5.0	40197	+.068	40195	-.006	40195	-.062
10.0	40388	+.727	40387	+.654	40387	+.597
15.0	40579	1.387	40579	+1.314	40581	+1.264
20.0	40771	2.021	40772	1.956	40773	1.904
25.0	40964	2.614	40964	2.588	40966	2.527
30.0	41157	3.238	41157	3.195	41158	3.148
35.0	41348	3.872	41349	3.822	41348	3.781
40.0	41545	4.557	41544	4.499	41545	4.462
45.0	41732	5.254	41732	5.200	41732	5.145*
40.0	41545	4.549			41545	4.451
35.0	41345	3.842			41348	3.770
30.0	41155	3.206	41158	3.177	41158	3.135
25.0	40962	2.581			40966	2.507
20.0	40772	1.957			40773	1.888
15.0	40579	1.315			40582	1.254
10.0	40386	+.651	40389	+.621		*
5.0	40196	-.006			40197	-.070
1.0	40041	-.497			40043	-.566
.359	40016	-.572			40018	-.641
.035	40003	-.611	40004	-.648	40005	-.680

- NOTES: (1) See 45°F data (Fig. 2 ) for Wiancko reading.  
 (2) Thermal Transpiration is +0.10% to 70°F as Decker correction.  
 (\*) Transonics out between these points -- malfunction.

TABLE 2

EVALUATION OF DECKER LOW GAS PRESSURE TRANSDUCER VS. TEMPERATURE

AMBIENT TEMPERATURE: 39°F

TRANSDUCER TEMPERATURE: 45°F

Trans-Sonics Type 120 Pressure MM Hg	Calibration Number 1		Calibration Number 2		Calibration Number 3	
	Wiancko (1) Frequency 522B HP Counter CPS	Decker (2) Transducer Output Volts	Wiancko CPS	Decker Volts	Wiancko CPS	Decker Volts
.035	40005	-.680	40003	-.752	40004	-.678
.359	40016	-.654	40015	-.727	40016	-.646
1.00	40042	-.600	40040	-.675	40042	-.586
5.00	40195	-.273	40194	-.352	40194	-.227
15.0	40582	+.558	40578	+.459	40579	+.681
20.0	40774	.978	40771	.887	40772	1.145
25.0	40967	1.410	40963	1.365	40967	1.630
30.0	41158	1.859	41155	1.887	41160	2.167
35.0	41348	2.338	41346	2.472	41350	2.754
40.0	41545	2.872	41540	3.064	41543	3.398
45.0	41732	3.451	41730	3.693	41728	4.160
40.0	41545	2.875	41540	3.056		**
35.0			41347	2.415		
30.0	41158	1.849	41157	1.870		
25.0			40965	1.400		
20.0	40774	.965	40773	.973		
15.0	40582	.553	40580	.647		
10.0			40388	.215		
5.0	40195	-.275	40195	-.224		
1.0	40042	-.603	40042	-.576		
.359	40016	-.655	40018	-.623		
.035		-.680	40005	-.645		

NOTES: (1) Wiancko works 0-5 psi between 40,000 and 50,000 therefore 38.7 counts/mm Hg is to be added to 40,000 to obtain Wiancko pressure in mm Hg.  
 (2) System thermal creep is -0.31% at .359 mm to room temperature of 70°F for Decker transducer tube.  
 \*\* CO<sup>2</sup> exhausted; temp. began to rise  
 Trans-Sonics malfunctioned above 25 mm (used Wiancko only above 25 mm No. 1 cal).

TABLE 3

**ALPHATRON 718 CALIBRATION**

8.1 Volts on 5886 Screen

45° F Oven		45° F Tube	
Pressure M.M.Hg.	R.G.I. Inches of Oil	Wiancko Transducer 522B HP Counter	Alphatron Pressure Transducer Type 718 522B HP Counter
0.036	.0228	40,004	3652
0.359	.227	40,014	3724
1.00	.634	40,040	3772
5.00		40,194	3828
10.00		40,387	3853
15.00		40,580	3870
20.00		40,774	3892
25.00		40,967	3922
30.00		41,161	3951
35.00		41,354	3998
40.00		41,548	4043
45.00		41,741	4071
40.00		41,548	4068
35.00		41,354	4061
30.00		41,161	4042
25.00		40,967	4045
20.00		40,774	4078
15.00		40,580	4080
10.00		40,387	4058
5.00		40,194	4022
1.00		40,040	3946
0.359		40,014	3907
0.036		40,004	3897
0.359		40,014	3957
1.00		40,040	3994
5.00		40,194	4083
10.00		40,387	4125
15.00		40,580	4162
20.00		40,774	4215
25.00		40,967	4255
30.00		41,161	4267
35.00		41,354	4278
40.00		41,548	4308
45.00		41,741	4341
40.00		41,548	4343
35.00		41,354	4331
30.00		41,161	4317
25.00		40,967	4290

TABLE 4

**ALPHATRON 718 CALIBRATION**

45° F Oven		8.1 Volts on 5886 Screen 45° F Tube	
Pressure M.M.Hg.	R.G.I. Inches of Oil	Wiancko Transducer 522B HP Counter	Alphatron Pressure Transducer Type 718 522B HP Counter
20.00		40,774	4256
15.00		40,580	4221
10.00		40,387	4179
5.00		40,194	4129
1.00		40,040	4053
.359		40,014	4016
.036		40,004	3980
0.036		40,004	3980
0.359		40,014	4039
1.00		40,040	4072
5.00		40,194	4123
10.00		40,387	4171
15.00		40,580	4236
20.00		40,774	4295
25.00		40,967	4331
30.00		41,161	4371
35.00		41,354	4399
40.00		41,548	4448
45.00		41,741	4474
40.00		41,548	4447
35.00		41,354	4410
30.00		41,161	4376
25.00		40,967	4339
20.00		40,774	4298
15.00		40,580	4260
10.00		40,387	4213
5.00		40,194	4161
1.00		40,040	4082
0.359		40,014	4043
0.036		40,004	4007
0.359		40,014	4045
1.00		40,040	4085
5.00		40,194	4166
10.00		40,387	4217
15.00		40,580	4270
20.00		40,774	4303
25.00		40,967	4349
30.00		41,161	4387

TABLE 4 (Continued)

ALPHATRON 718 CALIBRATION

8.1 Volts on 5886 Screen

45°F Oven

45°F Tube

Pressure M.M. Hg.	R.G.I. Inches of Oil	Wiancko Transducer 522B HP Counter	Alphatron Pressure Transducer Type 718 522B HP Counter
----------------------	----------------------------	---	---

35.00		41,354	4414
40.00		41,548	4446
45.00		41,741	4474
40.00		41,548	4441
35.00		41,354	4408
30.00		41,161	4370
25.00		40,967	4331
20.00		40,774	4292
15.00		40,580	4252
10.00		40,387	4208
5.00		40,194	4153
1.00		40,040	4068
.359		40,014	4027
.036		40,004	3998
0.036		40,004	3986
0.359		40,014	4025
1.00		40,040	4063
5.00		40,194	4140
10.00		40,387	4193
15.00		40,580	4232
20.00		40,774	4274
25.00		40,967	4325
30.00		41,161	4345
35.00		41,354	4372
40.00		41,548	4390
45.00		41,741	4413
40.00		41,548	4375
35.00		41,354	4350
30.00		41,161	4334
25.00		40,967	4293
20.00		40,774	4255
15.00		40,580	4213
10.00		40,387	4164
5.00		40,194	4115
1.00		40,040	4028
0.359		40,014	4003
0.036		40,004	3963

TABLE 4 (Continued)



ALPHATRON 718 CALIBRATION

74° Oven		8.1 Volts on 5886 Screen T. C. 74°	
Pressure M.M. Hg.	R. G. I. Inches of Oil	Wiancko Transducer 522B HP Counter	Alphatron Pressure Transducer Type 718 522B HP Counter
.036	.0228	40,004	2745
.359	.227	40,015	2766
1.00	.634	40,041	2770
5.00		40,193	2824
10.00		40,387	2867
15.00		40,580	2896
20.00		40,774	2935
25.00		40,967	2966
30.00		41,161	2997
35.00		41,354	3026
40.00		41,548	3054
45.00		41,741	3082
40.00		41,548	3051
35.00		41,354	3021
30.00		41,161	2990
25.00		40,967	2959
20.00		40,774	2924
15.00		40,580	2889
10.00		40,387	2853
5.00		40,193	2809
1.00	.634	40,041	2751
.359	.227	40,015	2720
.036	.0228	40,004	2706
.359		40,014	2727
1.00		40,041	2759
5.00		40,193	2811
10.00		40,387	2852
15.00		40,580	2891
20.00		40,771	2934
25.00		40,967	2954
30.00		41,161	2983
35.00		41,354	3013
40.00		41,548	3043
45.00		41,741	3076
40.00		41,548	3043
35.00		41,387	3021
30.00		41,161	2982

TABLE 5

*Contrails*

ALPHATRON 718 CALIBRATION

8.1 Volts on 5886 Screen

74° Oven Pressure M.M.Hg.	R.G.I. Inches of Oil	T. C. 74° Wiancko Transducer 522B HP Counter	Alphatron Pressure Transducer Type 718 522B HP Counter
25.00		40,967	2951
20.00		40,774	2918
15.00		40,580	2891
10.00		40,387	2854
5.00		40,193	2809
1.00		40,041	2752
.359		40,015	2732
.036		40,004	2708

TABLE 5 (Continued)

**ALPHATRON 718 CALIBRATION**

8.1 Volts on 5886 Screen

160°F Oven Pressure M.M.Hg.	R.G.I. Inches of Oil	159°F Tube T/C Wiancko Transducer 522B HP Counter	Alphatron Pressure Transducer Type 718 522B HP Counter
.036	0.0228	40,002	1881
.359	0.227	40,014	1901
1.00	0.634	40,041	1904
5.00		40,194	1914
10.00		40,387	1922
15.00		40,580	1927
20.00		40,774	1932
25.00		40,967	1936
30.00		41,161	1939
35.00		41,354	1941
40.00		41,548	1943
45.00		41,741	1944 1941
40.00		41,548	1938
35.00		41,354	1936
30.00		41,161	1933
25.00		40,967	1929
20.00		40,774	1924
25.00		40,580	1917
10.00		40,387	1911
5.00		40,194	1904
1.00	0.634	40,041	1891
0.359	0.227	40,014	1877
0.036	0.0228	40,003	1845
0.359	.227	40,014	1869
1.00	.634	40,040	1884
5.00		40,194	1998
10.00		40,387	1903
15.00		40,580	1908
20.00		40,774	1914
25.00		40,967	1918
30.00		41,161	1921
35.00		41,354	1923
40.00		41,548	1926
45.00		41,741	1927
40.00		41,548	1925
35.00		41,354	1922
30.00		41,161	1919

TABLE 6

ALPHATRON 718 CALIBRATION

8.1 Volts on 5886 Screen

160°F Oven

159°F Tube T/C

Pressure M.M. Hg	R.G.I. Inches of Oil	Wiancko Transducer 522B HP Counter	Alphatron Pressure Transducer Type 718 522B HP Counter
25.00		40,967	1916
20.00		40,774	1910
15.00		40,580	1905
10.00		40,387	1898
5.00		40,194	1892
1.00		40,041	1879
.359		40,014	1867
0.036	0.0228	40,002	1814
0.359	0.227	40,015	1878
1.00	0.634	40,040	1897
5.00		40,193	1910
10.00		40,387	1917
15.00		40,580	1923
20.00		40,774	1930
25.00		40,967	1935
30.00		41,161	1939
35.00		41,354	1942
40.00		41,548	1945
45.00		41,741	1947
40.00		41,548	1944
35.00		41,354	1941
30.00		41,161	1937
25.00		40,967	1932
20.00		40,774	1926
25.00		40,580	1919
10.00		40,387	1912
5.00		40,194	1904
1.00		40,040	1889
1.00	.634	40,040	1891
.359	.227	40,014	1875
1.000	.634	40,040	1896
5.00		40,194	1902
10.00		40,387	1908
15.00		40,580	1917
20.00		40,774	1922
25.00		40,967	1927
30.00		41,161	1932

TABLE 6 (Continued)

*Contrails*

ALPHATRON 718 CALIBRATION

8.1 Volts on 5886 Screen

160°F Oven

159°F Tube T/C

Pressure M.M. Hg	R. G. I. Inches of Oil	Wiancko Transducer 522B HP Counter	Alphatron Pressure Transducer Type 718 522B HP Counter
35.00		41,354	1936
40.00		41,548	1938
45.00		41,741	1940
40.00		41,578	1938
35.00		41,354	1934
30.00		41,161	1929
25.00		40,968	1924
20.00		40,774	1919
15.00		40,580	1912
10.00		40,387	1905
5.00		40,194	1897
1.00	0.634	40,040	1882
0.359	0.227	40,014	1860
0.036	0.0228	40,003	1824

TABLE 6 (Continued)

REV SYM \_\_\_\_\_

<b>BOEING</b>	NO. D2-81314-1
	SECT.   PAGE 47

ALPHATRON 718 CALIBRATION

8.1 Volts on 5886 Screen

212°F

Pressure M.M. Hg	R.G.I. Inches of Oil	Wiancko Transducer 522B HP Counter	Alphatron Pressure Transducer Type 718 522B HP Counter
0.036	0.0228	40,002	1616
0.359	0.227	40,014	1594
1.00	0.634	40,040	1577
5.00		40,193	1546
10.00		40,387	1532
15.00		40,580	1520
20.00		40,774	1511
25.00		40,967	1503
30.00		41,161	1493
35.00		41,354	1482
40.00		41,548	1469
45.00		41,741	1456 1453
40.00		41,548	1466
35.00		41,354	1477
30.00		41,161	1486
25.00		40,967	1494
20.00		40,774	1502
15.00		40,580	1509
10.00		40,387	1519
5.00		40,194	1533
1.00	.634	40,040	1561
.359	.227	40,014	1577
1.00	.634	40,040	1561
5.00		40,194	1534
10.00		40,387	1519
15.00		40,580	1512
20.00		40,774	1503
25.00		40,967	1493
30.00		41,161	1485
35.00		41,354	1478
40.00		41,548	1462
45.00		41,741	1449
40.00		41,548	1462
35.00		41,354	1472
30.00		41,161	1482
25.00		40,968	1490

TABLE 7



ALPHATRON 718 CALIBRATION

8.1 Volts on 5886 Screen

212°F

Pressure M.M. Hg	R.G.I. Inches of Oil	Wiancko Transducer 522B HP Counter	Alphatron Pressure Transducer Type 718 522B HP Counter
20.00		40,774	1499
15.00		40,580	1507
10.00		40,387	1516
5.00		40,194	1531
1.00		40,040	1558
0.359		40,014	1572
0.036		40,003	1588

TABLE 7 (Continued)

**ALPHATRON PRESSURE TRANSDUCER, TYPE 718  
CALIBRATION AT 120°F.**

Trans-Sonics Alpatron 718

M.M. Hg	Pulses/Sec	Pulses/sec	Pulses/sec	Pulses/sec	Pulses/sec	Pulses/sec
.035	1919	1897	↙			
.359	2011	1989				
1.00	2038	2017	20	19	→	20
5.00	2076	2058	91	90		91
10.00	2094	2078	181	178		180
15.00	2107	2094	270	267		270
20.00	2120	2108	356	352		356
25.00	2131	2120	441	436		441
30.00	2140	2131	523	518		523
35.00	2148	2141	602	598		602
40.00	2158	2153	683	679		683
45.00	2166	↑	756	↑		758

The poor repeatability of the first two cycles with the screen of the 5886 at 8.1 volts can be compared to that of the next three cycles with the screen of the 5886 at 5.1 volts. The trans-sonics diaphragm hysteresis now shows up against the Alpatron 718 count.

TABLE 8

**CALIBRATION OF ALPHATRON 718 PRESSURE TRANSDUCER -  
FULL PRESSURE RANGE  
CALIBRATION AT 78°F**

Trans-Sonics MM Hg	Alphatron Pulses/Sec					
	78°F		80°F		81°F	
.035	MS BP * 745	MS BP 850 →	MS BP 750	MS BP 824 →	MS BP 720	MS BP 832
.359	MS PP 85	MS PP 88	MS PP 87	MS PP 90	MS PP 86	MS PP 90
1.00	31	30	30	29	30	30
5.00	144	142	141	139	141	141
10.00	286	282	279	276	281	280
15.00	428	423	418	414	421	419
20.00	565	560	552	548	556	554
25.00	699	693	683	678	687	686
30.00	831	825	811	808	817	817
35.00	960	954	937	934	945	943
40.00	1090	1087	1066	1064	1073	1073
45.00	1214	↑	1187	↑	1197	↑

Screen Voltage of 5.1 Volts

\* MS BP is milliseconds between pulses

TABLE 9

**CALIBRATION OF ALPHATRON 718 PRESSURE  
TRANSDUCER AT 80°F - to 5 TORR**

Trans-Sonics MM Hg	ALPHATRON	
	Pulses/Sec	Millivolts, D.C.
.359	12	9.00
1.00	30	11.20
2.00	60	21.50
3.00	83	29.30
4.00	111	39.00
5.00	136	47.90
4.00	110	38.80
3.00	83	29.50
2.00	60	21.50
1.00	30	11.10
.359	12	7.00
.359	13	7.00
1.00	30	11.20
2.00	60	21.50
3.00	86	30.50
4.00	120	42.20
5.00	140	49.40
4.00	120	42.20
3.00	86	30.30
2.00	60	21.50
1.00	30	11.10
.359	12	7.00

The calibration was conducted with 5886 filament voltage 1.35 V, plate voltage 5.4 V and screen voltage 5.2 V.

TABLE 10

TRANS-SONICS 120 CALIBRATION DATA AT 78°F

Roger-Gilmont Oil Manometer Inches of Oil	Trans-Sonics M.M. Hg
0	0
.216	.360
.618	1.00
1.232	2.00
1.836	3.00
0	0
.022	.036
.214	.359
.615	1.00
1.228	2.00
1.836	3.00
1.238	2.00
.624	1.00
.216	.359
.025	.036
0	.001
.022	.036
.214	.359
.620	1.00
1.228	2.00
1.839	3.00
1.227	2.00
.620	1.00
.218	.359
.024	.036
0	.0015

TABLE II

TRANS-SONICS 120 CALIBRATION DATA AT 78°F

M.M. Hg	Wiancko Pulses/Sec	Trans-Sonics M.M. Hg
	40000	0
	40039	1.0
	40078	2.0
	40117	3.0
	40155	4.0
	40194	5.0
	40385	10.0
	40577	15.0
	40769	20.0
	40960	25.0
	41151	30.0
	41340	35.0
	41531	40.0
	41717	45
	41920	50
	41717	45
	41531	40
	41340	35
	41152	30
	40960	25
	40768	20
	40577	15
	40385	10
	40193	5
	40155	4
	40117	3
	40078	2
	40040	1
	40002	.0024
	40001	.0014
	40383	10.00
	40767	20.00
	41150	30.00
	41529	40.00
	41916	50.00

TABLE 11 (Continued)



*Contracts*

TRANS-SONICS 120 CALIBRATION SUMMARY FOR 78°F

Roger Gilmont Oil Manometer		Trans-Sonics	Wiancko	
Average Inches of Oil	M.M. Hg	M.M. Hg	Pulses/Sec	M.M. Hg
0.0	0.0	.0006		
0.023	.0364	.036		
0.216	.345	.359		
0.621	.983	1.00	40039	1.01
1.230	1.945	2.00	40078	2.02
1.837	2.90	3.00	40117	3.02
		4.00	40155	4.00
		5.00	40194	5.02
		10.00	40385	9.95
		15.00	40577	14.92
		20.00	40769	19.90
		25.00	40960	24.8
		30.00	41151	29.9
		35.00	41340	34.6
		40.00	41531	39.6
		45.00	41717	44.4

TABLE 12

U3 4288 2000 REV. 3/64

41

REV SYM \_\_\_\_\_

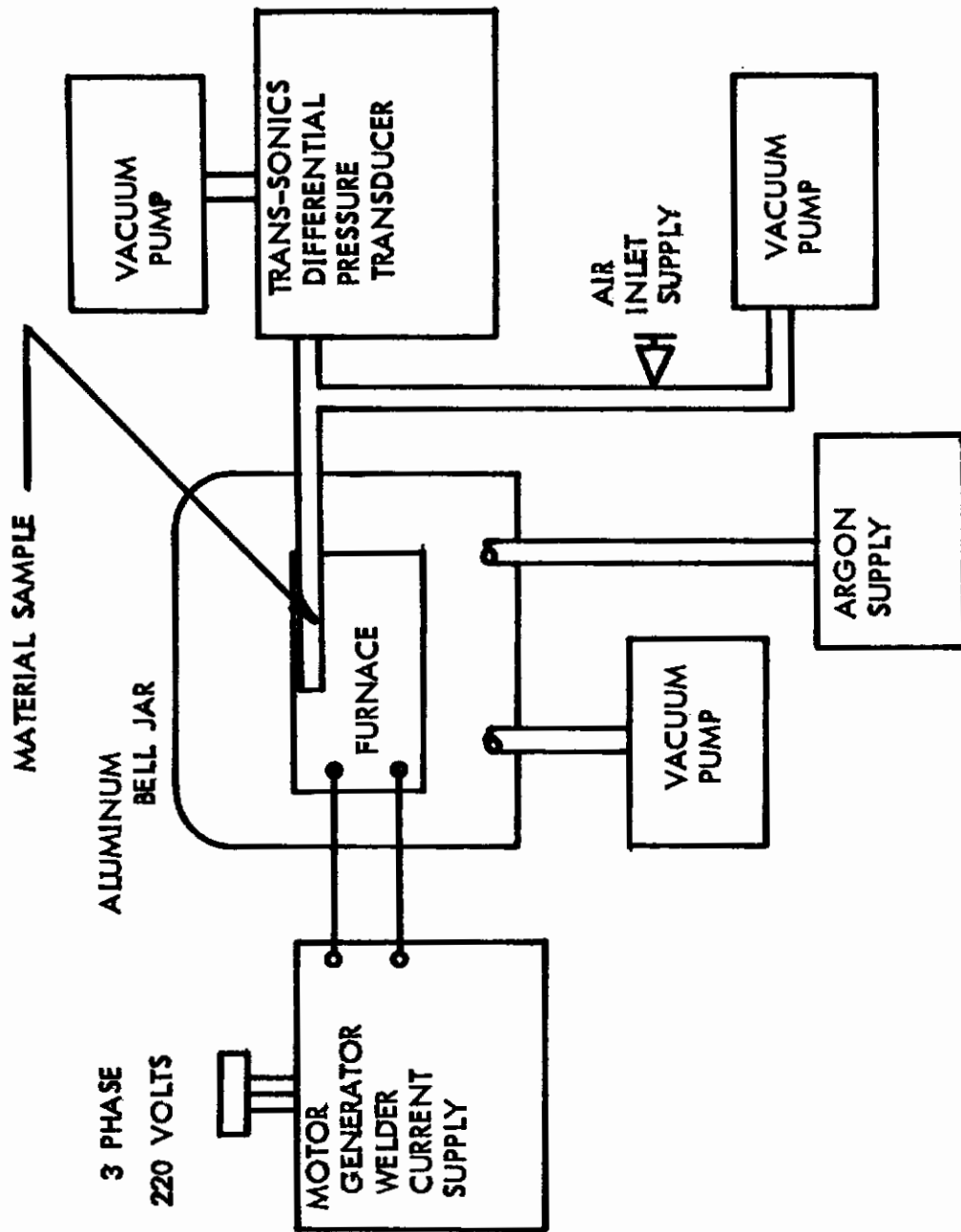
**BOEING**

NO.

D2-81314-1

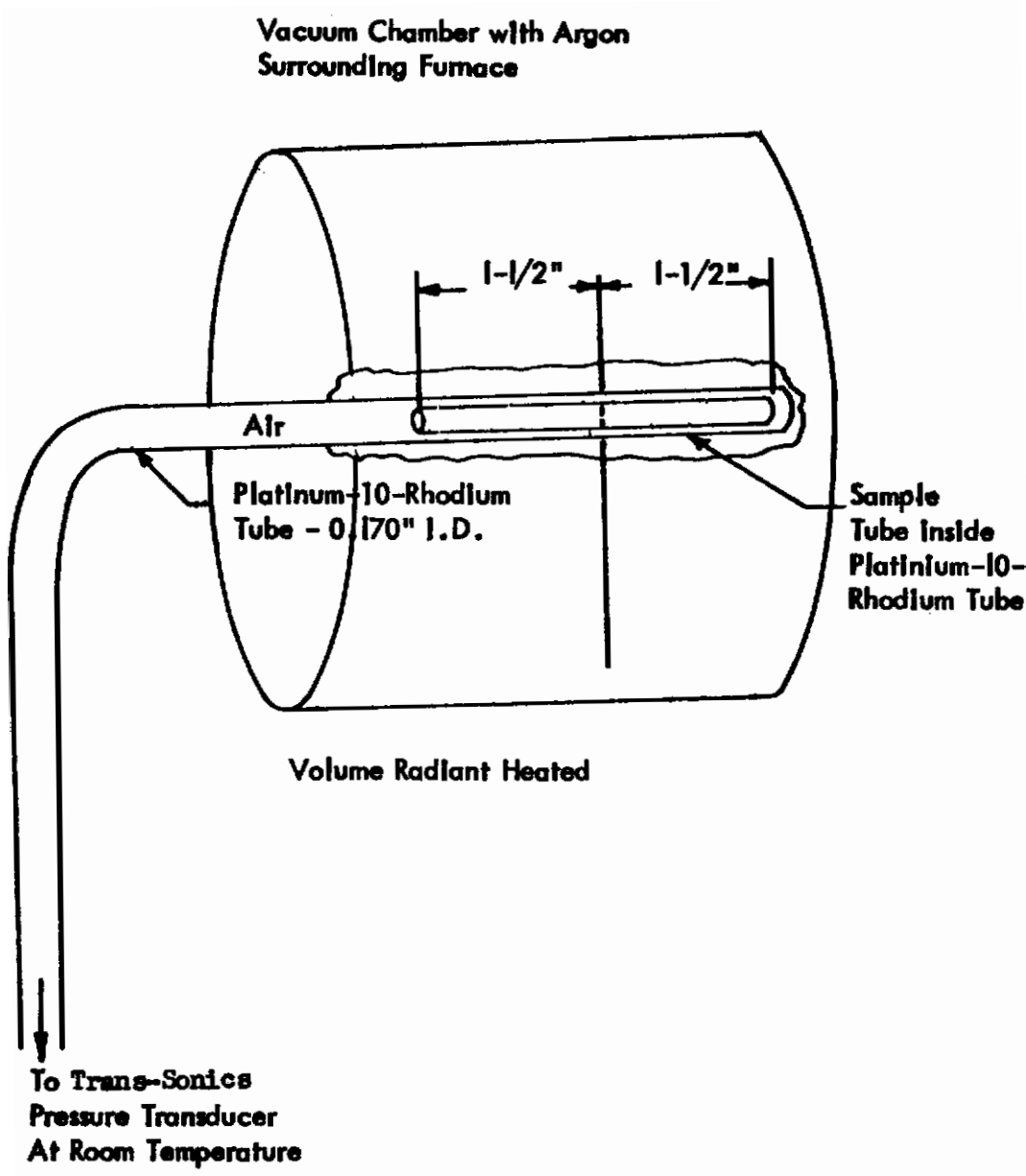
PAGE

55



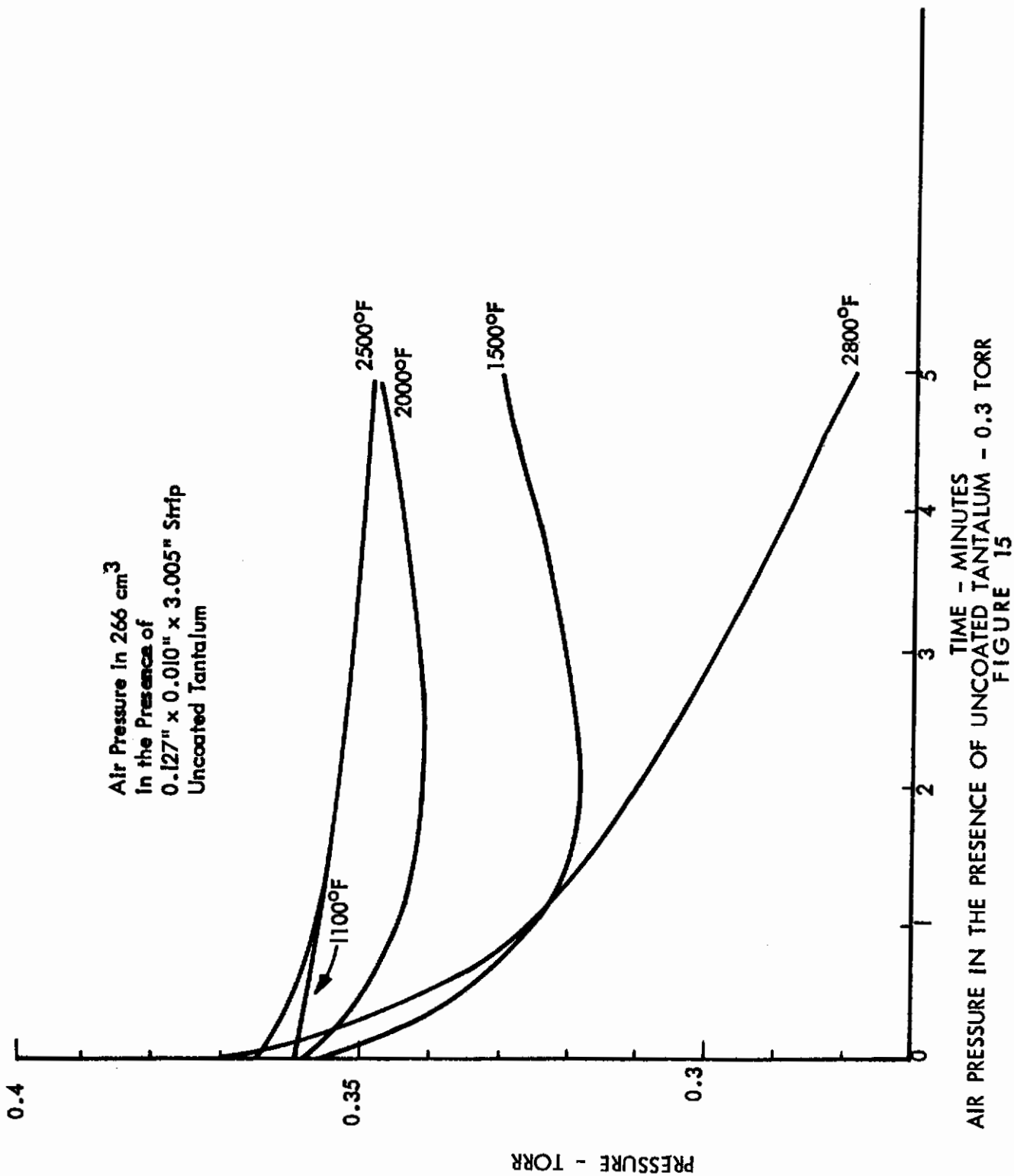
PLATINUM TUBING FACILITY TO MEASURE EFFECT OF AIR PLUS TUBE MATERIAL UPON PRESSURE MEASUREMENT

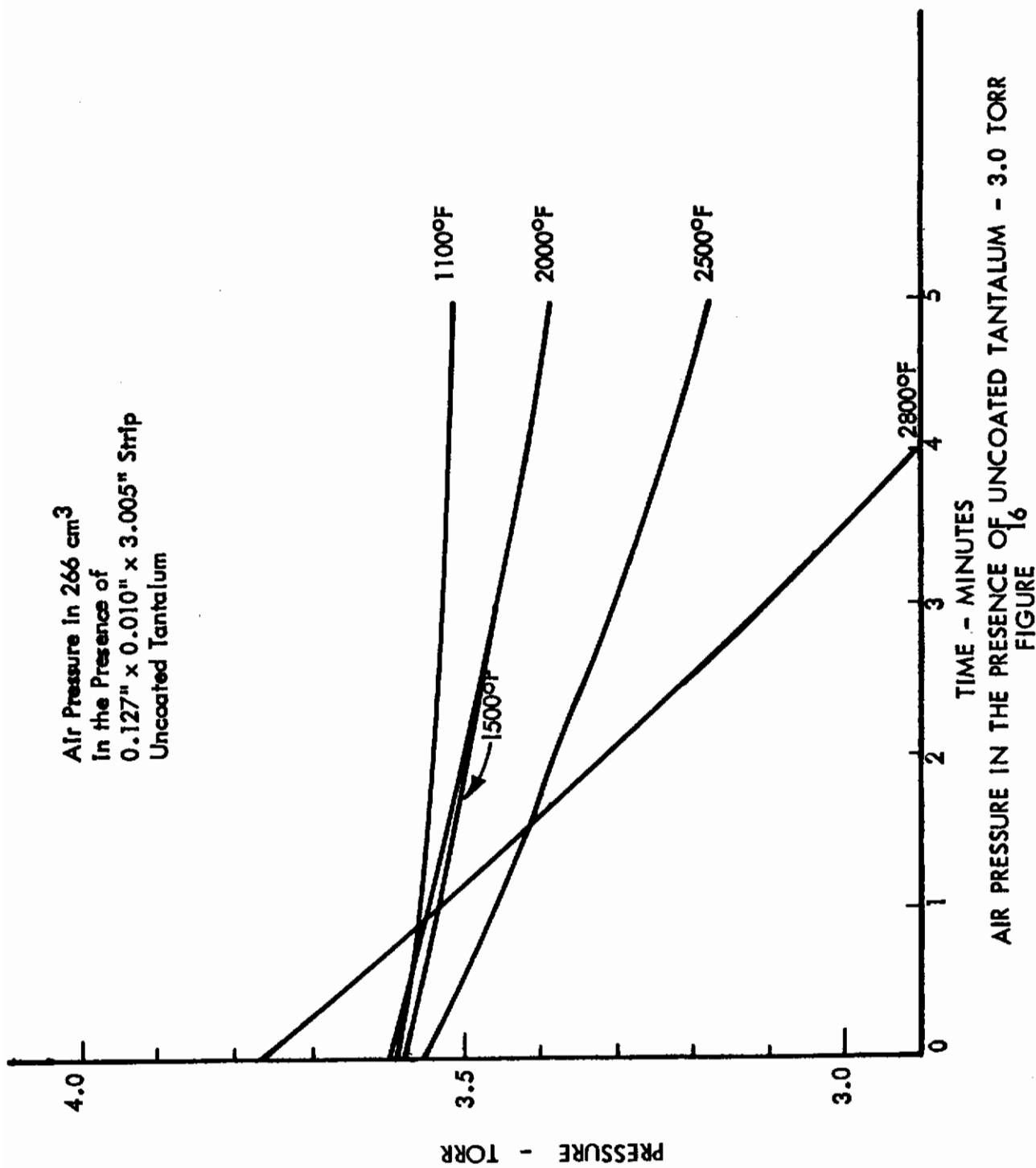
FIGURE 13

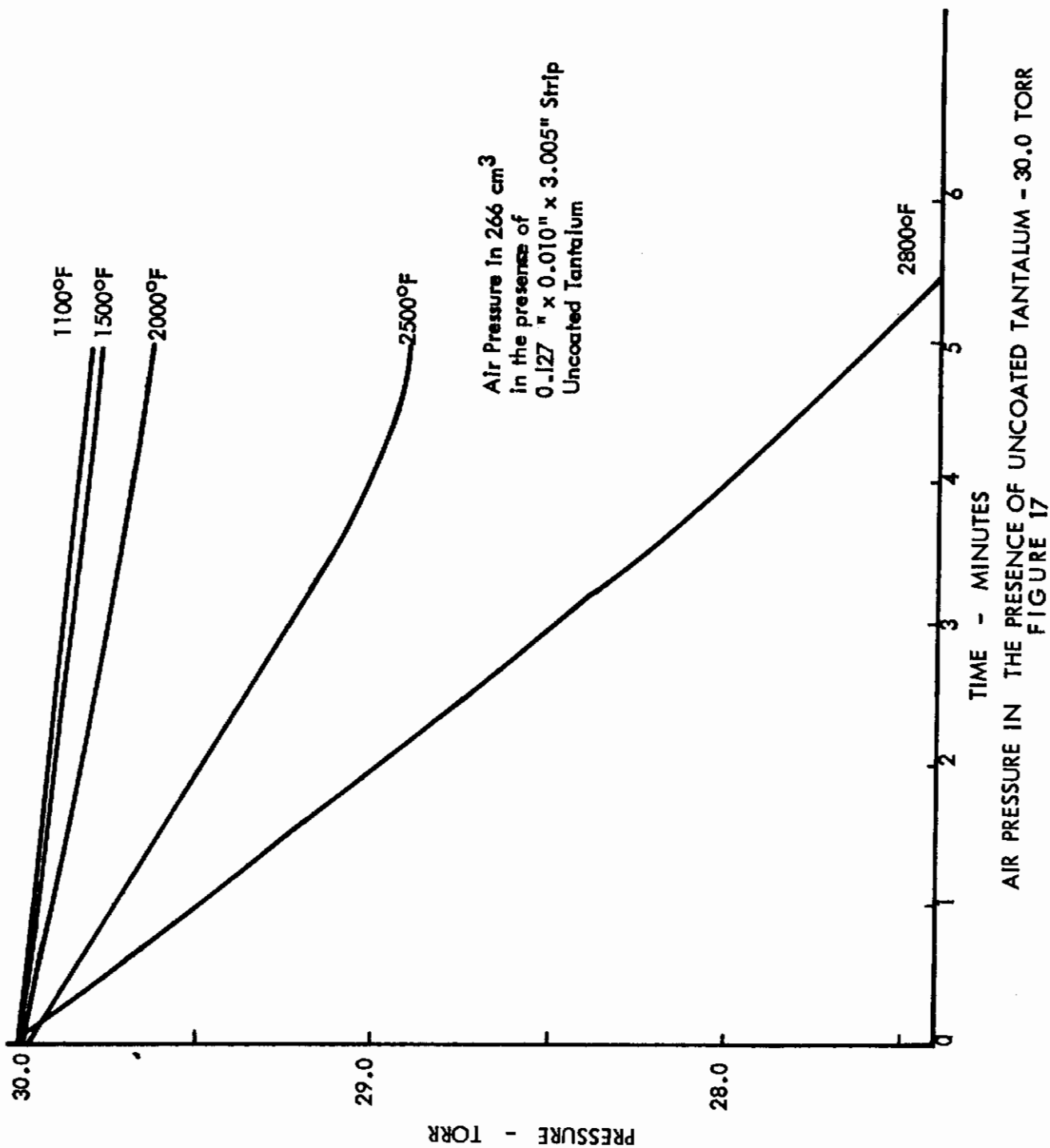


Facility to Measure Effect of Air Plus Tube Material Upon Pressure Measurement:  
1-100 p.s.f., 65-2800°F

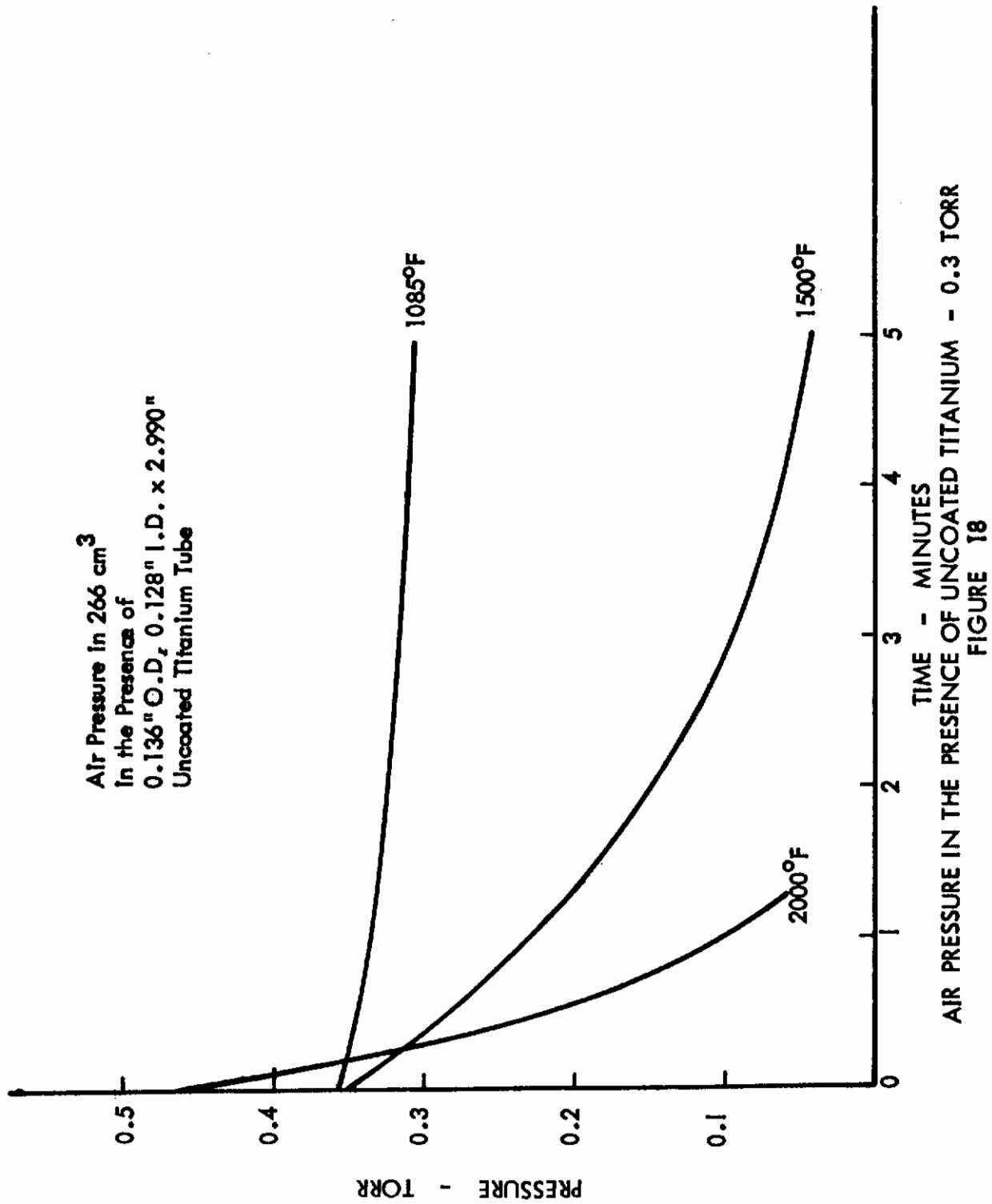
FIGURE 14

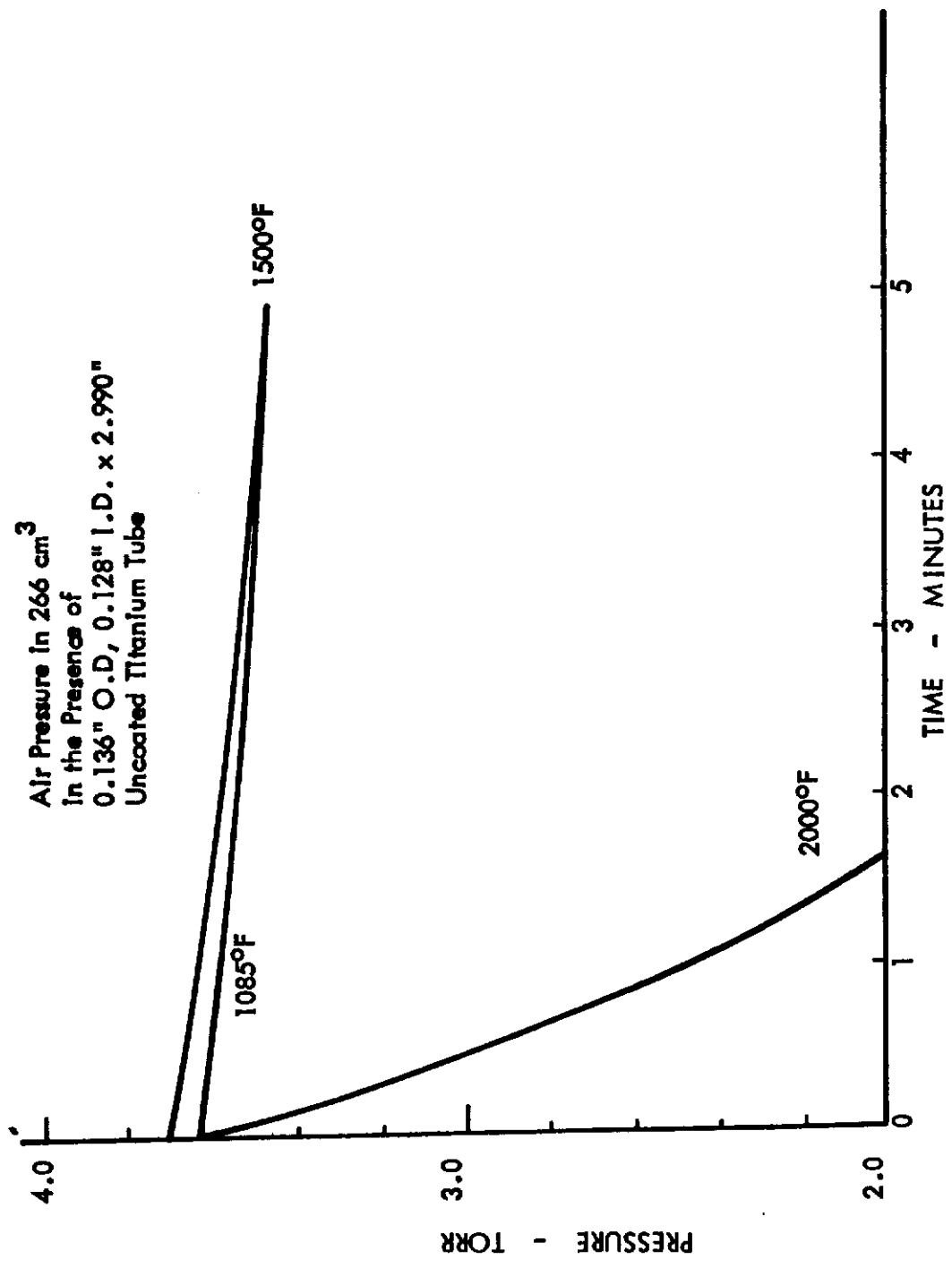




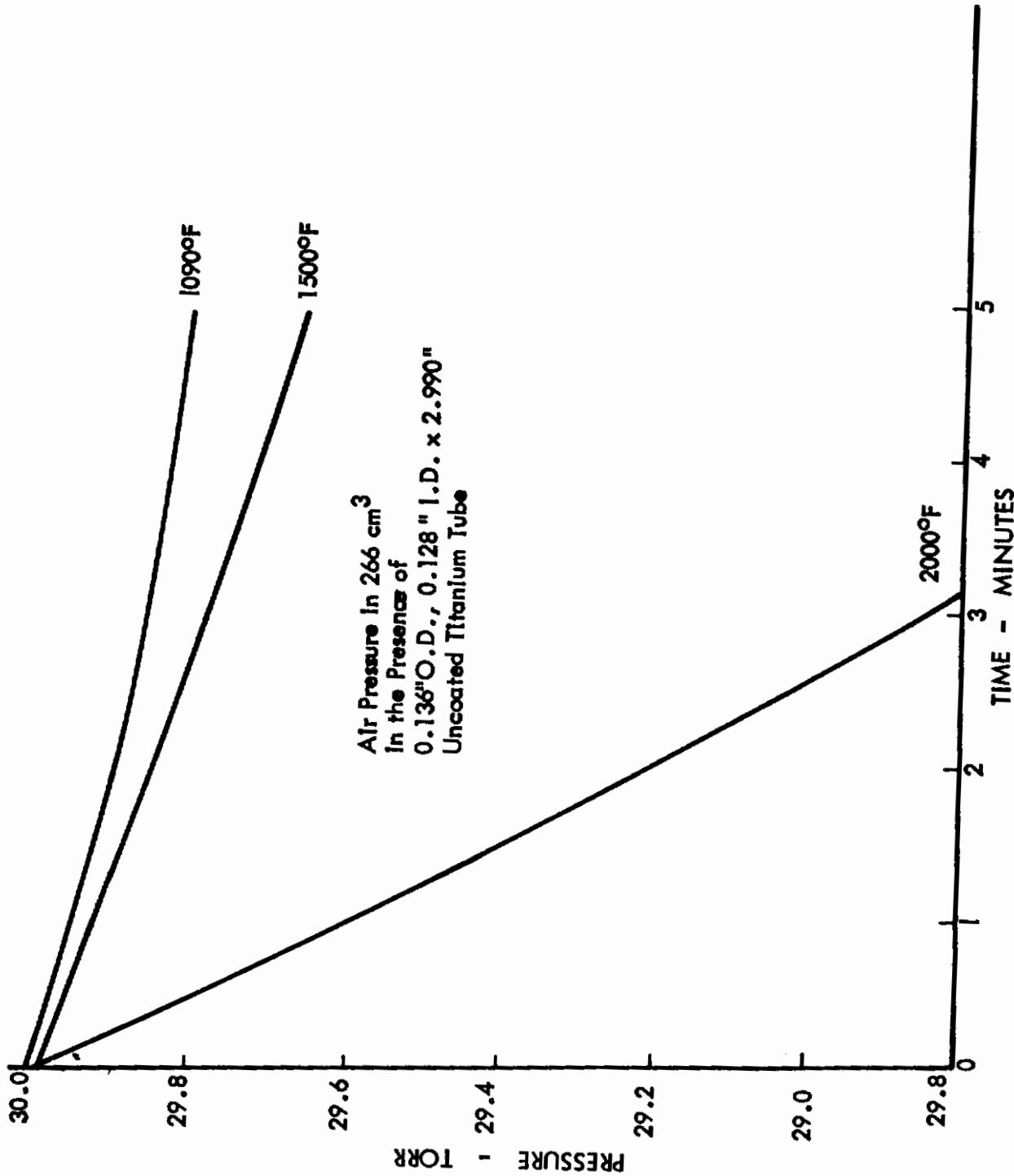






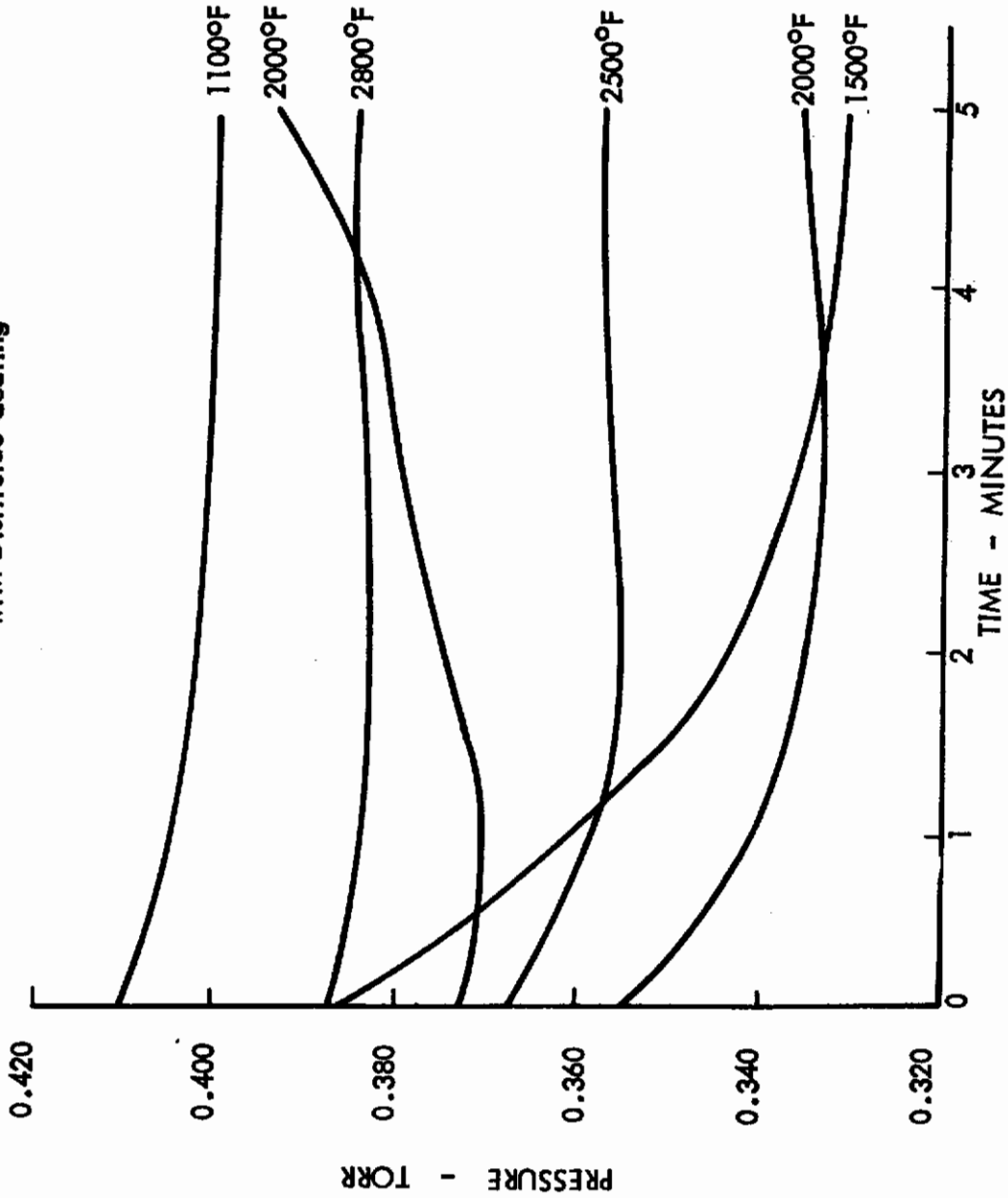


AIR PRESSURE IN THE PRESENCE OF UNCOATED TITANIUM - 3.0 TORR  
FIGURE 19



AIR PRESSURE IN THE PRESENCE OF UNCOATED TITANIUM - 30.0 TORR  
FIGURE 20

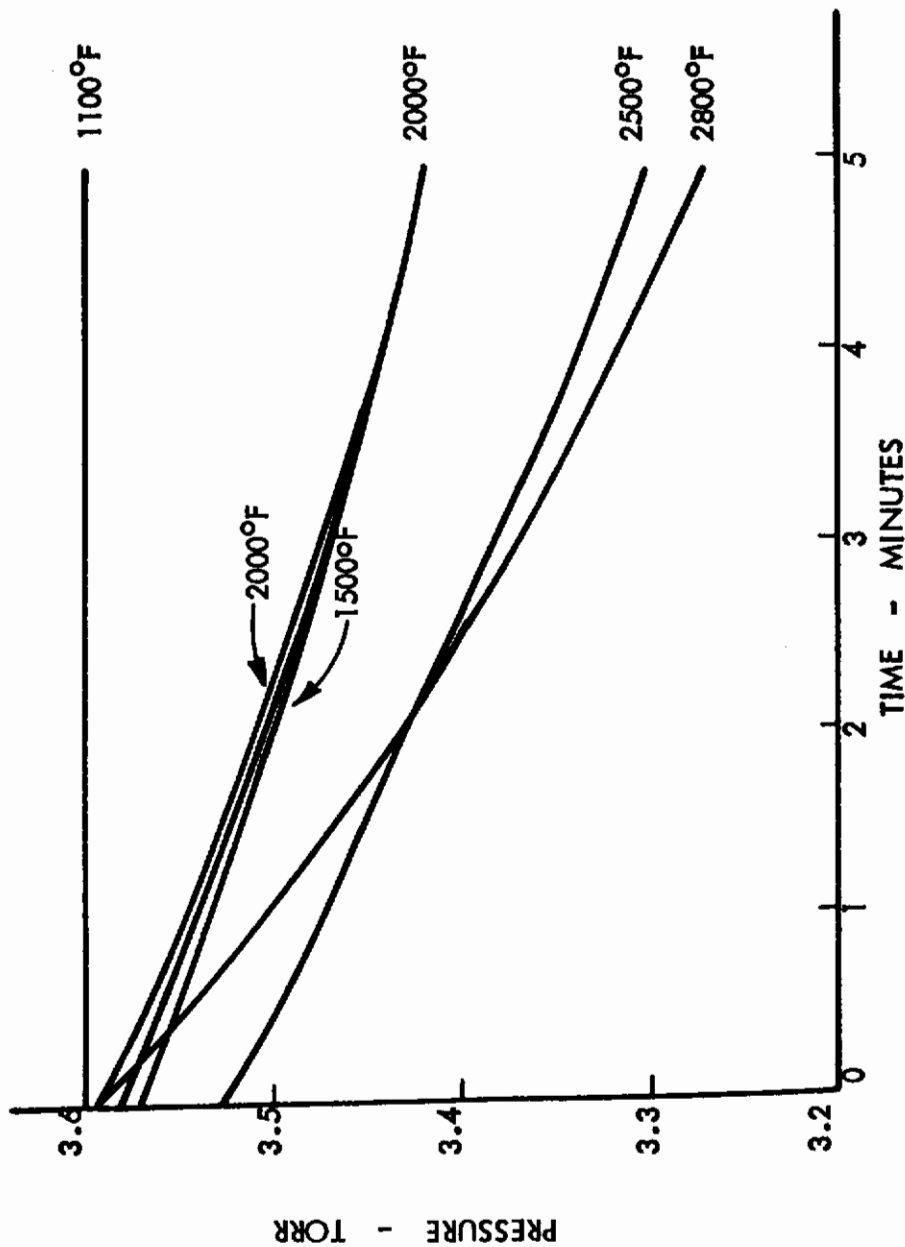
Air Pressure In  $266 \text{ cm}^3$   
In the Presence of  
 $0.127'' \times 0.010'' \times 3.005''$  Tantalum Strip  
with Disilicide Coating



AIR PRESSURE IN THE PRESENCE OF DISILICIDED TANTALUM - 0.3 TORR

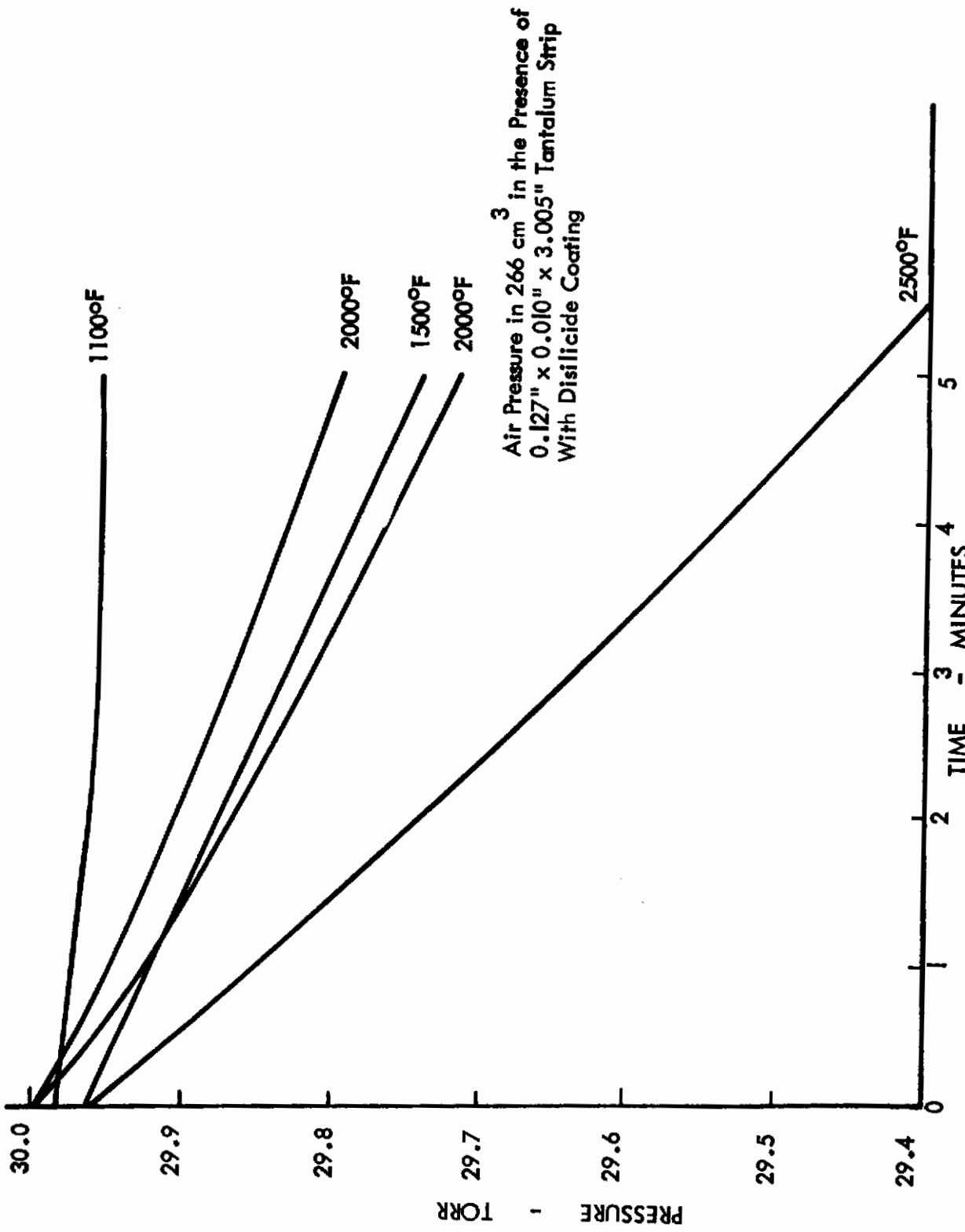
FIGURE 21

Air Pressure In  $266 \text{ cm}^3$   
In the Presence of  
 $0.127'' \times 0.010'' \times 3.005''$  Tantalum Strip  
With Disilicide Coating



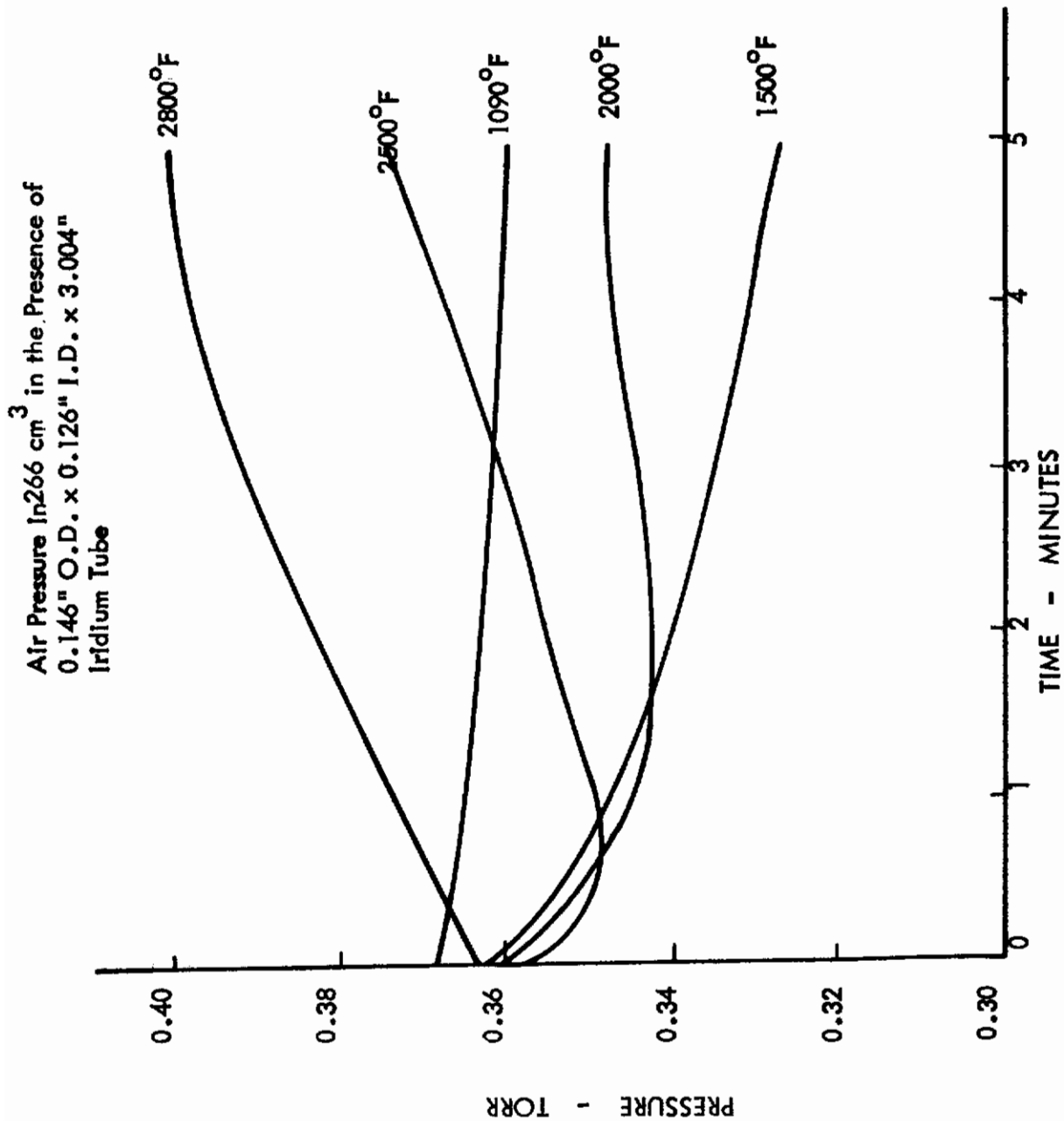
AIR PRESSURE IN THE PRESENCE OF DISILICIDED TANTALUM-3.0 TORR

FIGURE 22

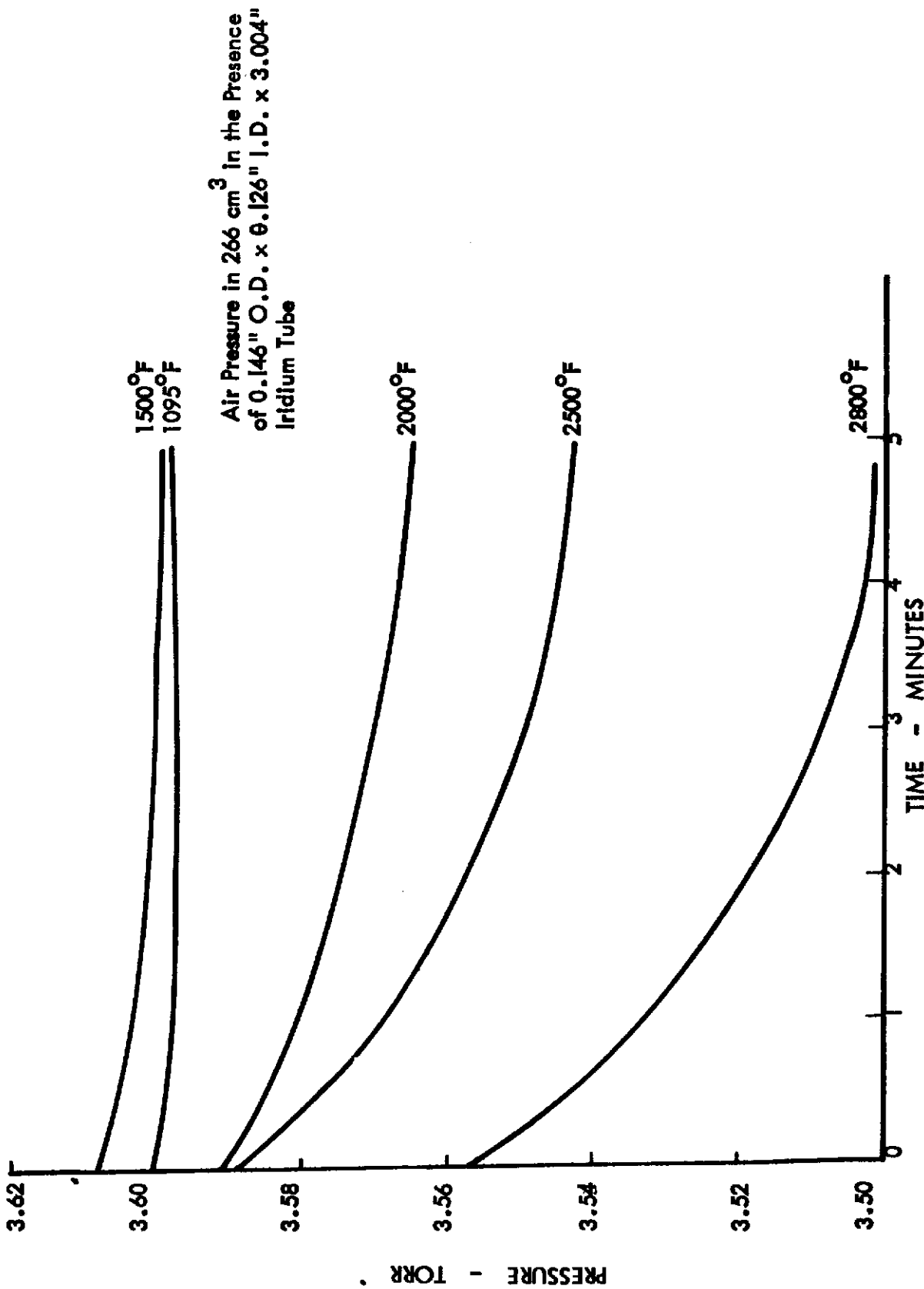


AIR PRESSURE IN THE PRESENCE OF DISILICIDED TANTALUM-30.0 TORR  
FIGURE 23



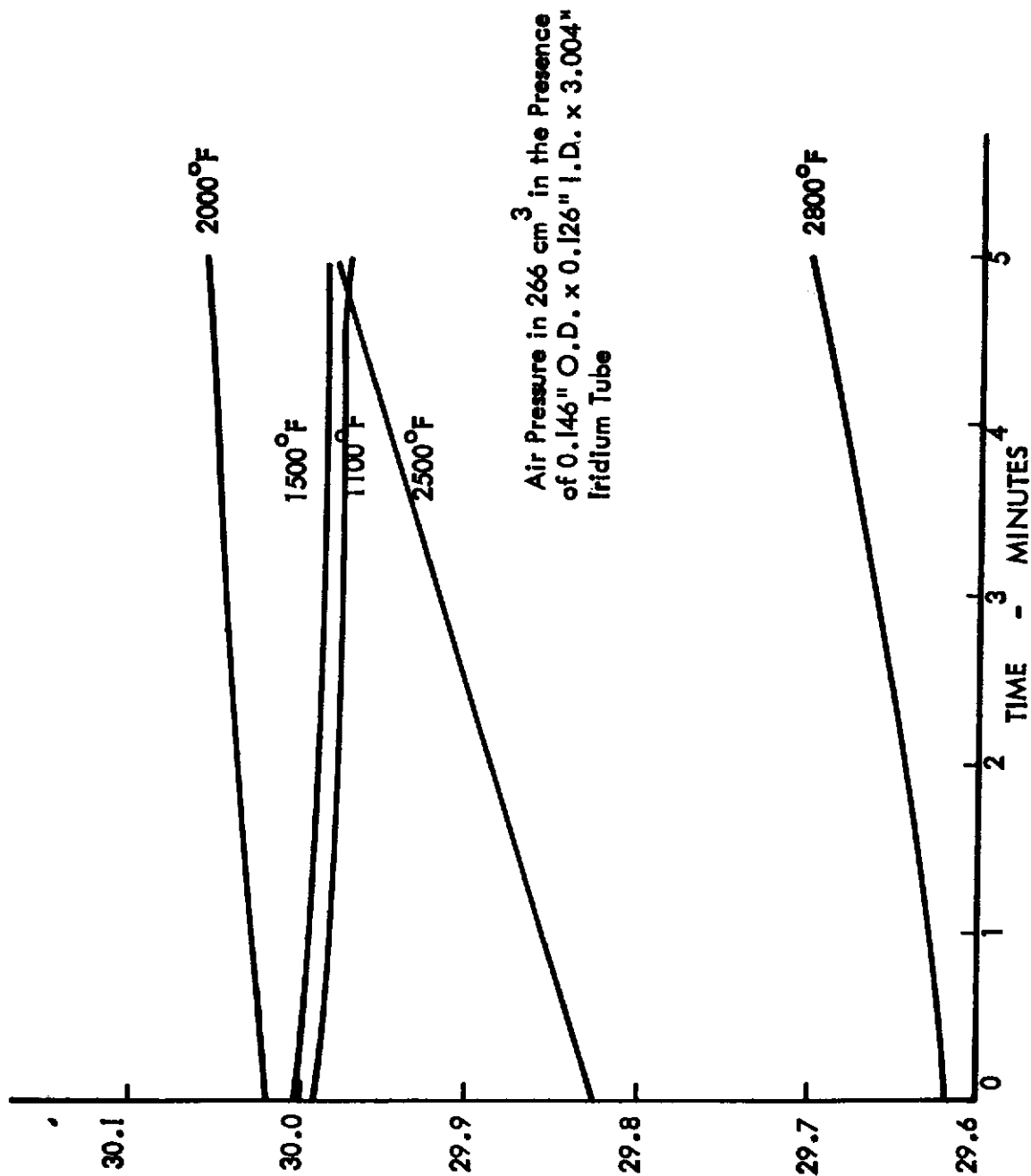


AIR PRESSURE IN THE PRESENCE OF IRIIDIUM - 0.3 TORR  
FIGURE 24



AIR PRESSURE IN THE PRESENCE OF IRIIDIUM - 3.0 TORR

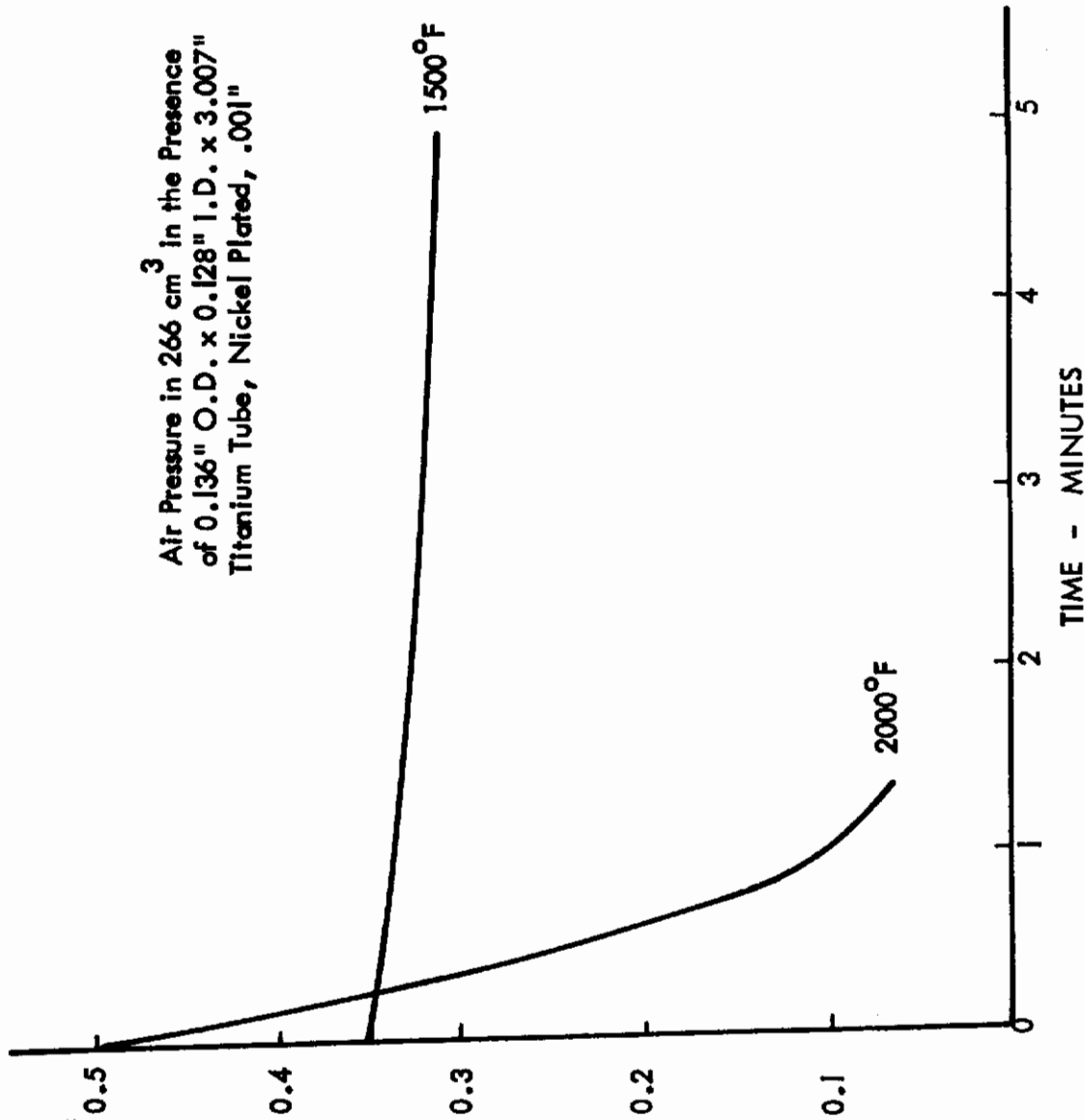
FIGURE 25



Air Pressure in 266 cm<sup>3</sup> in the Presence of 0.146" O.D. x 0.126" I.D. x 3.004" Iridium Tube

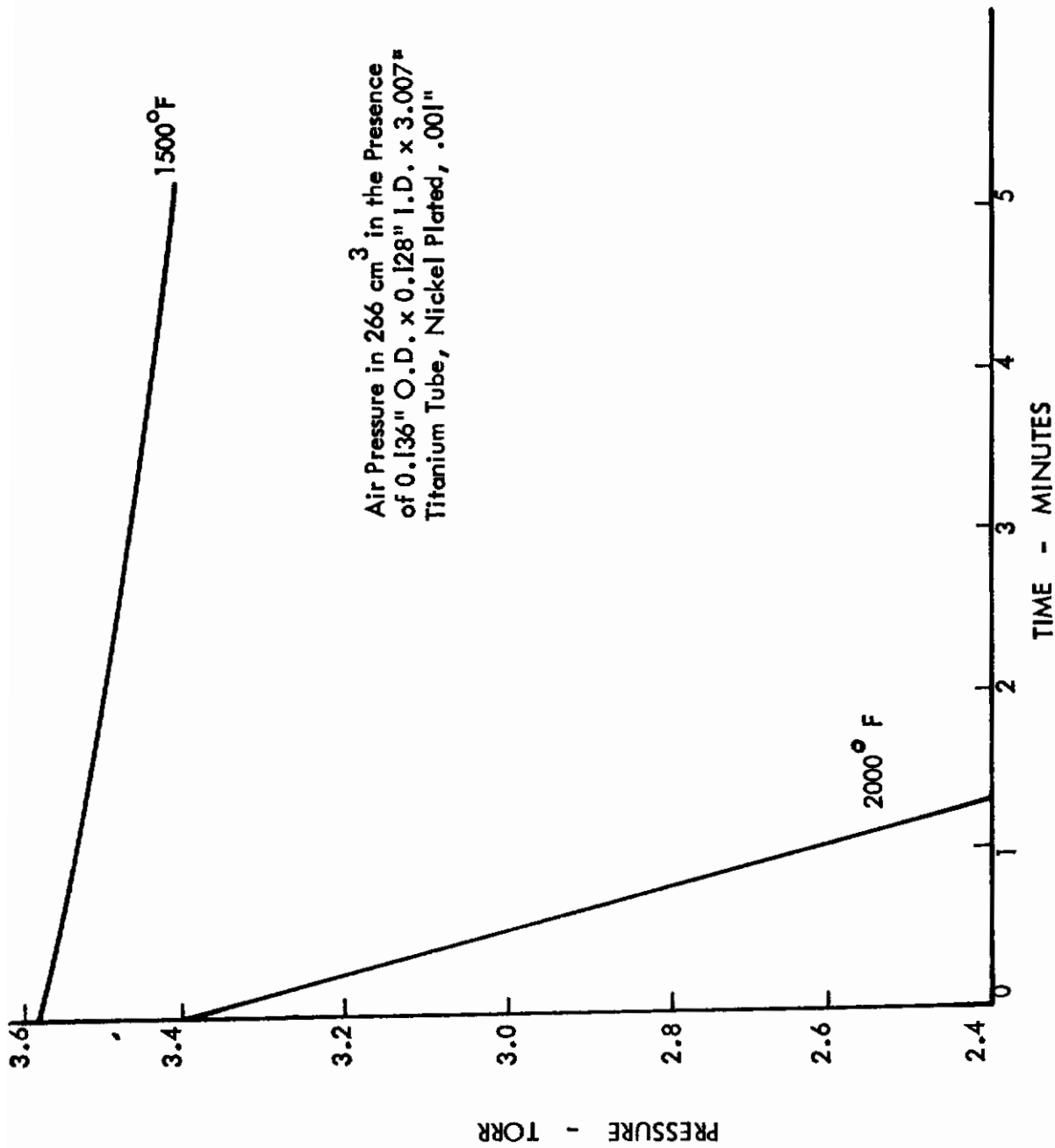
AIR PRESSURE IN THE PRESENCE OF IRIIDIUM - 30.0 TORR

FIGURE 26



AIR PRESSURE IN THE PRESENCE OF NICKEL PLATED TITANIUM - 0.3 TORR

FIGURE 27



AIR PRESSURE IN THE PRESENCE OF NICKEL PLATED TITANIUM - 3.0 TORR  
FIGURE 28

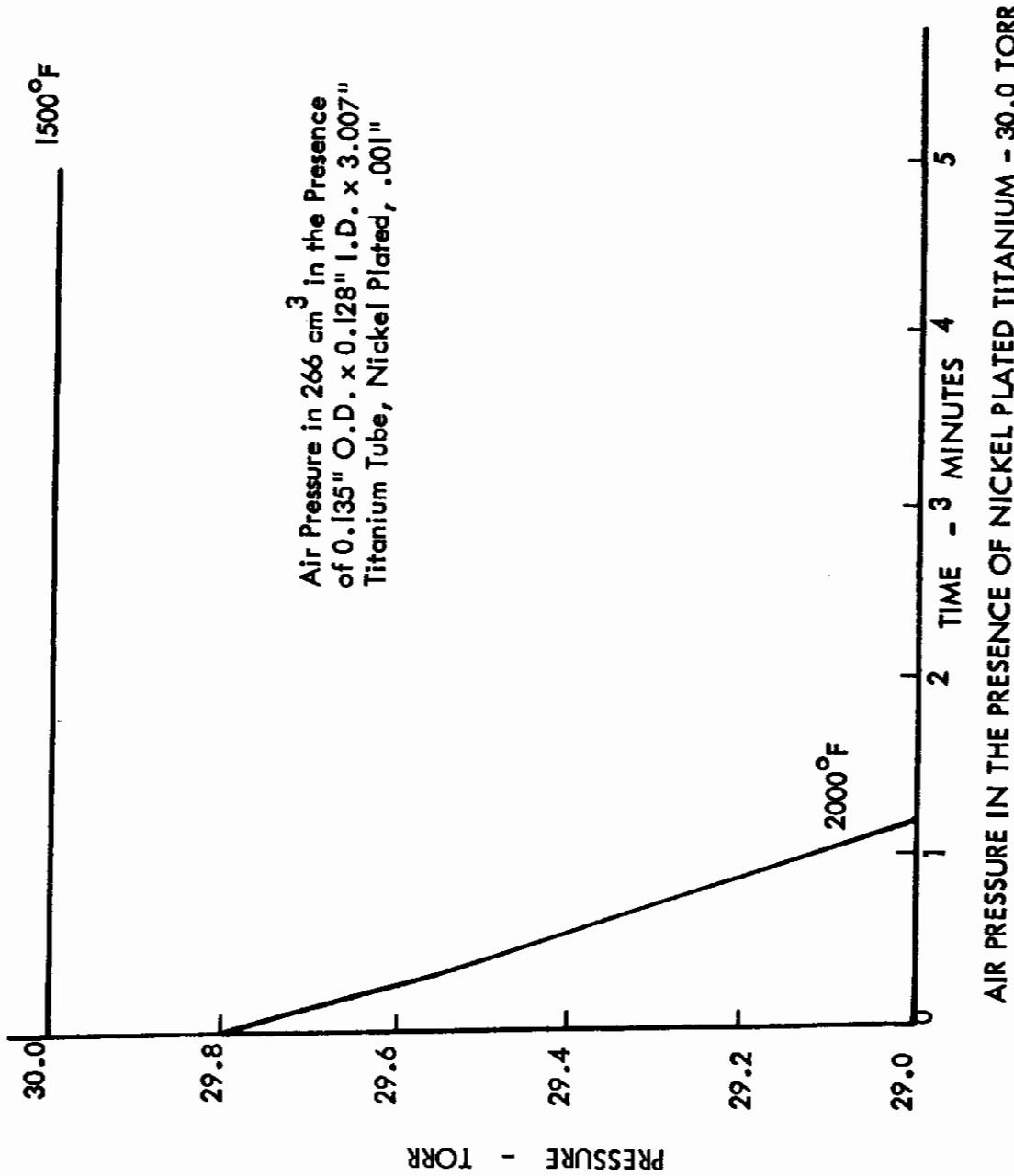
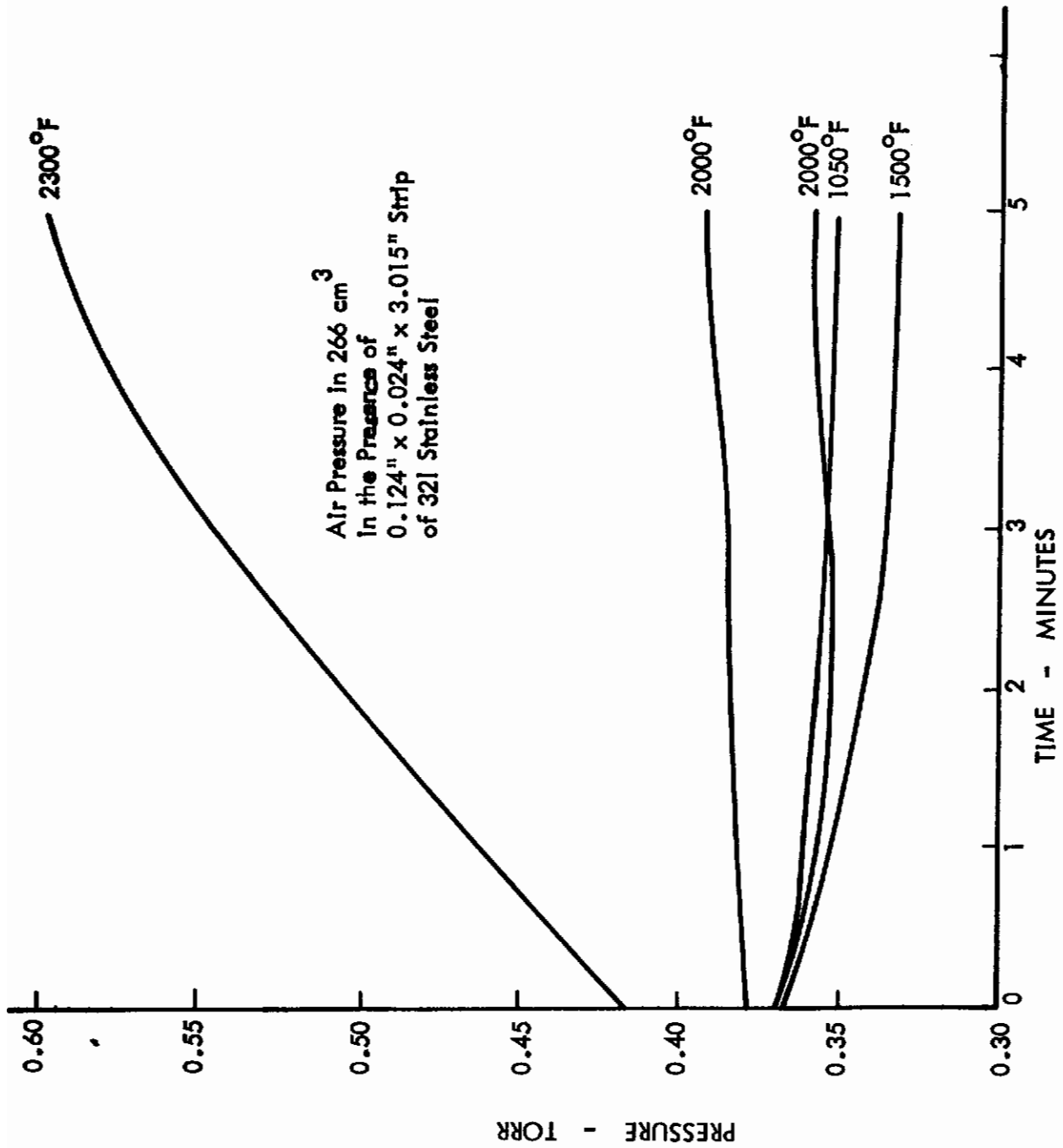
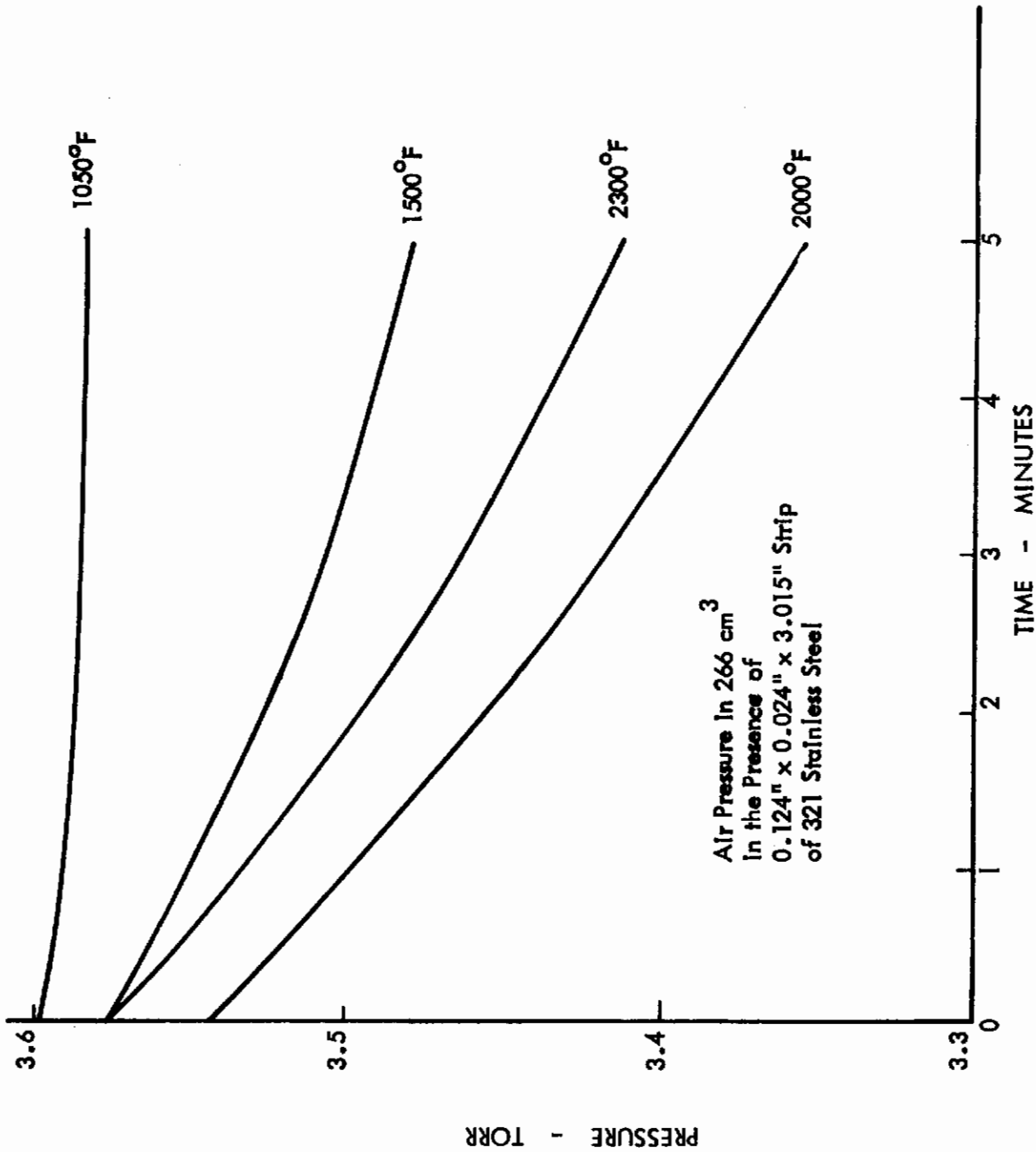


FIGURE 29



AIR PRESSURE IN THE PRESENCE OF 321 STAINLESS STEEL - 0.3 TORR  
FIGURE 30

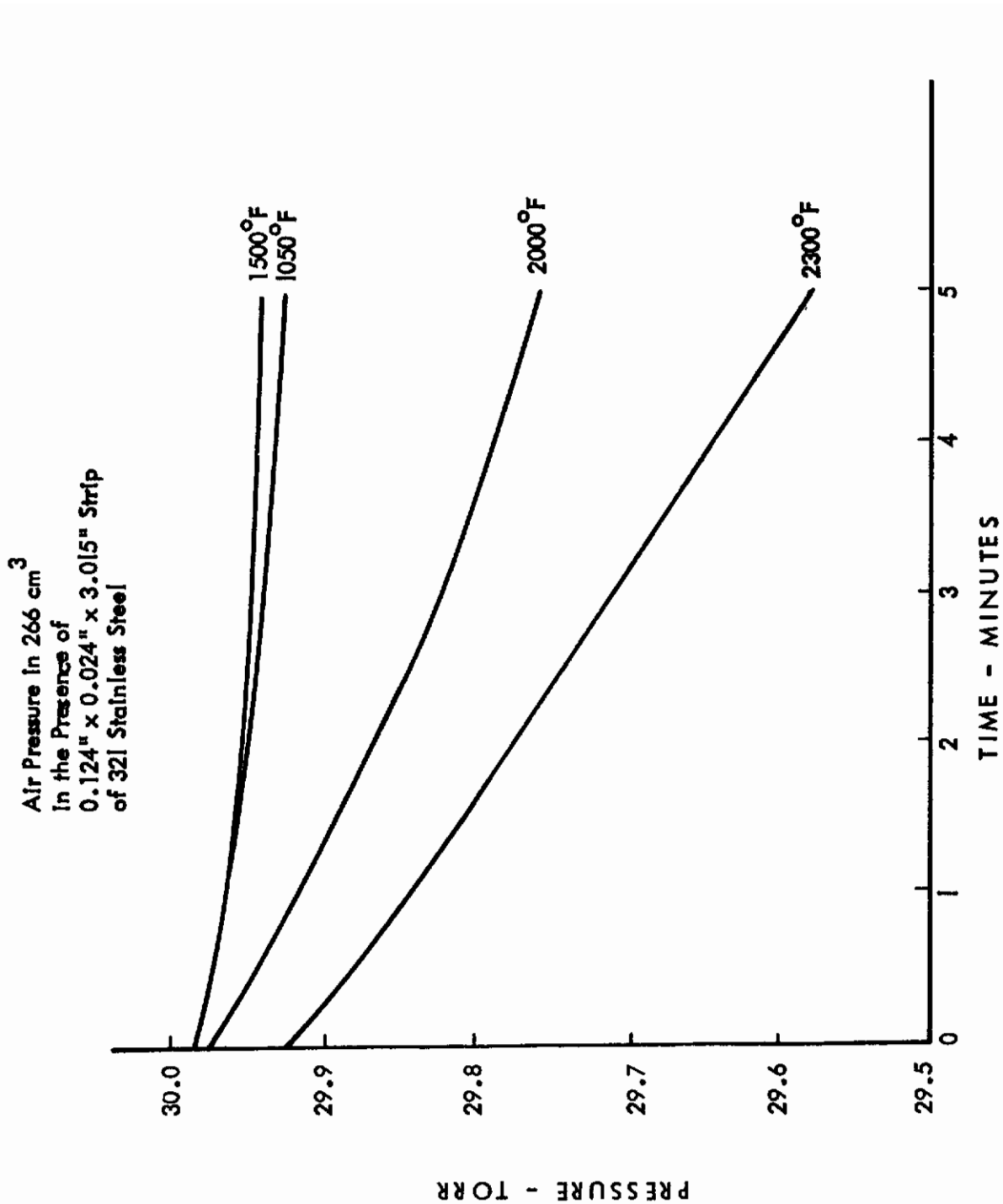


Air Pressure In  $266 \text{ cm}^3$   
In the Presence of  
 $0.124'' \times 0.024'' \times 3.015''$  Strip  
of 321 Stainless Steel

AIR PRESSURE IN THE PRESENCE OF 321 STAINLESS STEEL - 3.0 TORR

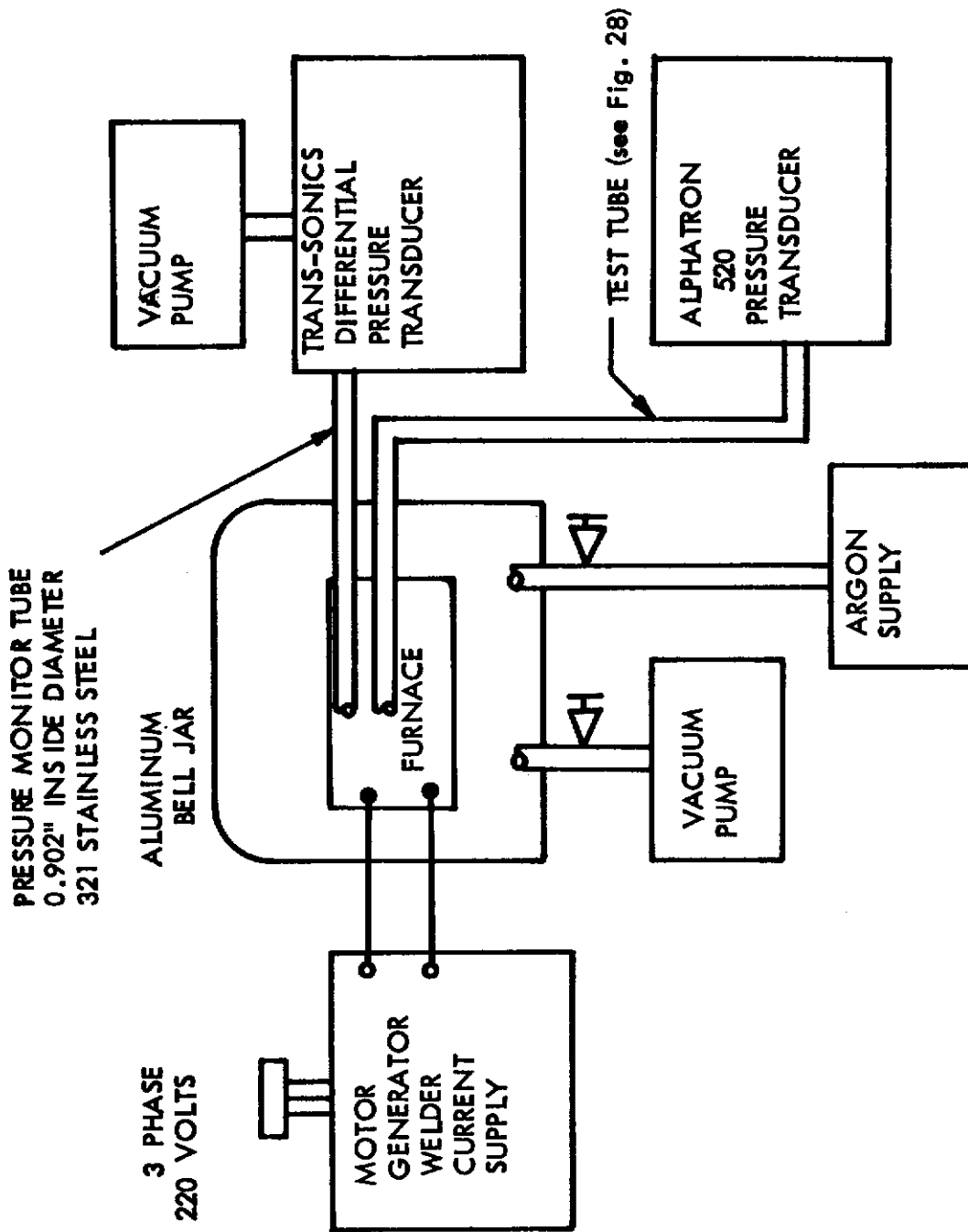
FIGURE 3I





AIR PRESSURE IN THE PRESENCE OF 321 STAINLESS STEEL - 30.0 TORR

FIGURE 32

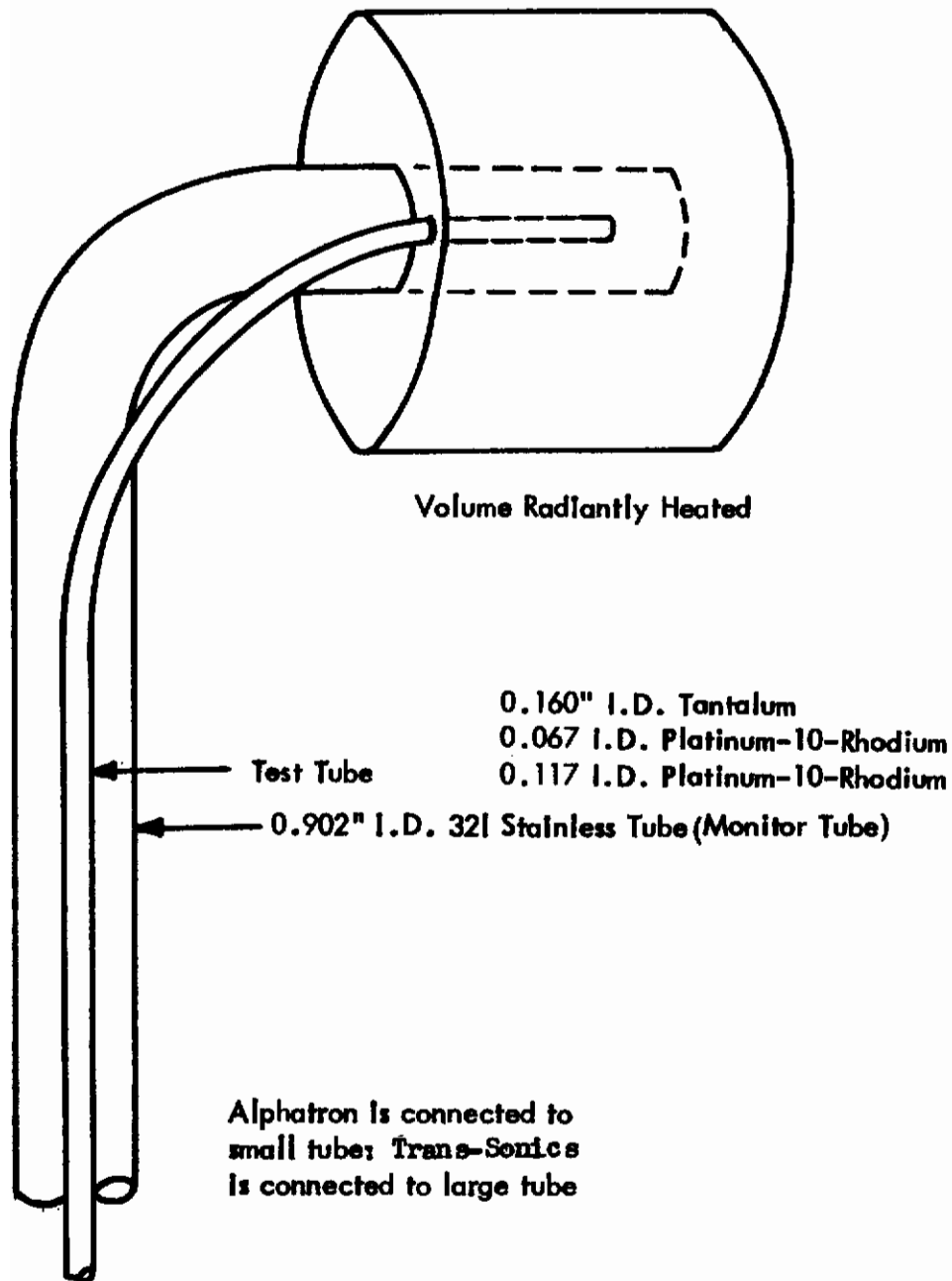


OPEN TUBE FACILITY FOR LOW PRESSURE ARGON MEASUREMENT

FIGURE 33

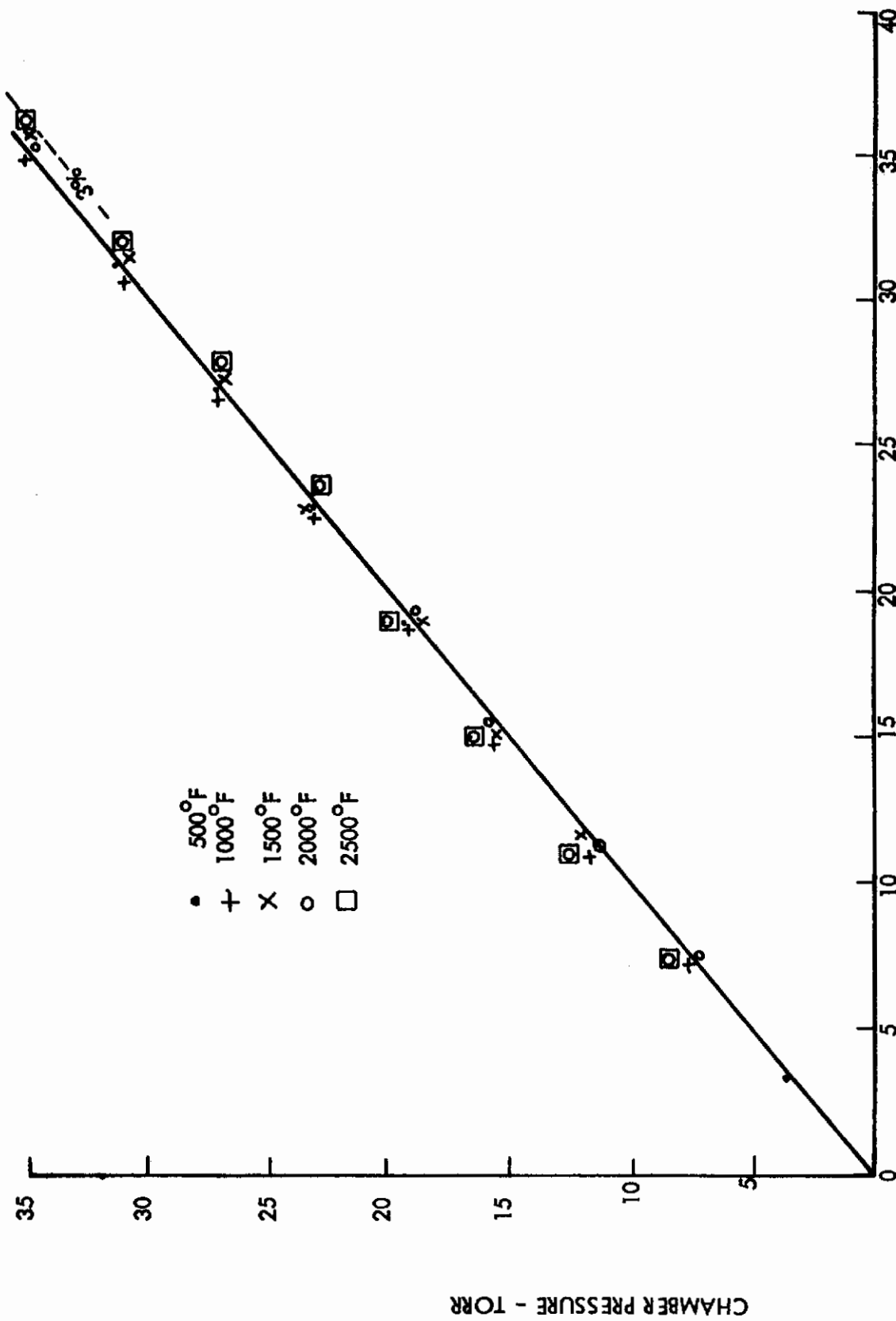
# Contrails

The dotted sections were added to the system for the second series of measurements.



Detail of  
Open Tube Assembly For Low  
Pressure Argon Measurement

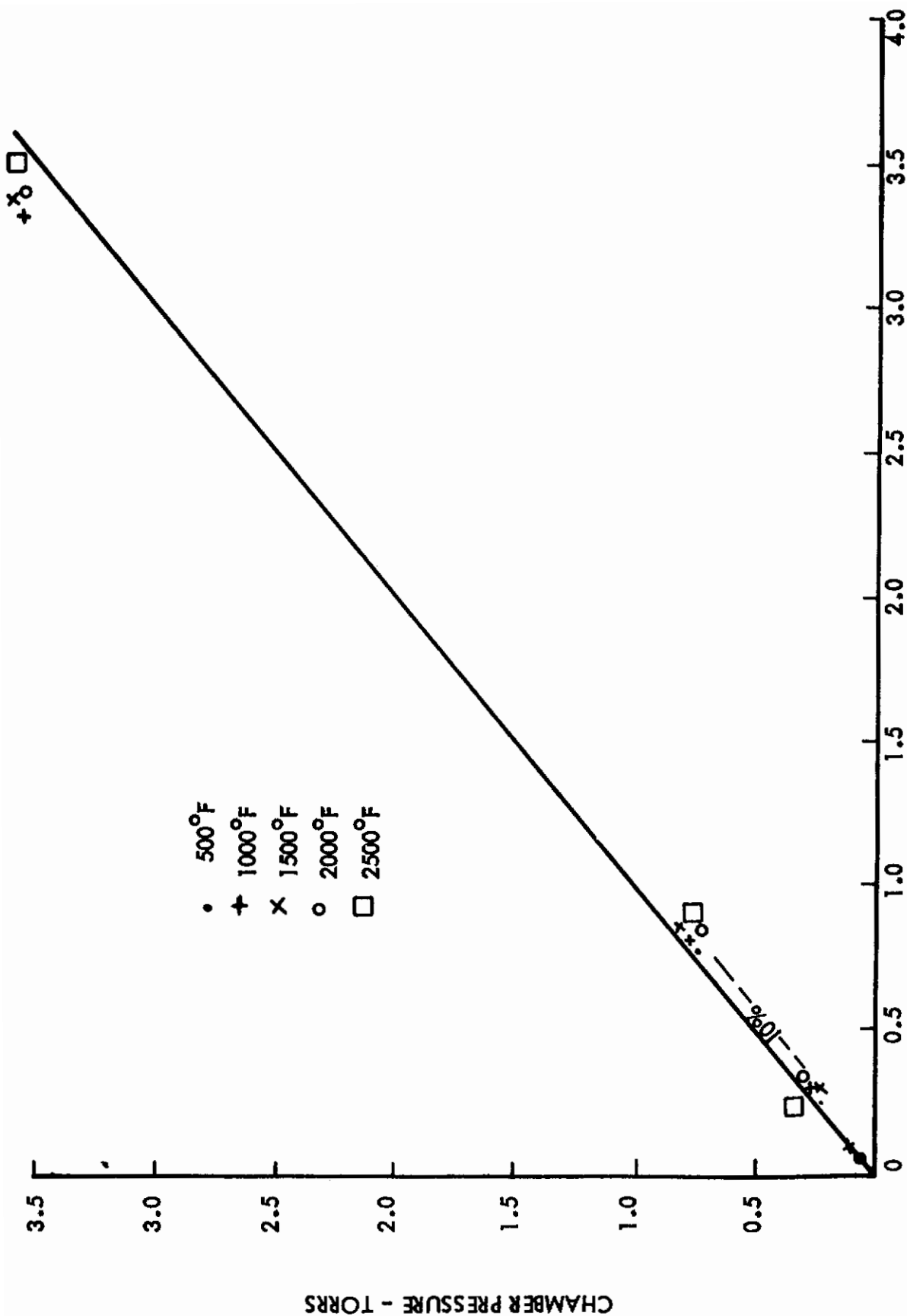
FIGURE 34



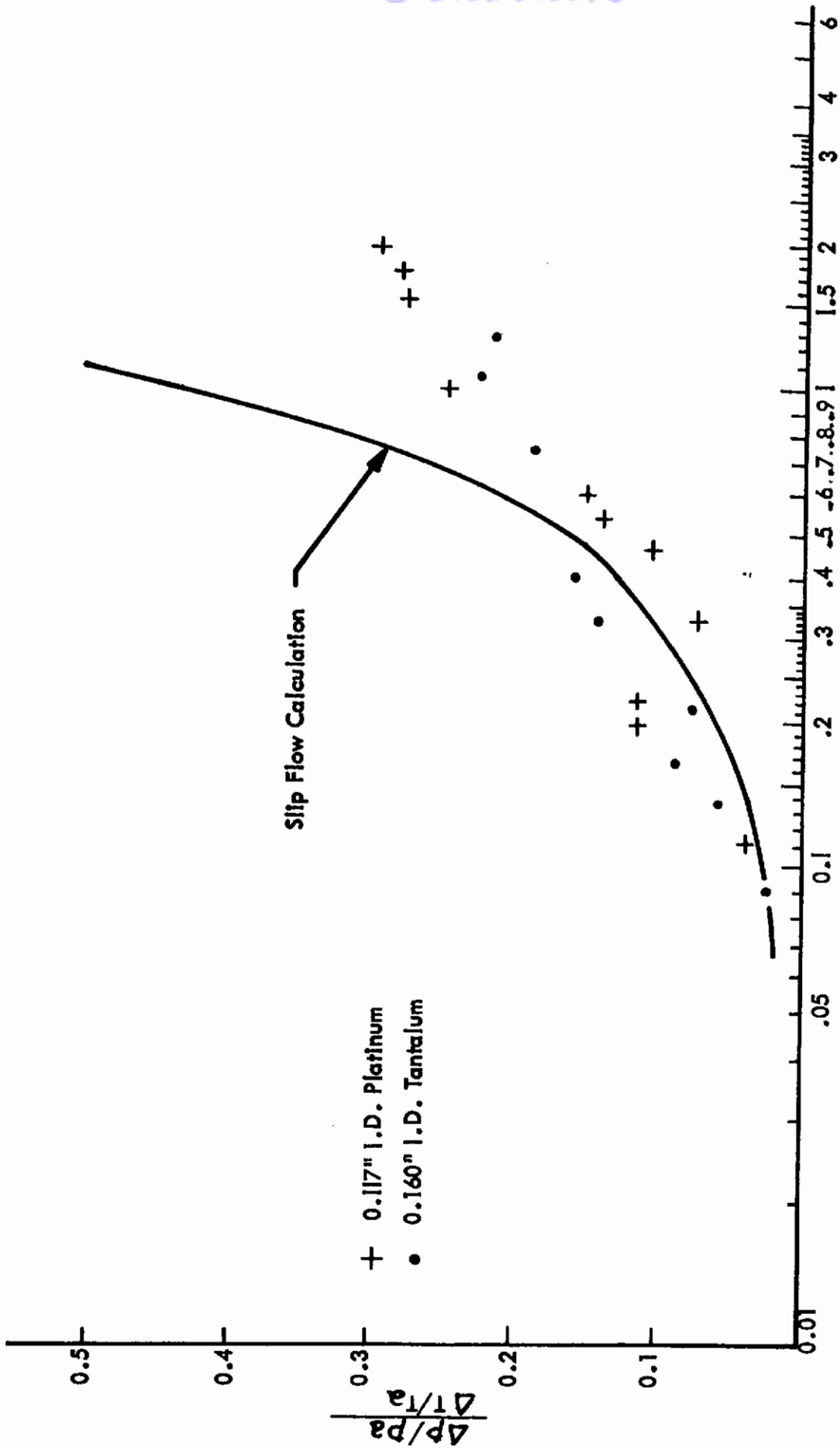
HOT MONITOR TUBE PRESSURE - TORR

CALIBRATION OF MONITOR TUBE PRESSURE AGAINST CHAMBER PRESSURE

FIGURE 35

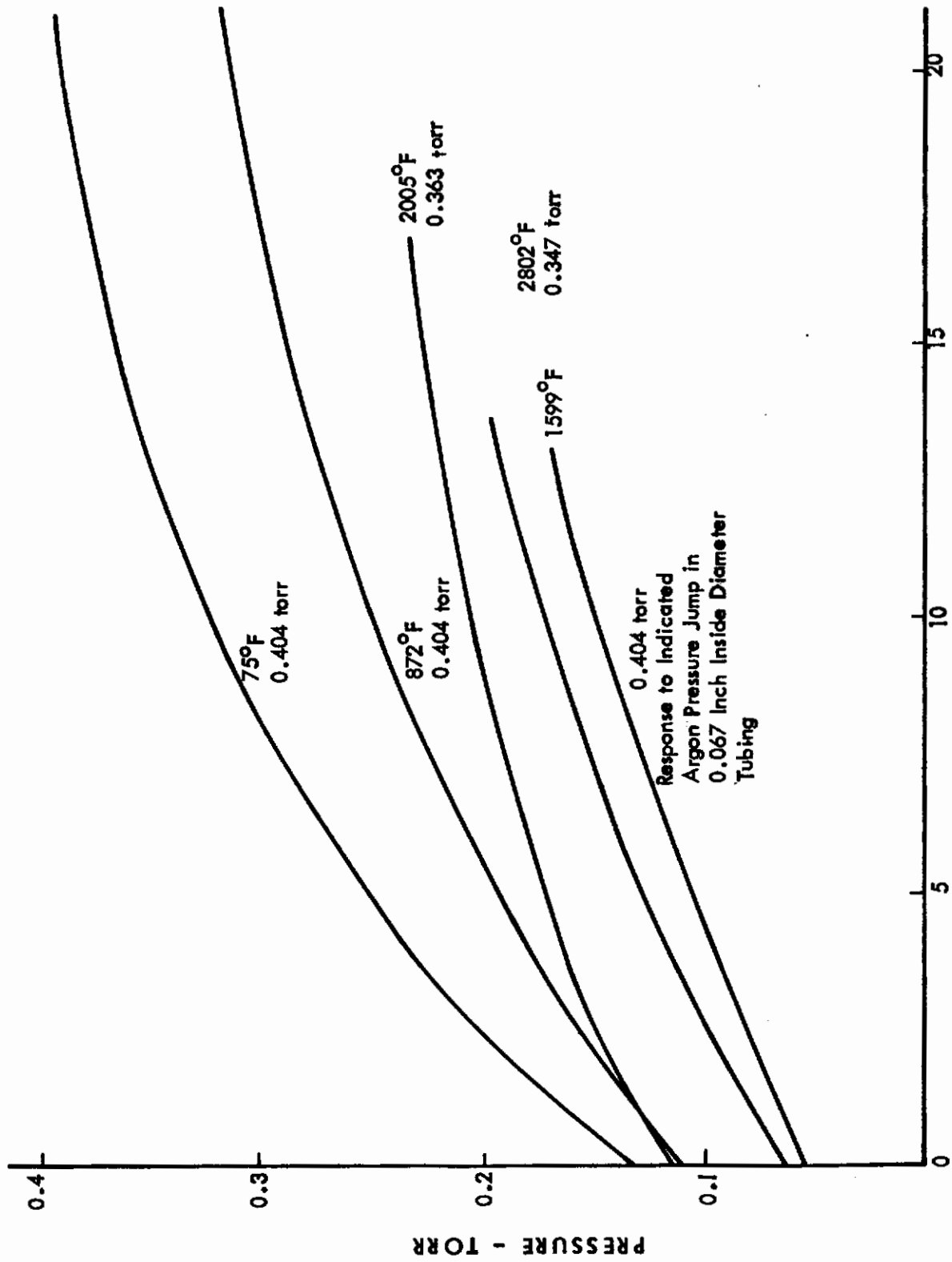


HOT MONITOR TUBE PRESSURE - TORRS  
CALIBRATION OF MONITOR TUBE PRESSURE AGAINST CHAMBER PRESSURE  
FIGURE 36



ARGON STATIC PRESSURE DIFFERENCE VS  $K_n$  IN AN OPEN TUBE

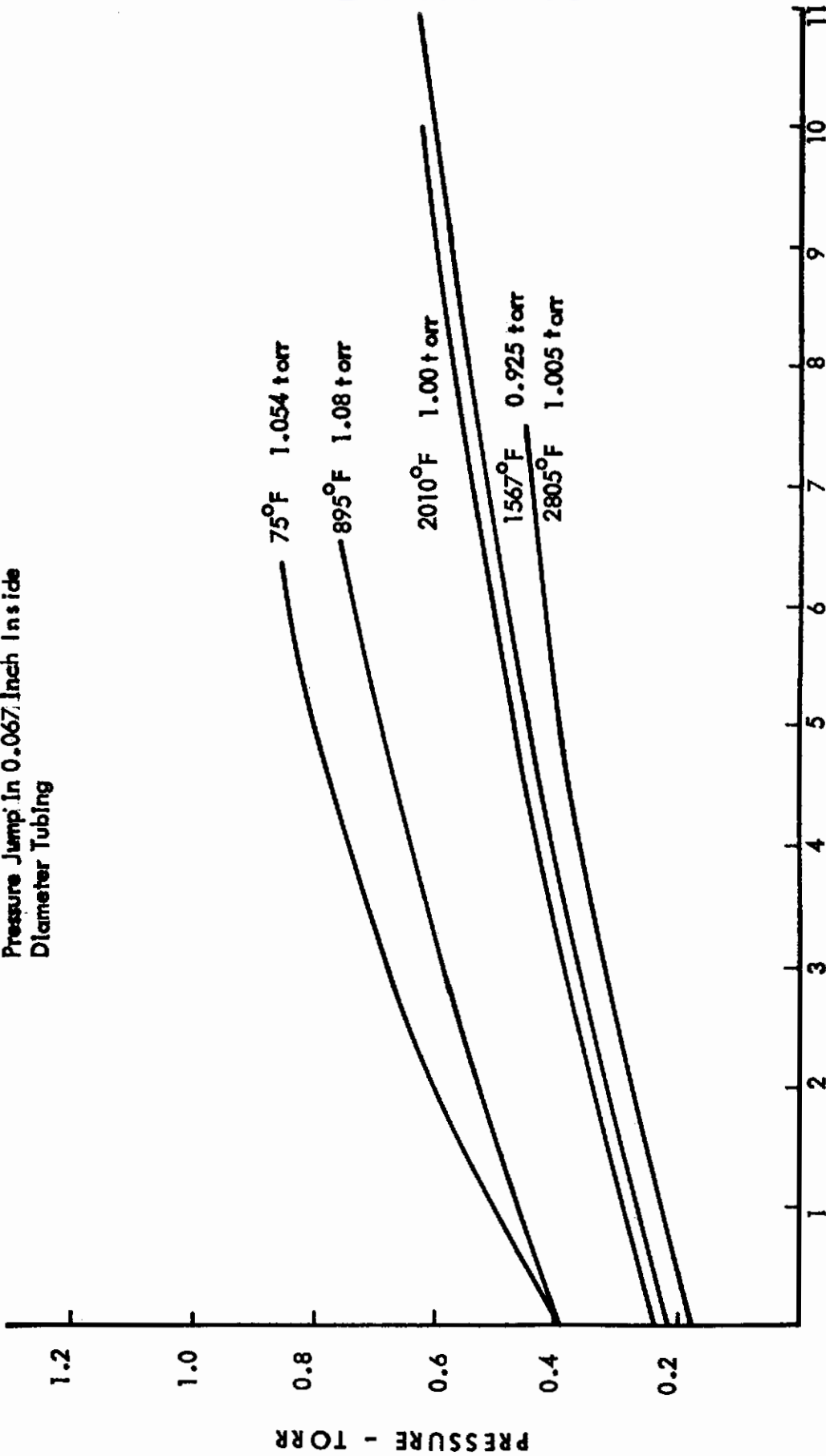
FIGURE 37



Response to Indicated  
Argon Pressure Jump in  
0.067 Inch Inside Diameter  
Tubing

TIME RESPONSE - ARGON TO 0.4 TORR - 0.067" TUBE  
FIGURE 38

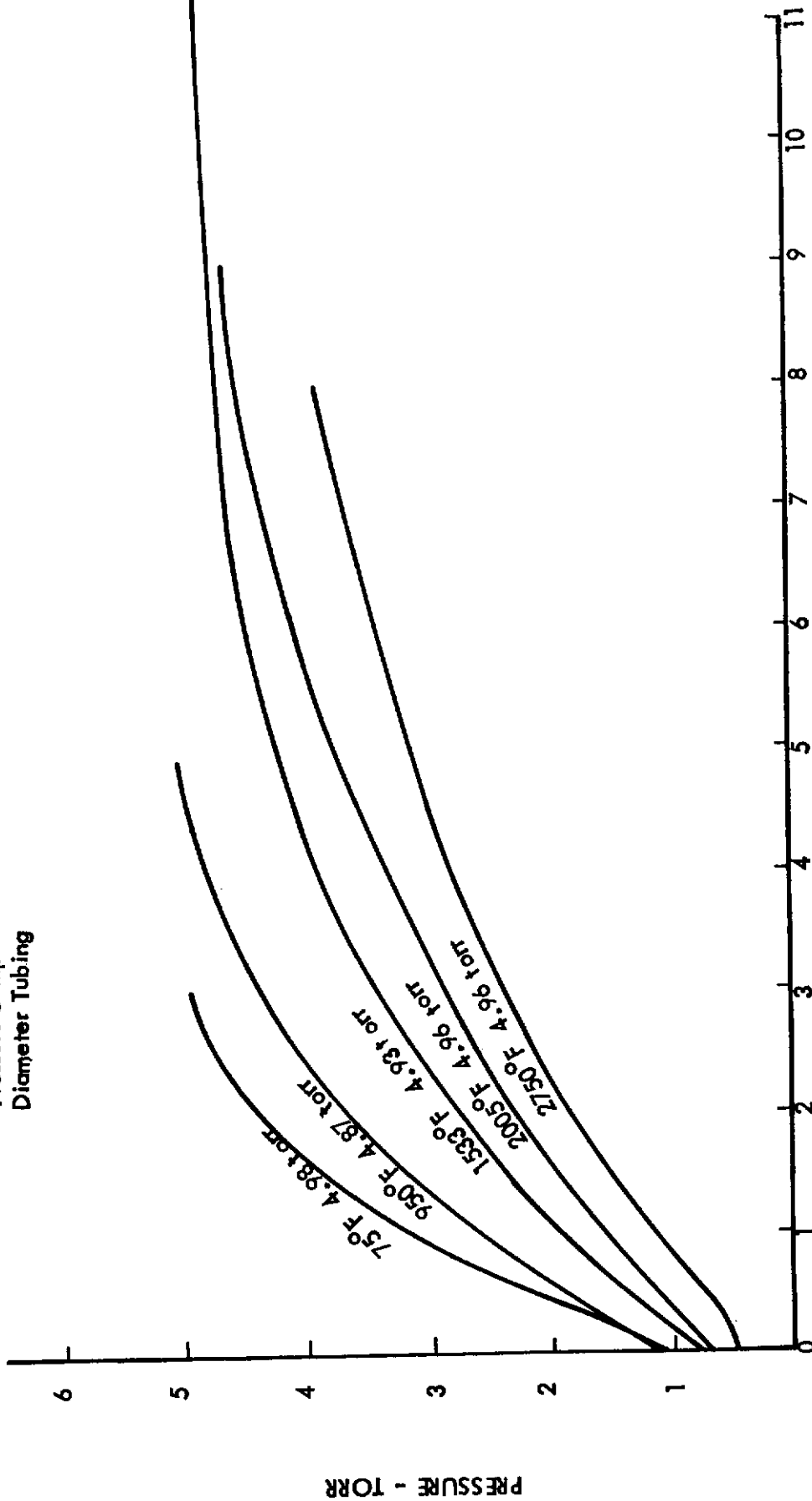
Response to Indicated Argon  
Pressure Jump in 0.067 Inch Inside  
Diameter Tubing



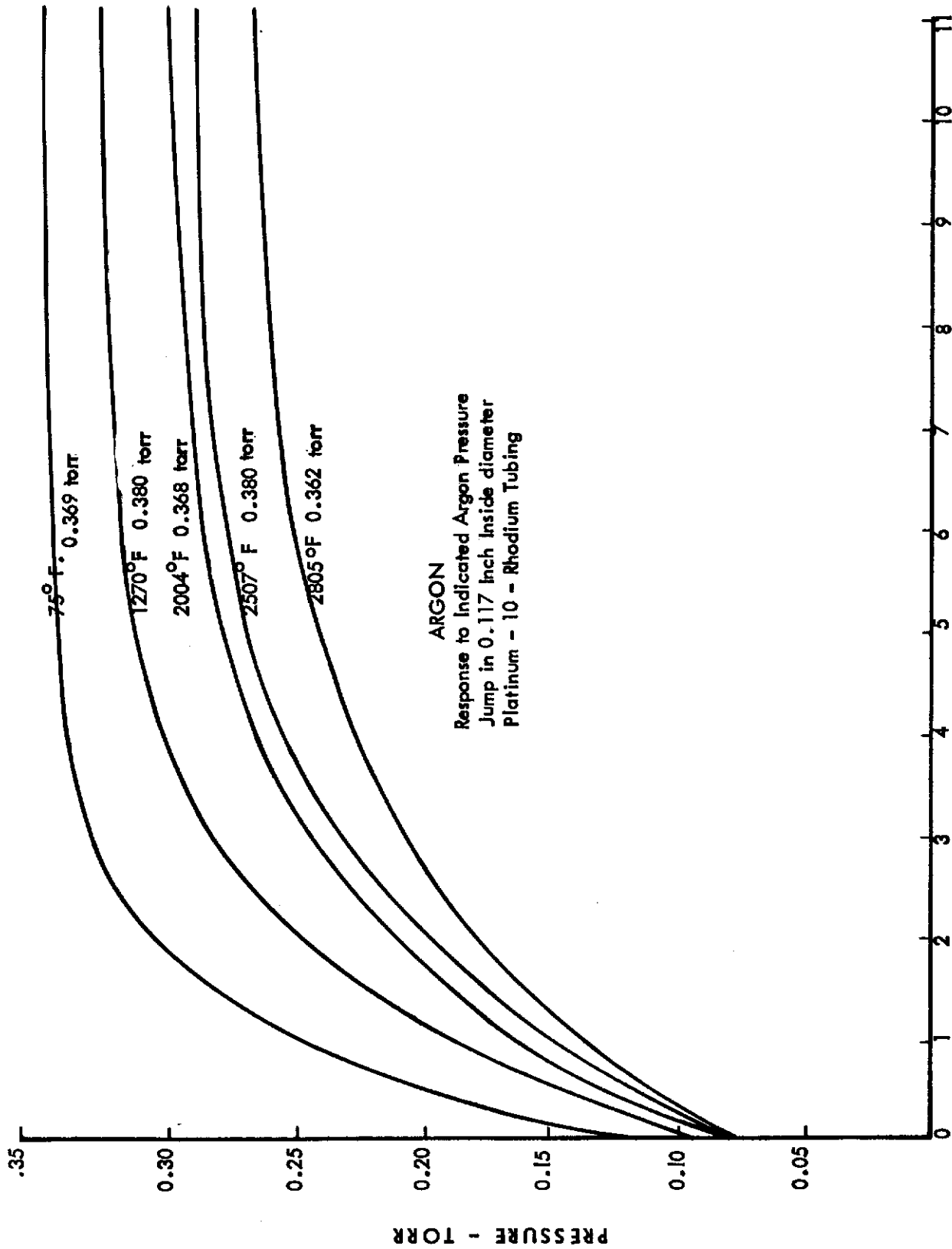
TIME RESPONSE - ARGON TO 1.0 TORR - 0.067" TUBE  
FIGURE 39



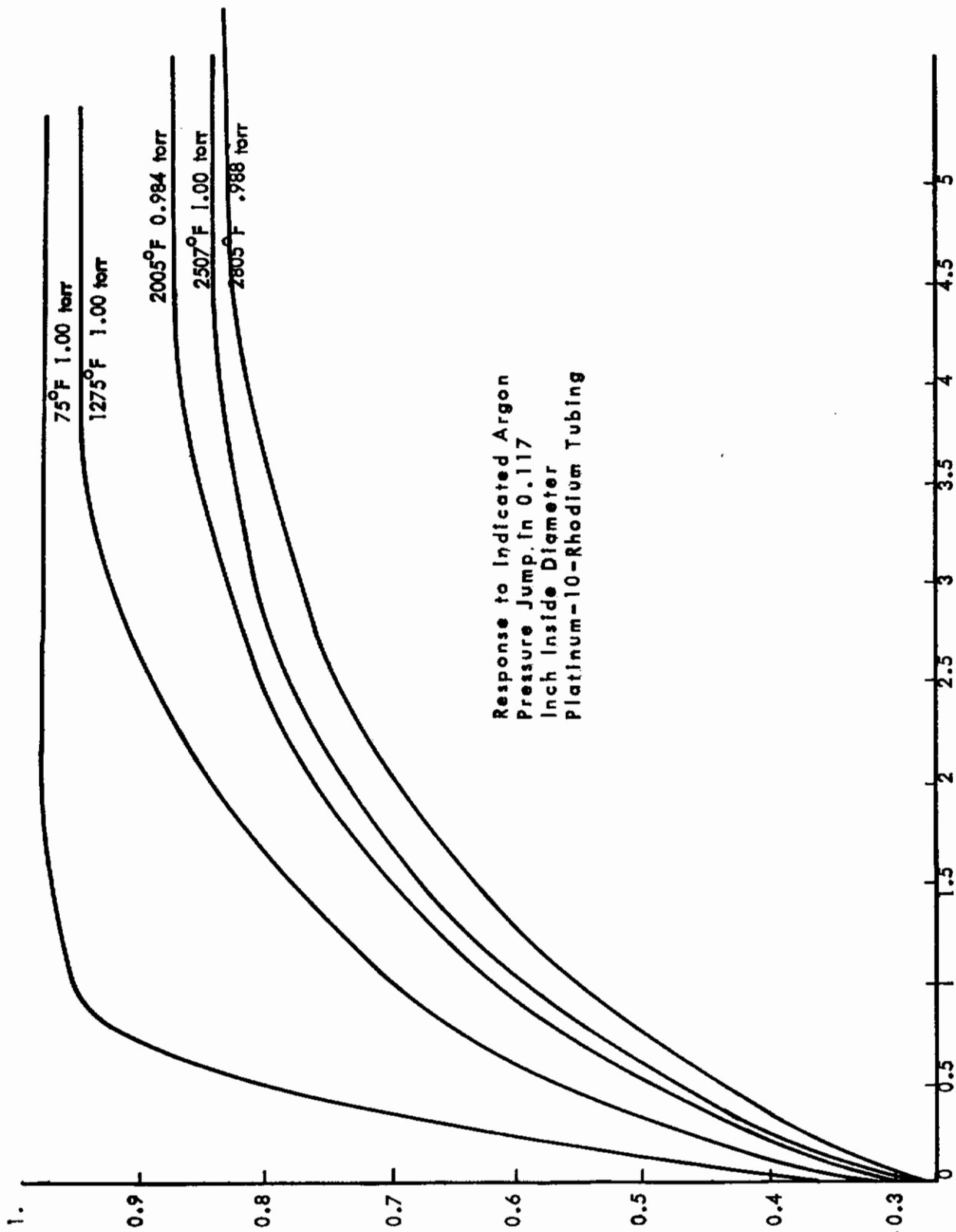
Response to Indicated Argon  
Pressure Jump in 0.067" Inside  
Diameter Tubing

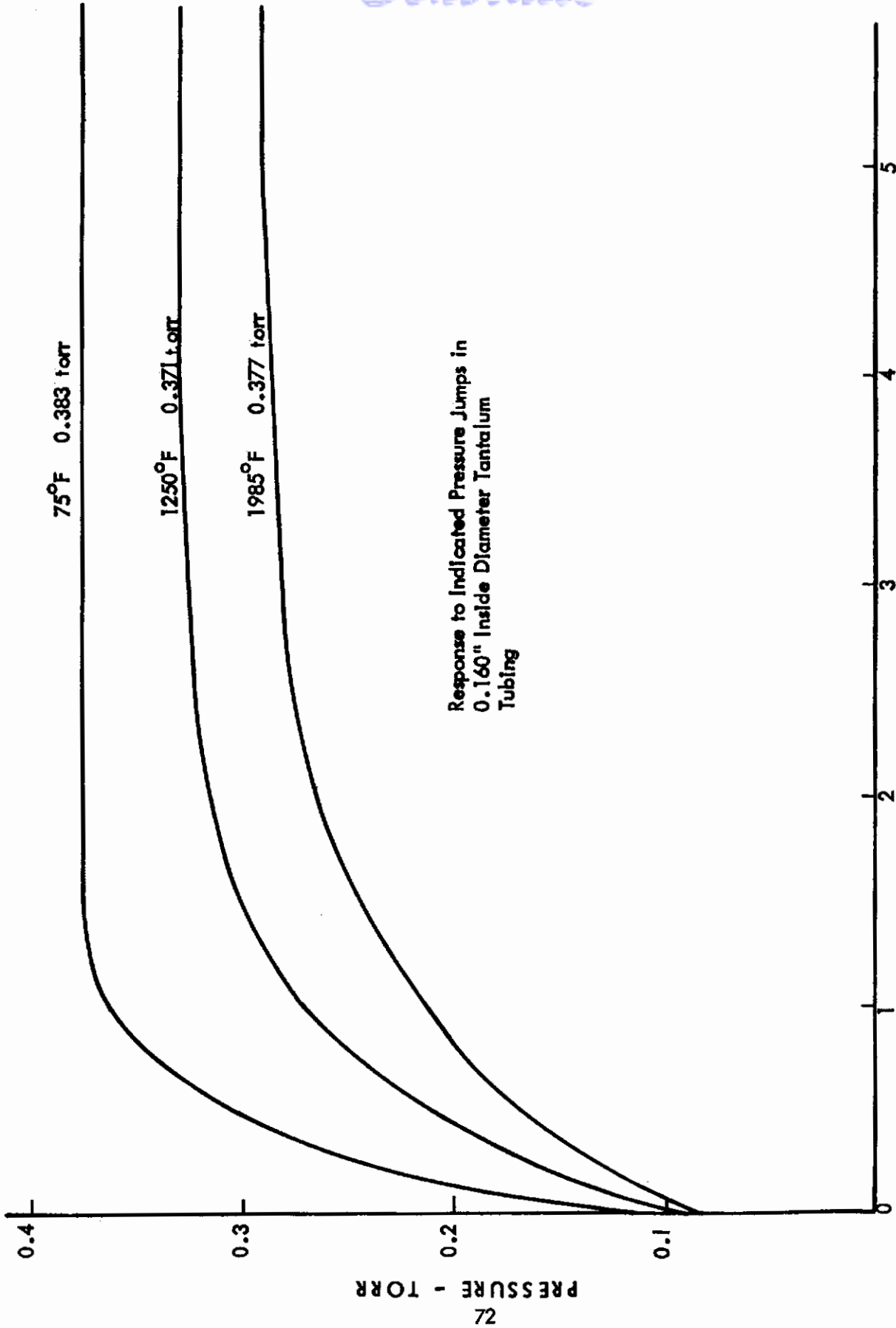


TIME - MINUTES  
TIME RESPONSE - ARGON TO 5.0 TORR - 0.067" TUBE  
FIGURE 40



TIME RESPONSE - ARGON TO 0.4 TORR - 0.117 TUBE  
FIGURE 41





Response to Indicated Pressure Jumps in  
0.160" Inside Diameter Tantalum  
Tubing

TIME RESPONSE - ARGON TO 0.4 TORR - 0.160 TUBE  
FIGURE 43

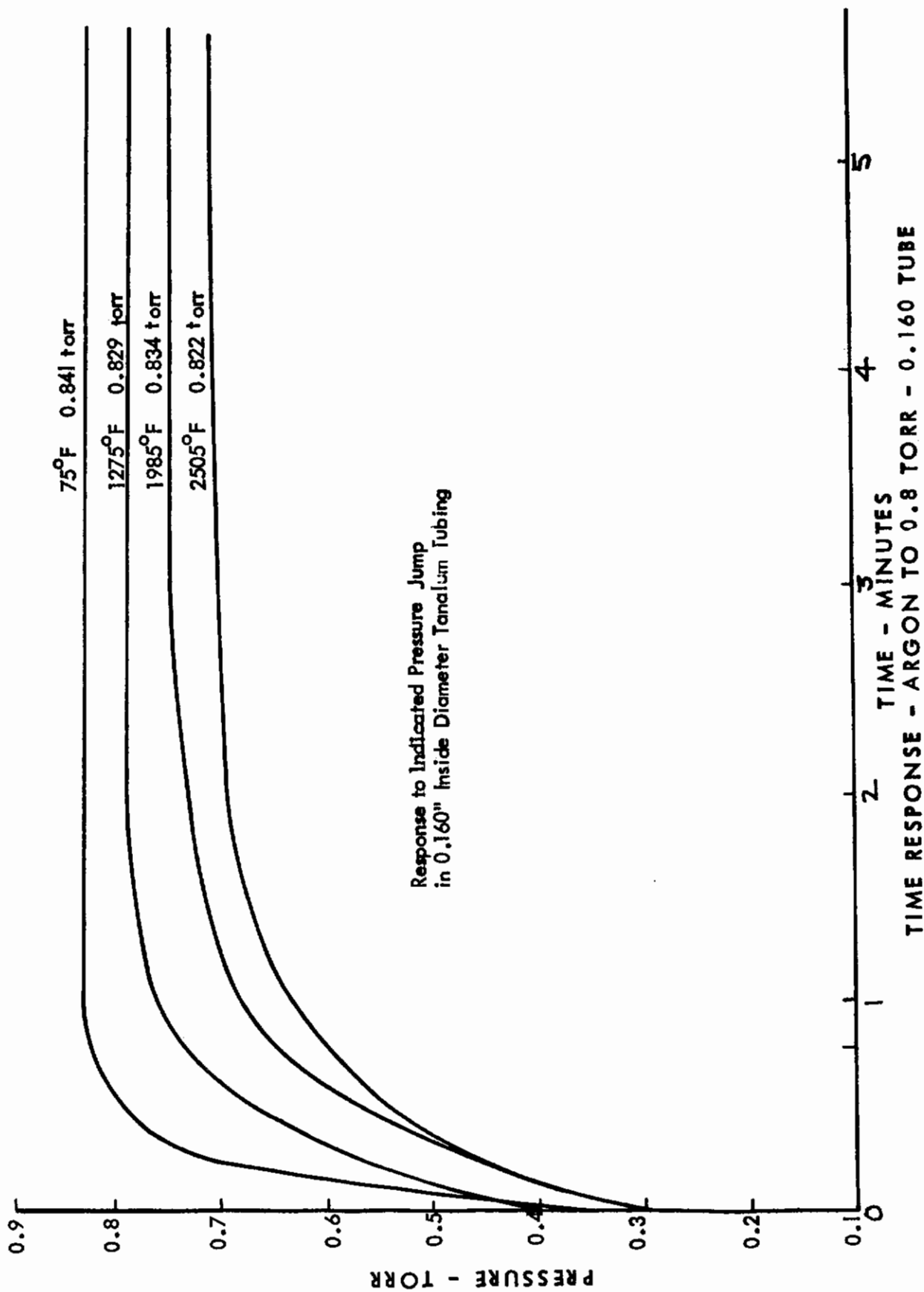
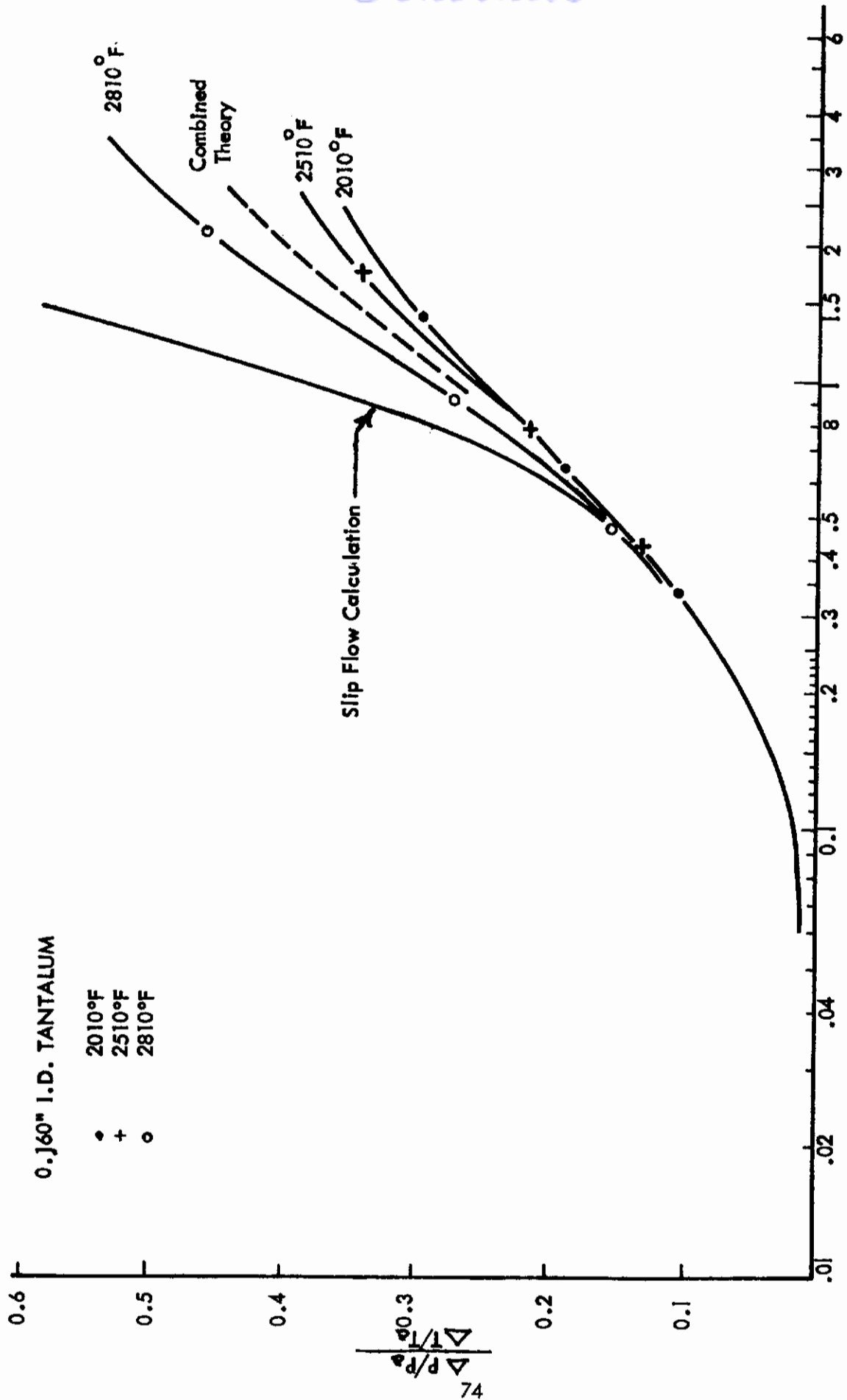


FIGURE 44



ARGON STATIC PRESSURE DIFFERENCE VS  $K_n$  IN AN OPEN TUBE  
FIGURE 45

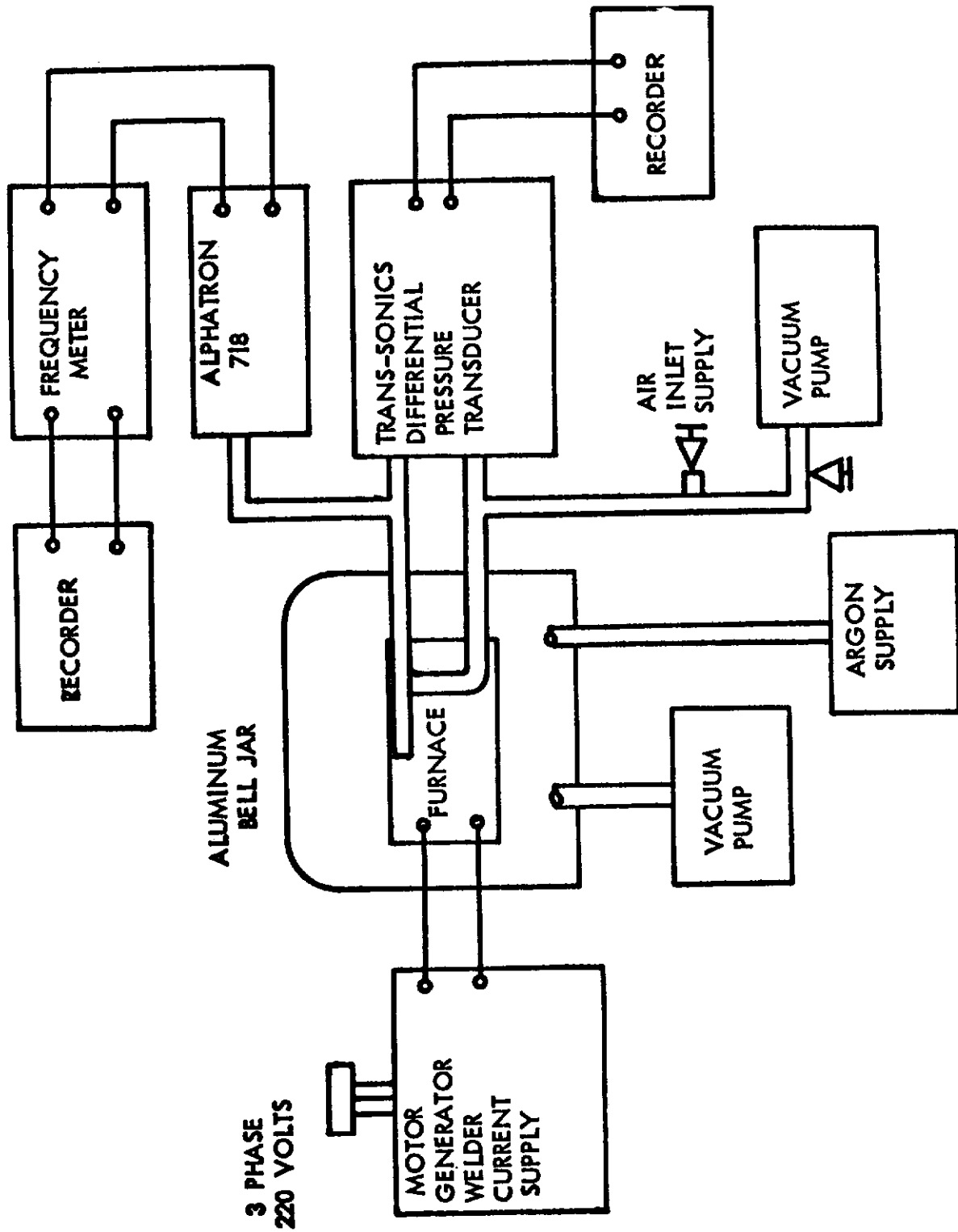
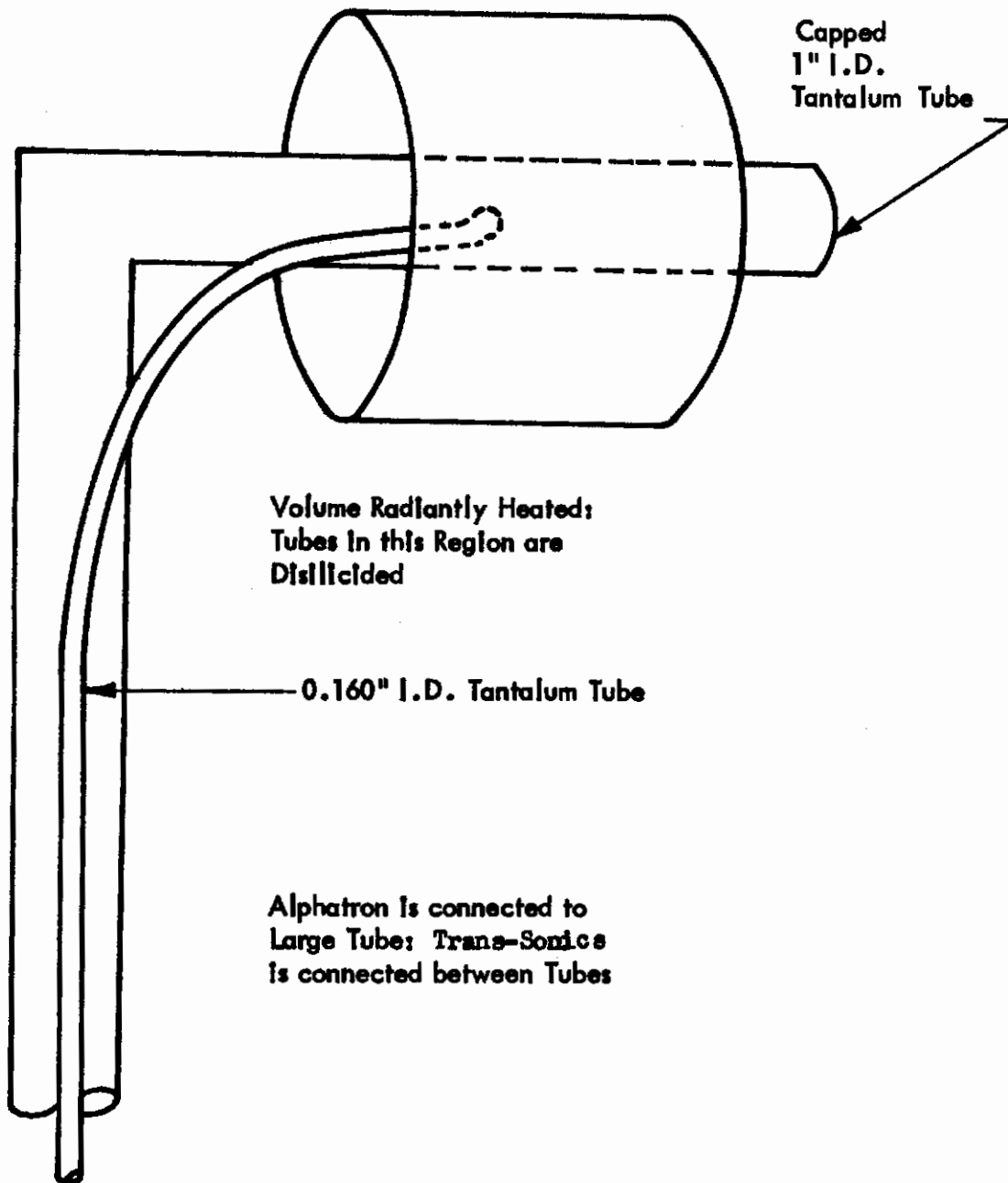


FIGURE 46  
TANTALUM TUBE FACILITY FOR LOW PRESSURE AIR MEASUREMENT



Tantalum Tube Assembly for Low  
Pressure Air Measurement

FIGURE 47

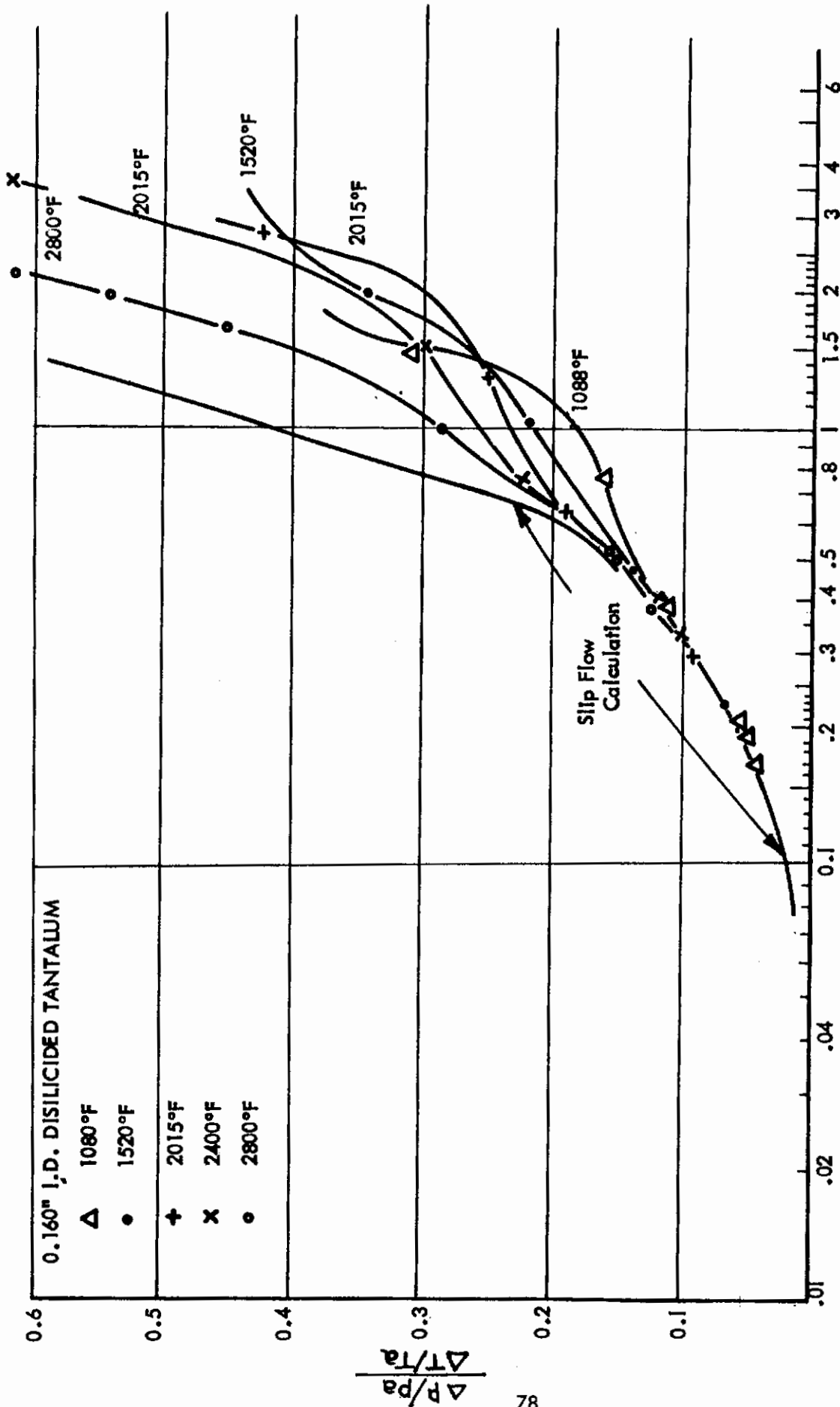


# Contrails

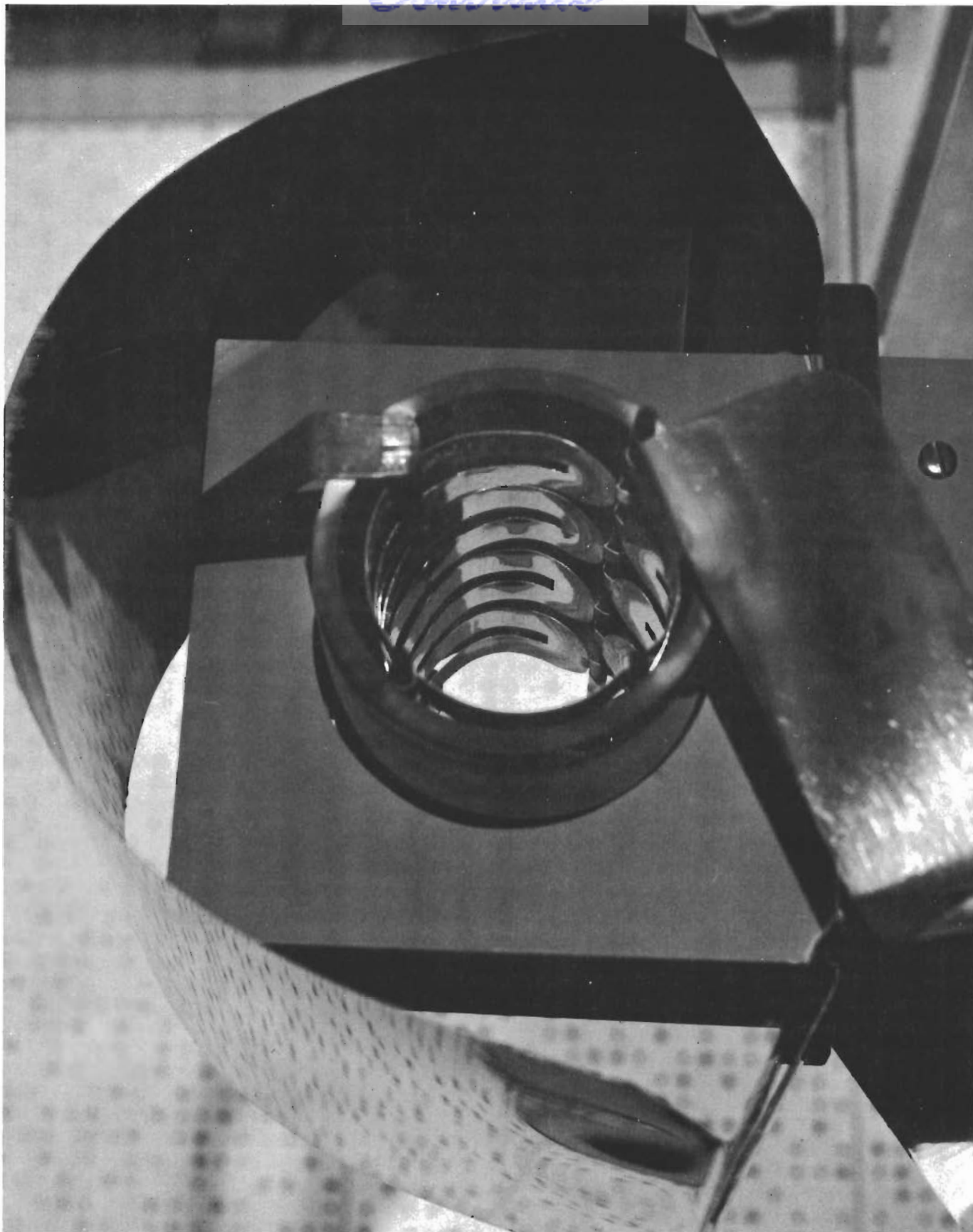
TIME RESPONSE OF TANTALUM TUBE TO AIR WITH STATIC PRESSURE DIFFERENCES BETWEEN IT AND MONITOR TUBE, $d = 0.160"$ , ROOM TEMPERATURE = $80^{\circ}\text{F}$						
	TEST	$p_1$ -torr	$\Delta p_1$ -microns	$p_1$ -torr	$\Delta p_1$ -microns	$(\tau) \cdot (p_1)$ -torr-sec
$80^{\circ}\text{F}$	1	.099		.355		.192
	2	.098		.431		.194
	3	.099		.397		.189
	4	.099		.443		.202
	5	.099		.419		.194
$855^{\circ}\text{K}$	1	.098	14	.335	18	.251
	2	.097	13	.419	17	.278
	3	.098	9	.360	18	.254
$1100^{\circ}\text{K}$	1	.098	22	.387	29	.334
	2	.099		.508	27	.375
	3	.098		.392	29	.330
	4	.098		.443	28	.347
$1366^{\circ}\text{K}$	1	.097	23	.387	40	.363
	2	.095	26	.382	41	.350
	3	.095	27	.387	41	.357
$1590^{\circ}\text{K}$	1	.099	37	.377	52	.362
	2	.099	33	.339	51	.349
	3	.099	33	.392	50	.390
$1805^{\circ}\text{K}$	1	.099	49	.308	65	.314
	2	.100	42	.321	66	.311
	3	.102	42	.397	64	.363

DATA FOR AIR IN CLOSED TUBE

FIGURE 48



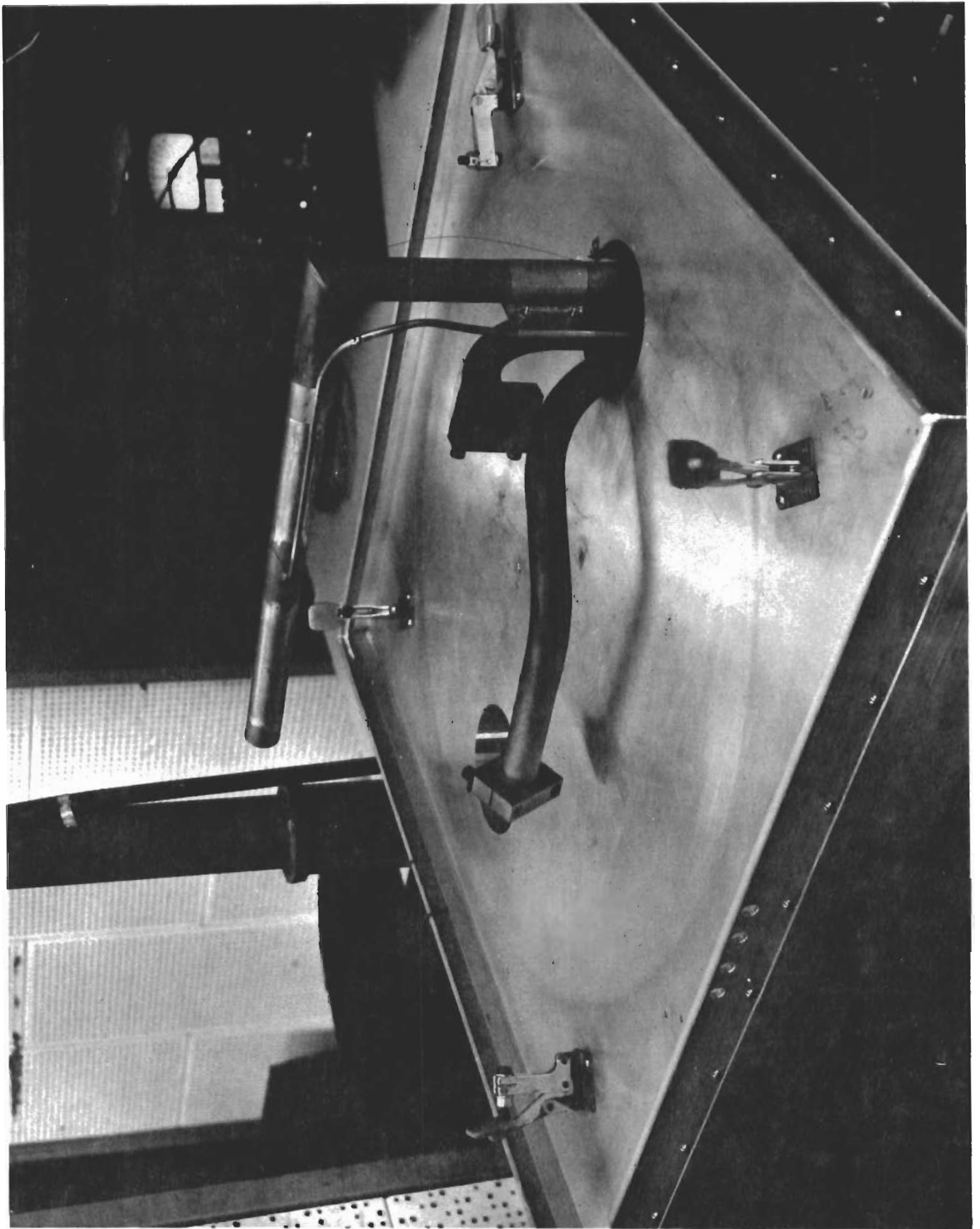
AIR STATIC PRESSURE DIFFERENCE VS  $K_n$  IN A CLOSED TUBE  
 FIGURE 49



PHOTOGRAPH OF FURNACE TO HEAT TANTALUM TUBES

FIGURE 50

79

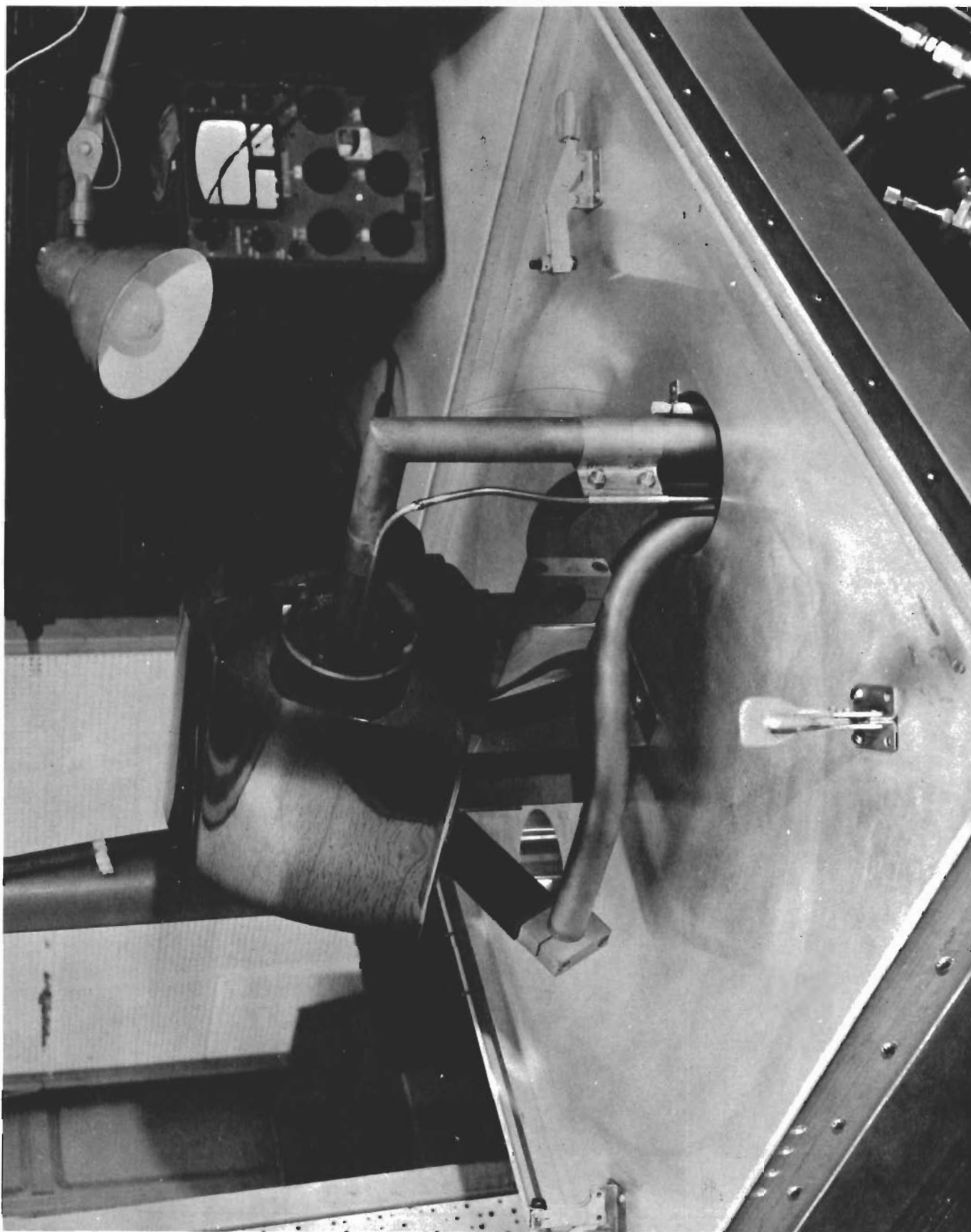


PHOTOGRAPH OF TANTALUM TUBE ASSEMBLY

FIGURE 51

80

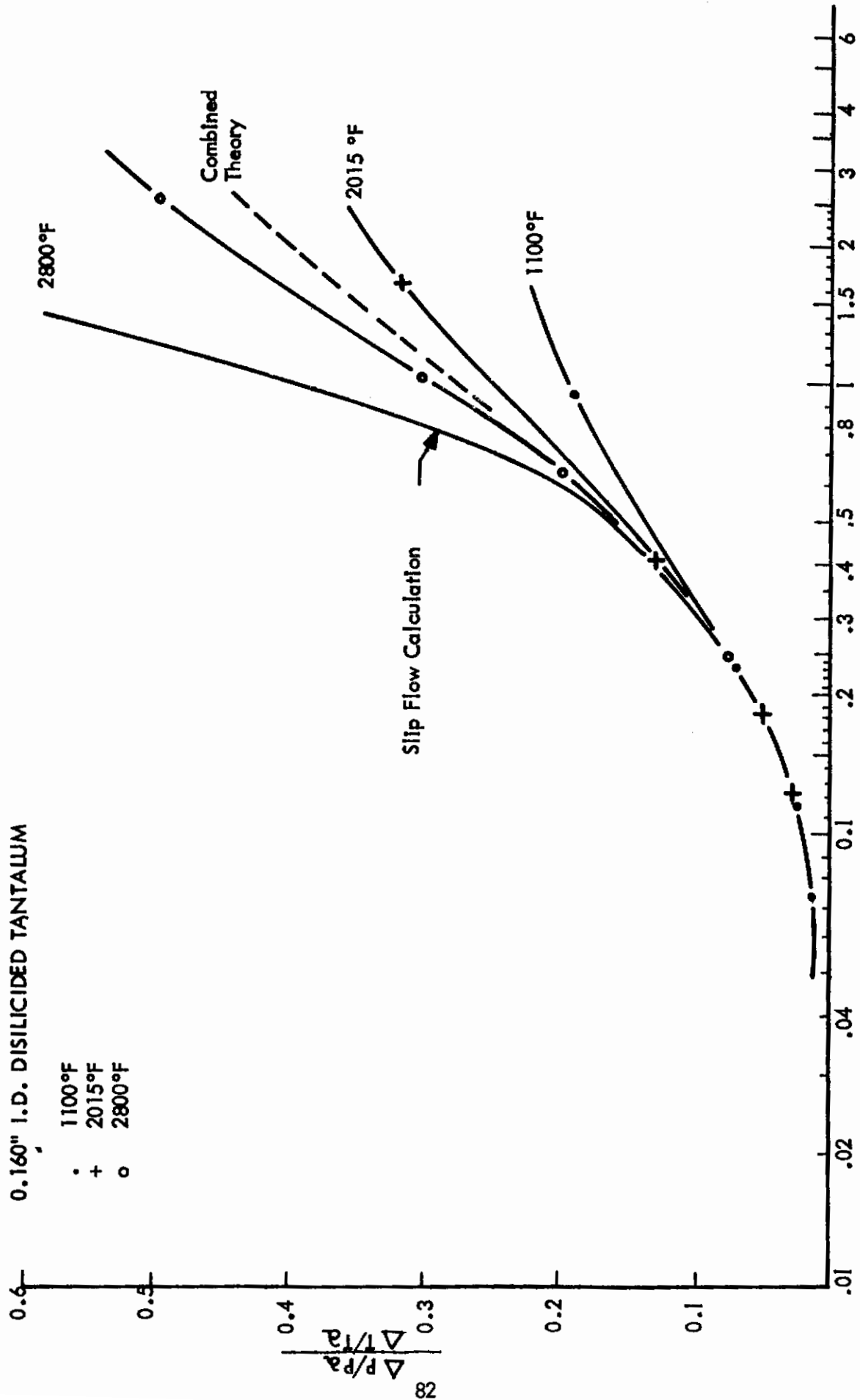


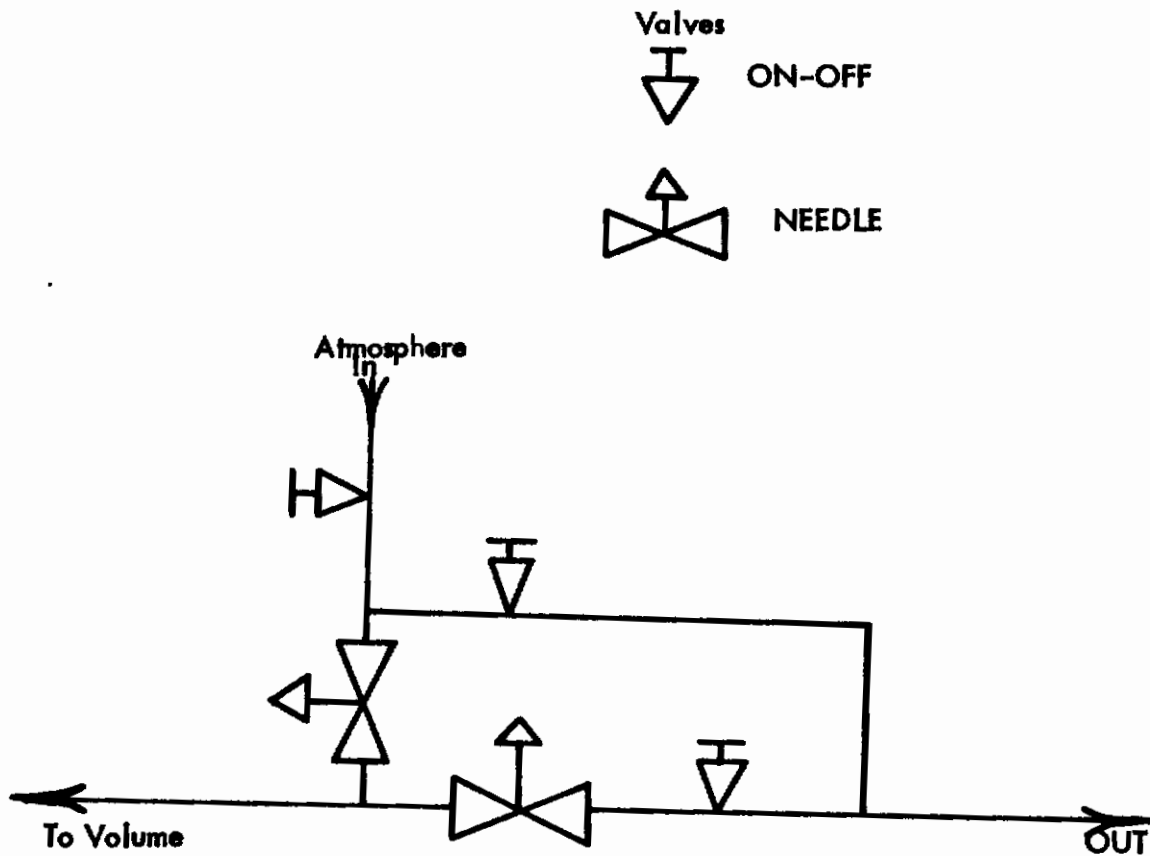


PHOTOGRAPH OF TANTALUM TUBE MOUNTED IN FURNACE

FIGURE 52

81

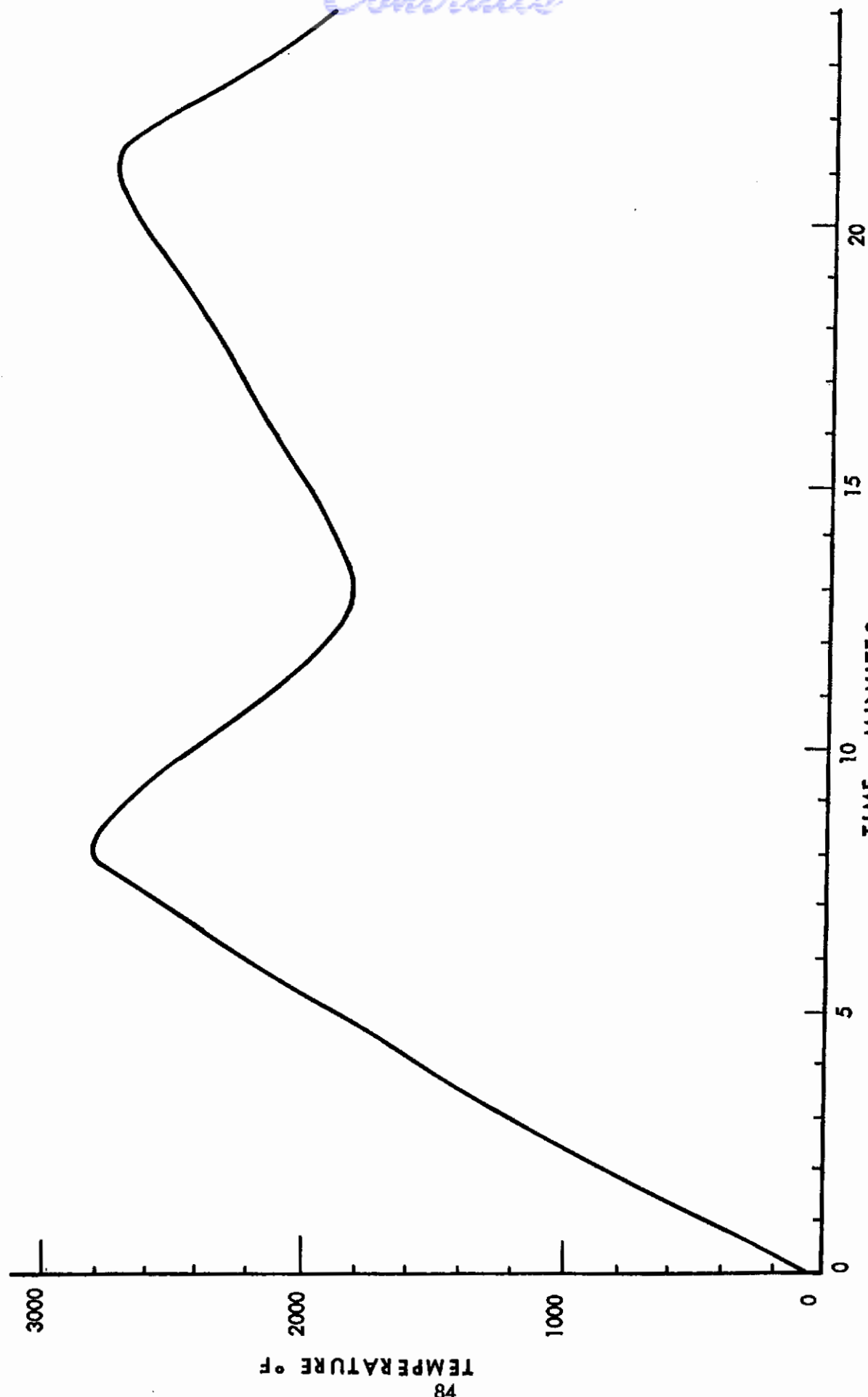




VALVE NETWORK FOR ATMOSPHERIC ENTRY TEST

FIGURE 54

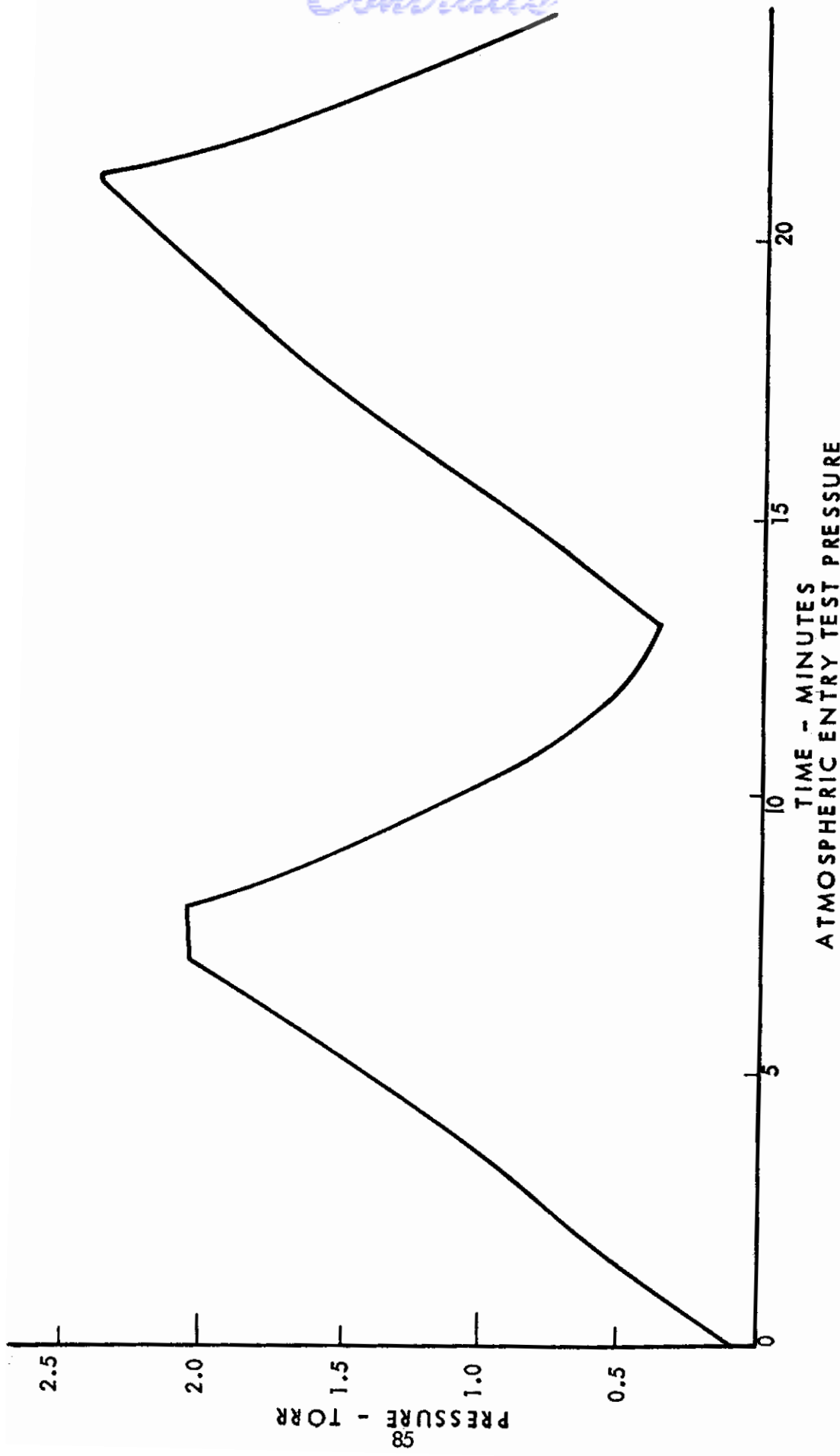
*Contrails*



ATMOSPHERIC ENTRY TEST TEMPERATURE  
FIGURE 55



*Contrails*



ATMOSPHERIC ENTRY TEST PRESSURE  
TIME - MINUTES

FIGURE 56

## PRESSURE - TEMPERATURE HISTORY

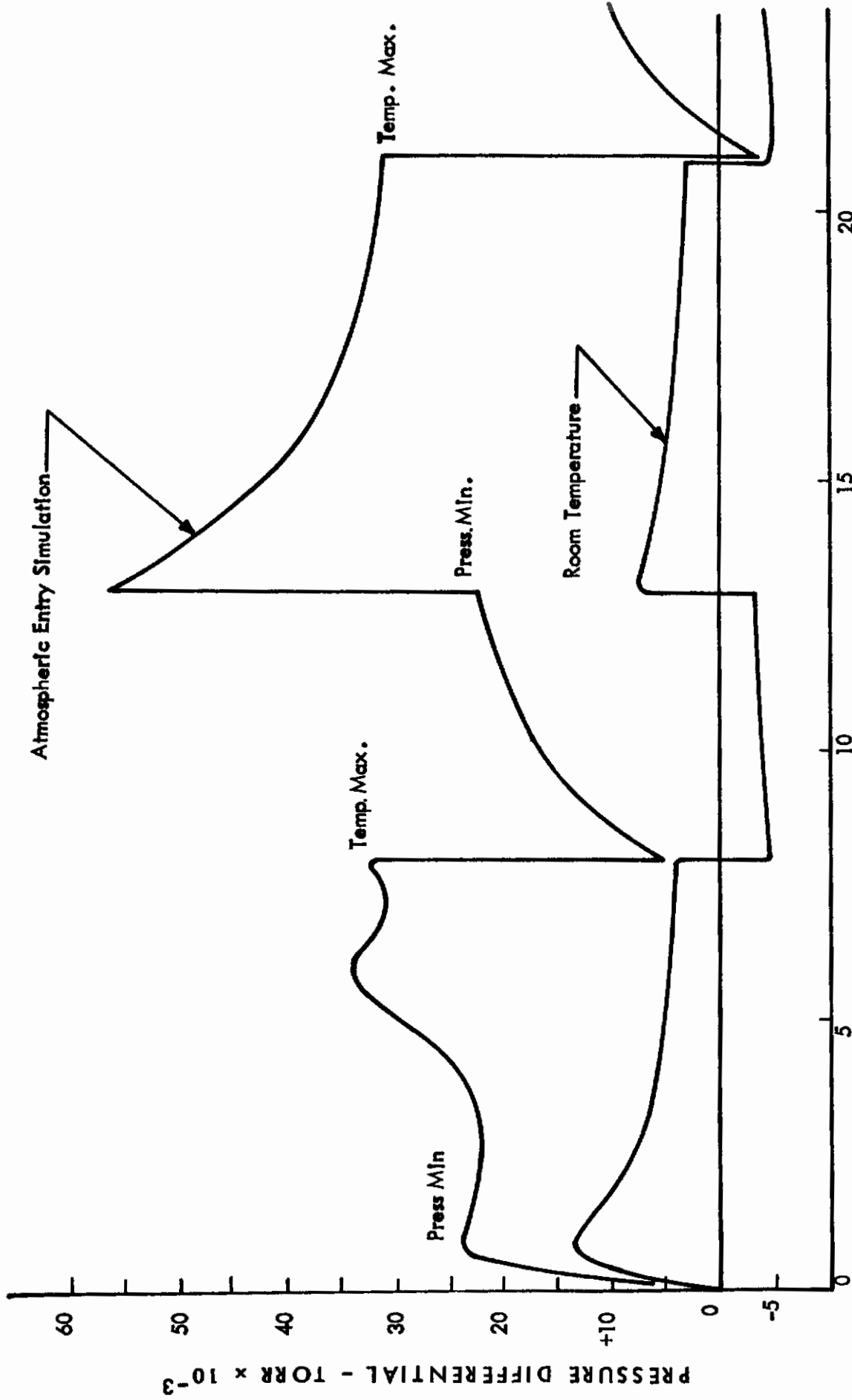
MINUTES	PRESSURE - torr	TEMPERATURE - °F	$\Delta P - \mu$	$\Delta P - \mu - 80^\circ\text{F}$
0	.095	80	+1.7	0.0
1	.355	427	+23.3	+13.3
2	.600	875	+22.0	+9.1
3	.885	1210	+22.0	+6.7
4	1.12	1540	+22.8	+5.5
5	1.42	1877	+28.8	+5.0
6	1.77	2220	+35.0	+4.7
7	2.04	2550	+30.4	+4.0
8	2.04	2800	+31.7, +5	+3.7, -4.7
9	1.51	2640	+11.7	-4.5
10	1.06	2377	+16.7	-4.2
11	0.690	2129	+18.3	-3.7
12	0.472	1900	+20.3	-3.3
13	0.350	1800	+21.7, 56.4	-3.3, +7.0
14	0.600	1870	+48.4	+6.7
15	0.872	1970	+42.0	+5.1
16	1.20	2110	+38.3	+4.8
17	1.44	2225	+36.2	+4.5
18	1.73	2340	+33.4	+3.8
19	1.90	2480	+31.6	+3.5
20	2.12	2630	+31.6	+3.3
21	2.36	2700	+31.0, -3.3	+3.3, -5.0
22	1.66	2480	+3.3	-5.0
23	1.10	2110	+7.5	-4.7
24	0.700	1870	+10.0	-4.2

## ATMOSPHERIC ENTRY TEST PRESSURE

## DIFFERENTIAL DATA

## FIGURE 57

*Contrails*



ATMOSPHERIC ENTRY TEST PLOT OF PRESSURE DIFFERENTIAL

FIGURE 58

# *Contrails*

UNCLASSIFIED

Security Classification

DOCUMENT CONTROL DATA - R&D		
<i>(Security classification of title, body of abstract and indexing annotation must be entered when the overall report is classified)</i>		
1. ORIGINATING ACTIVITY (Corporate author) The Boeing Company Aero-Space Division Seattle, Washington		2a. REPORT SECURITY CLASSIFICATION Unclassified
		2b. GROUP
3. REPORT TITLE  AIR PRESSURE MEASUREMENT IN THE RAREFIED GAS TRANSITION REGION		
4. DESCRIPTIVE NOTES (Type of report and inclusive dates) Final report April 1964 - March 1965		
5. AUTHOR(S) (Last name, first name, initial)  Brunschwig, Fred S.		
6. REPORT DATE August 1965	7a. TOTAL NO. OF PAGES 98	7b. NO. OF REFS 13
8a. CONTRACT OR GRANT NO. AF 33(615)-1793	9a. ORIGINATOR'S REPORT NUMBER(S)  AFFDL-TR-65-101	
b. PROJECT NO. 1469		
c. 146907		
d.	9b. OTHER REPORT NO(S) (Any other numbers that may be assigned this report)	
10. AVAILABILITY/LIMITATION NOTICES Foreign announcement and dissemination of this report by DDC is not authorized.		
11. SUPPLEMENTARY NOTES Report is continuation summary of transducer work started under X-20A program	12. SPONSORING MILITARY ACTIVITY Research & Technology Division Wright-Patterson Air Force Base Ohio	
13. ABSTRACT This report defines parameters and presents pressure corrections for a low air pressure (1-100 p.s.f.a.) measurement system consisting of a pressure transducer and tubing ported to a hot surface at temperatures to 2800°F. Included are results of laboratory measurements with argon and air under conditions of both thermal creep and slip flow occurring together in a pressure transmission tube under temperature gradients. Both temperature functions, thermal creep and slip flow, were found to affect the system pressure. Dynamically, the temperature dependance of slip flow affects time response for tubes since it has the temperature dependancy of gas viscosity. Integration of the tubular time constant, modified for slip flow along the tube's temperature gradient, is carried out and compared to measurements; fair agreement is shown.  For pressure correction, the static (steady state pressure and temperature) differential predicted by Knudsen is found to hold for a closed tubular volume. Additionally, the plotted static results are sufficiently accurate to clearly show the effect of temperature upon viscosity as predicted by integration of Maxwell's viscosity function along the tube.  Other laboratory work reported herein includes calibration of a commercial airborne alpha emission pressure transducer (National Research Corp. Alphation 718). Also, there is considerable data presented on adsorption/oxidation at temperature for pressure tubing material.		

DD FORM 1 JAN 64 1473

UNCLASSIFIED

Security Classification

14. KEY WORDS	LINK A		LINK B		LINK C	
	ROLE	WT	ROLE	WT	ROLE	WT
Transducer Pressure Measurement Pressure Transducer Refractory Metal Pressure Tubing Atmospheric Re-entry Conditions Hot Surface Gas Dynamics Transition Flow Slip Flow Thermal Creep Hardware Development Testing X-20A Dynasoar Continuation Effort						

INSTRUCTIONS

1. **ORIGINATING ACTIVITY:** Enter the name and address of the contractor, subcontractor, grantee, Department of Defense activity or other organization (*corporate author*) issuing the report.
- 2a. **REPORT SECURITY CLASSIFICATION:** Enter the overall security classification of the report. Indicate whether "Restricted Data" is included. Marking is to be in accordance with appropriate security regulations.
- 2b. **GROUP:** Automatic downgrading is specified in DoD Directive 5200.10 and Armed Forces Industrial Manual. Enter the group number. Also, when applicable, show that optional markings have been used for Group 3 and Group 4 as authorized.
3. **REPORT TITLE:** Enter the complete report title in all capital letters. Titles in all cases should be unclassified. If a meaningful title cannot be selected without classification, show title classification in all capitals in parenthesis immediately following the title.
4. **DESCRIPTIVE NOTES:** If appropriate, enter the type of report, e.g., interim, progress, summary, annual, or final. Give the inclusive dates when a specific reporting period is covered.
5. **AUTHOR(S):** Enter the name(s) of author(s) as shown on or in the report. Enter last name, first name, middle initial. If military, show rank and branch of service. The name of the principal author is an absolute minimum requirement.
6. **REPORT DATE:** Enter the date of the report as day, month, year, or month, year. If more than one date appears on the report, use date of publication.
- 7a. **TOTAL NUMBER OF PAGES:** The total page count should follow normal pagination procedures, i.e., enter the number of pages containing information.
- 7b. **NUMBER OF REFERENCES:** Enter the total number of references cited in the report.
- 8a. **CONTRACT OR GRANT NUMBER:** If appropriate, enter the applicable number of the contract or grant under which the report was written.
- 8b, 8c, & 8d. **PROJECT NUMBER:** Enter the appropriate military department identification, such as project number, subproject number, system numbers, task number, etc.
- 9a. **ORIGINATOR'S REPORT NUMBER(S):** Enter the official report number by which the document will be identified and controlled by the originating activity. This number must be unique to this report.
- 9b. **OTHER REPORT NUMBER(S):** If the report has been assigned any other report numbers (*either by the originator or by the sponsor*), also enter this number(s).
10. **AVAILABILITY/LIMITATION NOTICES:** Enter any limitations on further dissemination of the report, other than those

imposed by security classification, using standard statements such as:

- (1) "Qualified requesters may obtain copies of this report from DDC."
- (2) "Foreign announcement and dissemination of this report by DDC is not authorized."
- (3) "U. S. Government agencies may obtain copies of this report directly from DDC. Other qualified DDC users shall request through \_\_\_\_\_."
- (4) "U. S. military agencies may obtain copies of this report directly from DDC. Other qualified users shall request through \_\_\_\_\_."
- (5) "All distribution of this report is controlled. Qualified DDC users shall request through \_\_\_\_\_."

If the report has been furnished to the Office of Technical Services, Department of Commerce, for sale to the public, indicate this fact and enter the price, if known.

11. **SUPPLEMENTARY NOTES:** Use for additional explanatory notes.
12. **SPONSORING MILITARY ACTIVITY:** Enter the name of the departmental project office or laboratory sponsoring (*paying for*) the research and development. Include address.
13. **ABSTRACT:** Enter an abstract giving a brief and factual summary of the document indicative of the report, even though it may also appear elsewhere in the body of the technical report. If additional space is required, a continuation sheet shall be attached.  
  
It is highly desirable that the abstract of classified reports be unclassified. Each paragraph of the abstract shall end with an indication of the military security classification of the information in the paragraph, represented as (TS), (S), (C), or (U).  
  
There is no limitation on the length of the abstract. However, the suggested length is from 150 to 225 words.
14. **KEY WORDS:** Key words are technically meaningful terms or short phrases that characterize a report and may be used as index entries for cataloging the report. Key words must be selected so that no security classification is required. Identifiers, such as equipment model designation, trade name, military project code name, geographic location, may be used as key words but will be followed by an indication of technical context. The assignment of links, rules, and weights is optional.